PREPARATION, CHARACTERIZATION AND ENCAPSULATION OF DIORGANOTIN COMPLEXES AS POTENTIAL ANTICANCER DRUGS

SITI NADIAH BINTI MOHD ROSELY

FACULTY OF SCIENCE
UNIVERSITY OF MALAYA
KUALA LUMPUR

2018

University of Malaya

PREPARATION, CHARACTERIZATION AND ENCAPSULATION OF DIORGANOTIN COMPLEXES AS POTENTIAL ANTICANCER DRUGS

SITI NADIAH BINTI MOHD ROSELY

DISSERTATION SUBMITTED IN FULFILLMENT OF THE REQUIREMENTS FOR THE DEGREE OF MASTER OF SCIENCE

DEPARTMENT OF CHEMISTRY
FACULTY OF SCIENCE
UNIVERSITY OF MALAYA
KUALA LUMPUR

2018

University of Malaya

UNIVERSITY OF MALAYA

ORIGINAL LITERARY WORK DECLARATION

Name of Candidate: Siti Nadiah Binti Mohd Rosely

Matric No: SGR 140043

Name of Degree: Master of Science

Title of Dissertation ("this Work"): Preparation, Characterization and Encapsulation of Diorganotin Complexes as Potential Anticancer Drugs

Field of Study: Inorganic Chemistry

I do solemnly and sincerely declare that:

(1) I am the sole author/writer of this Work;
(2) This Work is original;
(3) Any use of any work in which copyright exists was done by way of fair dealing and for permitted purposes and any excerpt or extract from, or reference to or reproduction of any copyright work has been disclosed expressly and sufficiently and the title of the Work and its authorship have been acknowledged in this Work;
(4) I do not have any actual knowledge nor do I ought reasonably to know that the making of this work constitutes an infringement of any copyright work;
(5) I hereby assign all and every rights in the copyright to this Work to the University of Malaya ("UM"), who henceforth shall be owner of the copyright in this Work and that any reproduction or use in any form or by any means whatsoever is prohibited without the written consent of UM having been first had and obtained;
(6) I am fully aware that if in the course of making this Work I have infringed any copyright whether intentionally or otherwise, I may be subject to legal action or any other action as may be determined by UM.

Candidate's Signature Date:

Subscribed and solemnly declared before,

Witness's Signature Date:

Name:

Designation:

University of Malaya

PREPARATION, CHARACTERIZATION AND ENCAPSULATION OF DIORGANOTIN COMPLEXES AS POTENTIAL ANTICANCER DRUGS

ABSTRACT

A series of diorganotin(IV) complexes with Schiff base ligands derived from 3-hydroxy-2-naphthoic hydrazide (NAH) and *tris*(hydroxymethyl)aminomethane (TRIS), were synthesized and characterized using infrared (IR), ^{1}H and ^{13}C nuclear magnetic resonance (NMR) spectroscopies and elemental analyses. Besides, the crystal structure of one of the complexes was determined by single crystal X-ray diffraction (SCXRD). The *in vitro* cytotoxic activities of the Schiff base ligands and their diorganotin(IV) complexes were evaluated against two human carcinoma cell lines, namely human colon carcinoma cell line (HT29) and hormone-dependent breast carcinoma cell line (MCF7). Among the synthesized complexes, [*N*'-(4-decyloxy-2-oxidobenzylidene)-3-hydroxy-2-naphthohydrazidato]dimethyltin(IV) (NA1) and (2-{[1,1-*bis*(hydroxymethyl)-2-oxidoethyl]iminomethyl}-4-dodecyloxy-2-oxidobenzylidene)dibutyltin(IV) (TB2) were the most active. The percentage of encapsulation efficiency and percentage of drug loading for niosome-encapsulated for seven diorganotin(IV) complexes were investigated. While only one niosomes-complex system was chosen as an exemplary detailed characterization, covering encapsulation efficiency and drug loading, size distribution, zeta potential and morphology of the carriers as well as an *in vitro* release study was performed. Niosomes with the mean diameter approximately 100 nm in size with low polydispersity index of 0.3 was prepared through ethanolic injection method. Niosome-loaded with ND2 complex exhibited high encapsulation efficiency in the range of between 80 - 99%. The results from a zeta potential measurement showed that the formulation is relatively stable with the value in a range of -25 to -36 mV. The drug release rate was slow, about 20% cumulative in three months.

Keywords: diorganotin(IV), Schiff base, anticancer, niosome-encapsulated, drug release

University of Malaya

PENYEDIAAN, PENCIRIAN DAN PENGKAPSULAN KOMPLEKS DIORGANOTIN SEBAGAI POTENSI UBAT ANTIKANSER

ABSTRAK

Satu siri kompleks diorganotin(IV) dengan ligan Schiff bes yang diperolehi daripada 3-hydroxy-2-naphthoic hydrazide (NAH) dan *tris*(hydroxymethyl)aminomethane (TRIS), telah disintesis dan dicirikan menggunakan spektroskopi inframerah (IR), ^{1}H dan ^{13}C resonans magnetik nuklear (NMR) dan analisis unsur. Di samping itu, struktur kristal salah satu kompleks telah ditentukan dengan difraksi X-ray kristal tunggal (SCXRD). Aktiviti sitotoksik *in vitro* ligan Schiff bes dan kompleks diorganotin(IV) nya telah diuji dengan dua garis sel kanser manusia, iaitu garis sel karsinoma kolon manusia (HT29) dan garis sel karsinoma payudara yang bergantung kepada hormon (MCF7). Antara kompleks yang disintesis, [*N*'-(4-decyloxy-2-oxidobenzylidene)-3-hydroxy-2-naphthohydrazidato]dimethyltin(IV) (NA1) dan (2-{[1,1-*bis*(hydroxymethyl)-2-oxidoethyl]iminomethyl}-4-dodecyloxy-2-oxidobenzylidene)dibutyltin(IV) (TB2) adalah yang paling aktif. Peratus kecekapan pengkapsulan dan muatan ubat bagi niosom-terkandung untuk tujuh kompleks diorganotin(IV) telah dikaji. Hanya satu sistem niosom-kompleks yang dipilih sebagai contoh pencirian terperinci, meliputi kecekapan pengkapsulan dan muatan ubat, taburan saiz, potensi zeta dan morfologi pembawa serta pelepasan ubat secara *in vitro* telah dilakukan. Niosom dengan diameter lebih kurang dalam saiz 100 nm dengan indeks polidispersiti rendah iaitu 0.3 telah disediakan dengan kaedah suntikan beretanol. Niosom-dimuatkan dengan kompleks ND2 mempamerkan kecekapan pengkapsulan yang tinggi diantara julat 80 - 99%. Keputusan dari pengukuran potensi zeta menunjukkan formulasi adalah agak stabil dengan nilai antara -25 hingga -36 mV. Kadar pelepasan ubat adalah perlahan, kira-kira 20% kumulatif dalam tiga bulan.

Katakunci: diorganotin(IV), Schiff bes, antikanser, niosom-terkandung, pelepasan ubat

University of Malaya

ACKNOWLEDGEMENTS

Alhamdulillah, all praise to Allah S.W.T for His greatness and giving me the strength, opportunity and motivation to complete this research.

I would like to thank my supervisors, Dr. Rusnah Syahila Duali Hussen and Dr. Lee See Mun for their guidance, patience and support throughout this research. This thesis would not be completed without their help. Their kindness and dedication in helping me in my research are very much appreciated.

I also would like to extend my appreciations to my seniors from all Chemistry Research Laboratory who have been very helpful and supportive in providing technical support, and to all staffs in the Chemistry Department, Science Faculty, University of Malaya, for their cooperation and kindness.

I would like to thank my parents Mohd Rosely and Raja Hamidah for their support, valuable advice and prayers and sincere gratitude to my siblings. Also to my friends especially Siti Amira, Syaidatul Atiqah, Siti Khalijah, Nur Zahidah and Nur Artikah for their full support and encouragement throughout this research. Thank you so much for all supports, time, manpower and sacrifices for me being able to finish this master research.

This research was financially supported by the scholarship from Fellowship Scheme Universiti Malaya (SBUM) from Institute of Graduate Studies, Postgraduate Research Fund (PPP) (PG102-2015A) and my supervisor's research grant.

University of Malaya

TABLE OF CONTENTS

University of Malaya

University of Malaya

University of Malaya

University of Malaya

University of Malaya

LIST OF FIGURES

University of Malaya

University of Malaya

LIST OF TABLES

University of Malaya

University of Malaya

LIST OF SCHEMES

University of Malaya

LIST OF SYMBOLS AND ABBREVIATIONS

AFM	:	Atomic force microscopy
Anal.	:	Combustion elemental analysis
B.M	:	Bohr Magneton
calcd	:	Calculated
$CDCl_3$	:	Deuterated chloroform
$CHCl_3$	:	Chloroform
DL	:	Drug loading
DMF	:	Dimethylformamide
DMSO	:	Dimethylsulfoxide
DTA	:	Differential thermal analysis
ESR	:	Electron spin resonance
FESEM	:	Field emission scanning electron microscopy
FTIR	:	Fourier transform infrared
HCl	:	Hydrochloric acid
HPLC	:	High-performance liquid chromatography
IC_{50}	:	Inhibitory concentration 50
ILCT	:	Intraligand charge transfer
IM	:	Intramuscular
IV	:	Intravenous
K_2CO_3	:	Potassium carbonate
KI	:	Potassium iodide
LUV	:	Large unilamellar vesicle
MCV	:	Microencapsulation vesicle method
$MgSO_4$	:	Magnesium sulphate
MLV	:	Multilamellar vesicle
MTT	:	3-(4,5-dimethylthiazol-2-yl)-2,5-diphenyl-tetrazolium
Mw	:	Molecular weight
NAH	:	3-hydroxy-2-naphtoic hydrazide
NMR	:	Nuclear magnetic resonance
PDI	:	Polydispersity index
SC	:	Subcutaneous
SCXRD	:	Single crystal X-ray diffraction

University of Malaya

SEM	:	Scanning electron microscopy
SUV	:	Small unilamellar vesicle
TEM	:	Transmission electron microscopy
TGA	:	Thermogravimetric analysis
TLC	:	Thin layer chromatography
TRIS	:	*Tris*(hydroxymethyl)aminomethane
Tween 80	:	Polyoxyethylene (20) sorbitan monooleate
w/o	:	Water-in-oil
w/o/w	:	Water-in-oil-in-water

University of Malaya

CHAPTER 1: INTRODUCTION

1.1 Overview

This chapter includes the introduction and background of diorganotin(IV) complexes and its potential characteristic as an anticancer agent, as well as the research benefit. The problem statements and the objectives of the study, including with the map of the thesis are also in this chapter.

1.2 Introduction of the research

Complexes of platinum(II), such as cisplatin, oxaliplatin, nedaplatin, and carboplatin have achieved clinical status as a result of intensive research on anticancer metal-based drugs (Sun et al., 2007; Kaluderović & Paschke, 2011). However, despite its reasonable therapeutic index, the applications of platinum(II) complexes are limited by significantly unfavorable side effect, poor water solubility and its acute toxicity (Prasad et al., 2010). Hence, non-platinum metals are being investigated to replace platinum drugs due to problems such as typical of heavy metal toxicity and the development of drug tolerance by the tumors (Arjmand et al., 2014). Therefore, the synthesis of non-platinum metal chemotherapeutics such as gold(III), copper(II), ruthenium(II), cobalt(II), and tin(IV), all of which exhibit positive, no or limited side effects towards the healthy cells, are preferred (Prasad et al., 2010). Several researchers have begun investigating the possible therapeutic applications of other metal-based drugs, often organometallic complexes, specifically organotin(IV) complexes as alternatives to platinum for biological activities (Koch et al., 2008).

Since the discovery of the cisplatin antitumor activity, great efforts have focused on the rational design of metal-based anticancer agents that can be potentially used in cancer chemotherapy (Muhammad & Guo, 2014). Tin(IV) complexes give great attention because of their unique properties in medicine, industrial applications and biological

University of Malaya

systems (Niu et al., 2014; Pourayoubi et al., 2015). Organotin(IV) complexes might be designed with good properties such as increased water solubility and lower general toxicity than platinum drugs (Kaluderović & Paschke, 2011). It has well been established that organotin(IV) complexes are very important in cancer chemotherapy due to their apoptosis-inducing character (Hadjikakou & Hadjiliadis, 2009). Organotin(IV) complexes are currently becoming crucial in cancer chemotherapy treatments. It has proven their significant effectively by controlling of toxicity problems and specifically targeted drug uptake only by the cancerous cells without affecting the healthy cells (apoptosis) (Arjmand et al., 2014).

Generally, the biochemical activity of organotin(IV) complexes is influenced prominently by several factors which are the coordination number, types of coordinated ligands and the structure of the molecule as well as the substituent alkyl groups of the tin(IV) atom (Hong et al., 2014). The ligands not only control the reactivity of the metal but also play important roles in determining the nature of interactions involved in the recognition of biological target sites such as deoxyribonucleic acid (DNA), enzymes and protein receptors (Sadler, 2009). Tin(IV) complexes normally have a tetrahedral, octahedral or trigonal bipyramidal structure. This difference in the molecular geometry might lead to the difference in binding to the target cells (Carraher & Roner, 2014). The coordination chemistry of diorganotin(IV) complexes with biologically or pharmacologically active *O,N,O, N,N,S* and *O,N,S* tridentate ligands may provide further information about the structural characteristics needed for their antitumor and cytotoxic activities (Dey et al, 2011; Lee et al., 2012). Due to the other works from the past with organotin(IV) complexes as chemotherapeutic agents, this research desired to work on preparation of diorganotin(IV) complexes derived from tridentate *O, N, O* ligands to study its anticancer activities and niosomal formulation.

University of Malaya

A number of studies have been conducted for metal complexes encapsulated in nanoparticles (Aryal et al., 2012), niosomal (Marianecci et al., 2013), and liposomal (Corvo et al. 2016) formulation for cancer therapies. Most of these complexes show poor water solubility, which reduces the anticancer efficacy. This could be circumvented *via* less polar solvents, such as dimethylsulfoxide or ethanol. However, these solvents strongly affect the *in vitro* and *in vivo* responses and are acutely toxic (Corvo et al., 2016). The formulation of the encapsulated metal complexes with relatively inert and nontoxic carriers has been found to reduce the side effects while improving therapeutic index, prolonging the product lifecycle, and eventually reduce health-care costs (Zhang et al., 2008). The drug carrier helps prolong the release of the drug while reducing destruction along the pathway to the target site (Puri et al., 2010). In this research, a nonionic surfactant will be used to prepare niosome for it to act as a drug carrier for the diorganotin(IV) complexes. Niosome is known to possess distinct advantages, such as long shelf life, lower toxicity, and biodegradability (Bagheri et al., 2014). The preparation of the carrier method, in addition, helps produce a variety of vesicle sizes, which is also an important parameter when determining the circulation half-life of vesicles. Both size and a number of bilayers eventually affect the amount of drug encapsulation in the vesicles (Akbarzadeh et al., 2013).

Injections are among the most common health care procedures throughout the world. Intravenous (IV), subcutaneous (SC), and intramuscular (IM) are three most commonly used injection routes in medication administration (Jin et al., 2015). In this research, the selected compounds were potential as an anticancer agent for breast cancer therapy. Therefore, a suitable drug administration route for the hormone-dependent breast carcinoma cell line (MCF7) is an intravenous (IV) injection. Thus, a smaller size of niosome in nano scale is preferred for injection route. Consequently, methods that will be used to formulate niosomal, must be able to produce smaller vesicle size. A suitable

University of Malaya

method such as ethanol injection method that known to produce a formulation with narrow distribution is appropriate to apply (Jaafar-Maalej et al., 2010) and also microencapsulation vesicle (MCV) method that through a 2-step emulsification and dispersion process (Nii & Ishii, 2007). A small size vesicle for IV injection is preferred for the delivery of anticancer drugs, as it helps avoid steric hindrance and can penetrate farther into the infected cell to deliver their contents. When administered by injection, the use of niosomes to encapsulate drugs reduces toxicity without decreasing the potency of the drugs (Vaage et al., 1997).

1.3 Research benefits

There is crucial need to develop and characterize new drugs with enhanced activity, selectivity, bioavailability and fewer side-effects than conventional drugs to treat current cancers (Low, 2015). The newly prepared diorganotin(IV) complexes derived from NAH and TRIS ligands as potential anticancer drugs are expected to be a more active MCF7 anticancer agent that is less toxic than the model drug, such as cisplatin. According to past research (Lee et al., 2013), the diorganotin((IV) complexes derived from NAH ligands such as NE1 (0.62 ± 0.01 μg mL^{-1}) and NF2 (0.69 ± 0.01 μg mL^{-1}) complexes that contain halides have better cytotoxicity than cisplatin (2.4 ± 0.6 μg mL^{-1}) in MCF7. The organotin(IV) also have a different mechanism of action than those of cisplatin and its analogs. Furthermore, several studies related to organotin(IV) also displayed lower median inhibitory concentration against different human cancer cell lines as compared to the recent clinical drugs used in cancer treatment (Gómez-Ruiz et al., 2008; Hadjikakou & Hadjiliadis, 2009).

1.4 Problem statements

Cancer is one of the leading causes of mortality and disease in the world. Platinum based-drugs have been used in many treatments due to its good therapeutic index,

University of Malaya

nevertheless, the platinum(II) complexes bring side effect to the healthy cells and its severe toxicity (Muhammad & Guo, 2014). Hence, many new organotin(IV) complexes are currently being synthesized to combat this disease by redesigning the existing chemical structure through ligand substitution or building the entire new compound with enhanced safety and cytotoxic profile (Hadjikakou & Hadjiliadis, 2009; Ndagi et al., 2017). With these reasons, it is important to stress the need for more research in the synthesis and characterization of new organotin(IV) with biologically active ligands (Garza-ortiz et al., 2013).

In this dissertation, two type of diorganotin(IV) complexes containing 3-hydroxy-2-naphthoic hydrazide (NAH) or *tris*(hydroxymethyl)aminomethane (TRIS) Schiff base ligands that involve different alkyl groups attached to the organotin(IV) moiety and different type of long alkoxy chain as substituents will be synthesized and characterized. The choice of NAH in this research was based on the literature findings concerning this hydrazide. Due to −NH−C(=O)− moiety in the structure, it can undergo keto-enol tautomerization, These hydrazones are able to modulate the number of negative charges in coordination systems and form stable complexes with metal ions in various oxidation states (Bikas et al., 2018). In a study, 1,2,4-triazoles derived from this hydrazide showed favorable *in vitro* anticancer activity against 60 human tumor cell lines (Dogan et al., 2005). While in the TRIS structure it contains an amino and three alcoholic groups which contribute to the characteristic of physiologically inert, non-corrosive, biodegradable, and is available commercially (Pandit et al., 2015). The TRIS ligand coordinates to metal not only through nitrogen but also through oxygen, hence, increasing the coordination number of metal (Kemula et al., 1962). The TRIS ligands also have been reported for their antimicrobial properties (Odabasoglu et al., 2007) and anticancer activities (Lee et al., 2015).

University of Malaya

However, diorganotin(IV) complexes are still toxic and its application also limited by their poor water solubility (Hong et al., 2013b). In order to reduce the toxicity and increase the bioavailability of the drugs, they will be encapsulated with nonionic drug carrier (Aryal et al., 2012). Niosome and other nanoparticles are precious tools in the chemical and pharmaceutical areas as they allow the release of drug in a controlled manner with improved bioavailability. Being nonionic, they are less toxic and improve the therapeutic index of drug and release the drug specifically to the target cell by controlling their action (Andresen et al., 2005; Mehta & Jindal, 2013).

1.5 Objectives of the research

The objectives of this study are listed below:

- To prepare two series of ligands and diorganotin(IV) complexes based on 3-hydroxy-2-naphthoic hydrazide (NAH) and *tris*(hydroxymethyl)aminomethane (TRIS). Two ligands and four complexes were prepared for NAH series and a similar number of ligands and complexes were synthesized for TRIS series.
- To characterize the structure of synthesized ligands and complexes using infrared (IR), ^{1}H and ^{13}C nuclear magnetic resonance (NMR) spectroscopies, elemental analyses and single crystal X-ray diffraction (SCXRD) where the tools are relevant and suitable.
- To study the encapsulation and drug release of selected diorganotin(IV) complexes as a model drug.
- To study the anticancer activities in the colon (HT29) and breast (MCF7) carcinoma cell lines of the synthetized ligands and diorganotin(IV) complexes.

University of Malaya

1.6 Dissertation map

This dissertation consists of five chapters. Chapter 1 introduces the background and significance of this research, problem statements and its objectives. Chapter 2 presents the theories and literature relevant to the research. Chapter 3 gives the details of the experimental part of the research and the synthesis of the involved complexes, the instrumental techniques used to characterize the ligands and complexes, the biological study, formulation, and characterization of niosome-encapsulated diorganotin(IV) complexes. Chapter 4 presents the results and discussions, while Chapter 5 concludes the work and some recommendations for future research related to this study. A list of references and publication paper presented are listed at the end of this dissertation.

University of Malaya

CHAPTER 2: LITERATURE REVIEW

2.1 Introduction

This chapter includes the discussion on applications, biological significance, structural variety and chemical properties of organotin(IV) complexes and other metal complexes with hydrazone ligands (Sedaghat et al., 2014). A few types of ligands, transition metals and metal complexes that used in the preparation of organotin(IV) complexes are the matters to discuss first. Organotin(IV) complexes are toxic to living organisms and to their immune system (Marianecci et al., 2013). These complexes also have poor solubility in water and are classified as a hydrophobic drug. Therefore, a drug carrier is needed to facilitate the drug delivery throughout the body *via* a suitable drug administration route. Thus, a literature review on the anticancer drug administration, types of drug carrier, as well as the preparation of drug carrier, are also included in this chapter.

2.2 Schiff base ligands

Schiff base is a nitrogen analogue of an aldehyde or ketone, where the C=O group is exchanged with the C=N-R group, with a general formula of $R_2C{=}N{-}R'$, where R and R' is an aryl or alkyl group that makes the Schiff base a stable imine as displayed in Figure 2.1 (Qin et al., 2013).

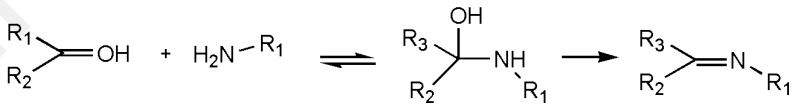

Figure 2.1: Schiff reaction of preparation of imines

Schiff bases play an important role in inorganic chemistry, as they can easily form stable complexes with most transition metal ions in the periodic table (Qurban, 2011). The coordination of these ligands with metal complexes can be monodentate, bidentate, tridentate and tetradentate.

University of Malaya

2.3 Hydrazone ligands

Hydrazone attracted special attention from researchers due to their well-known chelating capability and structural flexibility that can provide rigidity to the skeletal framework of the prepared metal complexes (Yang et al., 2016). The general formula of hydrazides, $RC{=}ONHNH_2$, is known for their fascinating chemical features. Hydrazides react with aldehydes RCHO to form hydrazones with the general formula of $R^1R^2C{=}N\text{-}NH_2$. Generally, the reaction is reversible under acid or base catalysis, or upon heating. The metal complexes of this hydrazone are generally studied due to the presence of more than two potential donor sites (Shelke et al., 2011). The ligands may coordinate to the metal center either in the 'keto' or 'enol' forms through nitrogen or oxygen (Al-Ne'aimi, 2012). The tautomeric keto or enol forms of ligands as shown in Figure 2.2 (Dey et al., 2011) were also indicated by ^{1}H-NMR spectroscopy by observing the enolic OH signal of enol forms of ligands or amide NH signal of keto forms. The evidence for enolization due to some shifted absorption frequencies showed in infrared (IR) spectrum. The absence of stretching band due to NH and strong *v*(C=O) was attributed to the presence of the enol tautomer (Saadeh, 2013).

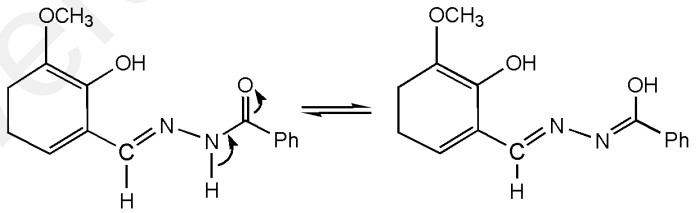

Figure 2.2: Tautomerism of the ligand, *N*'-(2-hydroxy-3-methoxybenzyl-idene)benzohydrazide (I)

Hydrazone derivatives containing an azomethine (-CONHN=CH-) group exhibit antiproliferative activities, and act as a cytotoxic agent with the ability to prevent cell progression in cancerous cells *via* different mechanisms (Onnis et al., 2009). Hydrazone bond linkage offers a proper system for pH-dependent release of anticancer drugs from

University of Malaya

drug-conjugates. The study on structure-activity relationships showed that the hydrazone derived from salicylaldehyde had much more inhibitory effects (Zheng et al., 2009). Based on literature, these ligands are widely used for anticancer applications (Abu-Dief et al., 2015), antioxidant (Dutta et al., 2005; Bhat et al., 2014), antimicrobial-like antibacterial (Sunitha et al., 2012), and antifungal (Chohan et al., 2010) and cytotoxic activities (Das et al., 2009; Qin et al., 2013).

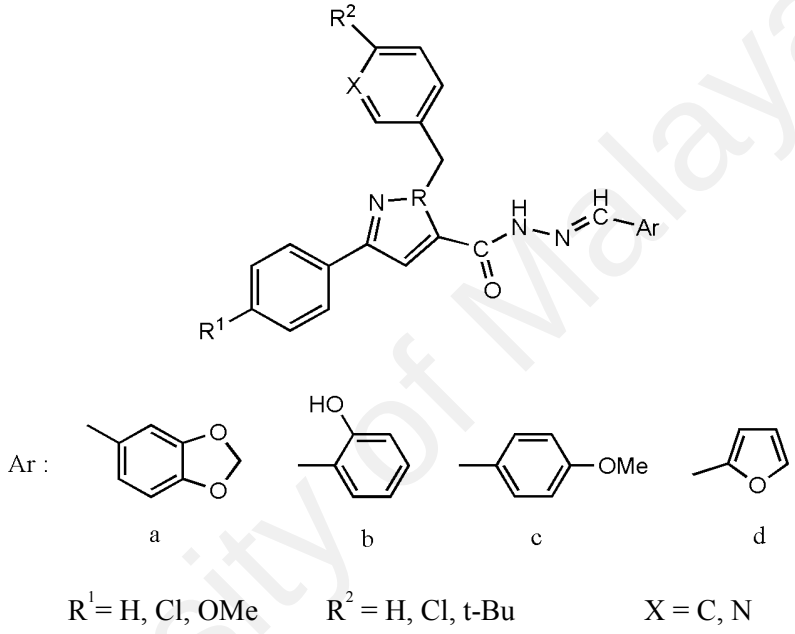

Figure 2.3: Hydrazone derivatives of 1-arylmethyl-3-aryl-1H-pyrazole-5-carbohydrazide

Xia et al., (2008) synthesized several 1-arylmethyl-3-aryl-1H-pyrazole-5 carbohydrazide hydrazone derivatives (Figure 2.3) with the intention to study its anticancer behavior. The results showed that all compounds had almost inhibitory effects on the growth of lung cancer cell lines (A549) using the (3-[4,5-dimethylthiazol-2-yl]-2,5-diphenyl-tetrazolium bromide, (MTT) cell proliferation assay. It was suggested that the potency of these compounds against A549 depended on its lipophilicity, as well as the capacity of the compound chelating metal ions. It was believed that metal ions play a vital role in cell growth. The research found that the nature and position of the substituent

University of Malaya

on the compound as shown in Figure 2.3 improve biological activities. The compound with substituents of R^2 = tert-butyl, X = C and R^1 were any of these three H, Cl, OMe will improve the biological activities.

5-nitrosalicylaldehyde benzoylhydrazone (5nSBH) and its derivatives were tested for *in vitro* cytotoxicity on an acute myeloid leukemia (HL60) and chronic myeloid leukemia cell lines (BV173). 5nSBH exerted the most noticeable cytotoxic effect against both cell lines compared to its derivatives. The trend of inhibitory concentration 50 (IC_{50}) for HL60 and BV173 was increasing from various ligands but decreases in lipophilicity. The existence of the nitro group in salicylaldehyde moiety slightly decreases the lipophilicity because the nitro group is polar and a strong attractor of electrons (Nikolova-Mladenova et al., 2009). A decreasing lipophilicity will improve solubility of the compounds and gives good absorption (Arnott & Planey, 2012).

Zheng et al., (2009) synthesized a series of novel 3-aryl-1-(4-tert-butylbenzyl)-1H-pyrazole-5-carbohydrazide (compound 3) ($R = R^2 = R^1 = H$) derivatives and tested against lung cancer cells (A549) growth. The result showed that the derivative of 3 which is 3e ($R = R^2 = Cl$; $R^1 = H$) held the highest growth inhibitory effect. 3e compound also induces apoptosis in A549. The apoptosis induction may be a mechanism by which compound 3e kills the cancer cells. From the IC_{50} result, it showed that the substituent of R groups in the hydrazone of compound 3 derivatives gave different cytotoxic activities.

2.3.1 Diorganotin(IV) complexes with hydrazone ligands

For many years, organotin(IV) complexes have been used in industries and biology, due to its anticancer behavior (Nikolova-Mladenova et al., 2009), antifungal properties (Piver, 1973), antitumor behavior (Ahmad et al., 2007; Koch et al., 2008), as well as pharmaceutical benefits (Wang et al., 2010).

University of Malaya

Dey et al., (2011) have synthesized three diorganotin(IV) complexes from the corresponding diorganotin(IV) dichlorides (Me_2SnCl_2, n-Bu_2SnCl_2, Ph_2SnCl_2) and ligand *N*'-(2-hydroxy-3-methoxy-benzylidene)benzohydrazide (I). The ligand can either act as a monobasic bidentate (I-A), monobasic tridentate (I-B) or dibasic tridentate (I-C) chelator, as illustrated in Figure 2.4. The ligand can undergo keto-enol tautomerism. But from the IR spectra of the ligand, it exists in the keto form in the solid state as there is a band at 1669 cm^{-1} for an amido carbonyl ν(C=O) vibration and consistent with the formation of an imine bond. In all three complexes Dey et al., (2011) have not found any -O-H and C=O stretching bands, which show that the ligand is coordinated to the metal in its deprotonated enol form.

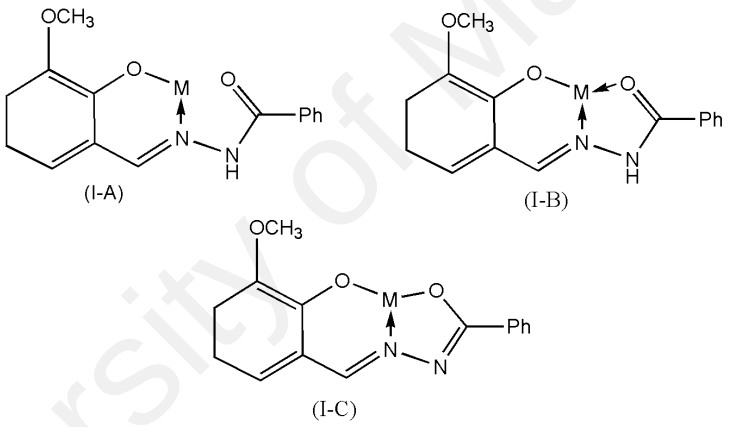

Figure 2.4: Three potential binding modes of the ligand, *N*'-(2-hydroxy-3-methoxy-benzylidene)benzohydrazide (I)

The diorganotin(IV) complexes of 2-hydroxy-1-naphthaldehyde-5-chloro-2-hydroxybenzoylhydrazone as shown in Figure 2.5 are selective against cells, while the type of alkyl groups attached to the organotin(IV) moiety affects antitumor activity. The dimethyltin(IV) **1** and diphenyltin(IV) **2** are monomeric structures, where the tin(IV) center is coordinated with the enolic tridentate ligand (L) in the *O,N,O* chelate mode. They exhibit five-coordinated trigonal bipyramidal geometry. While dibutyltin(IV) complex **3** exists as a rare one-dimensional chain polymeric structure but its coordination of tin(IV) is the same with complex **1** and **2** (Hong et al., 2013a).

University of Malaya

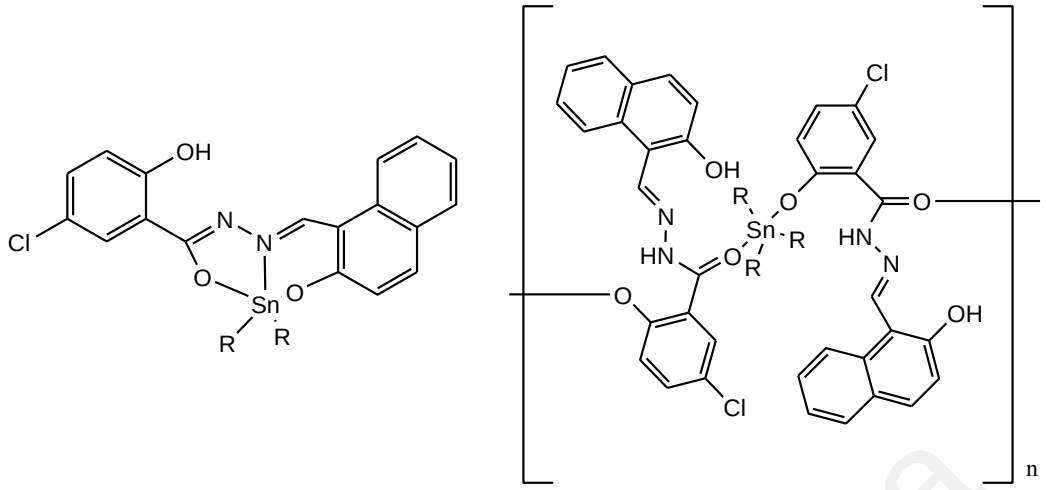

R = Me (**1**); Ph (**2**) R = Bu (**3**)

Figure 2.5: Structure of diorganotin(IV) complexes of 2-hydroxy-1-naphthaldehyde-5-chloro-2-hydroxybenzoylhydrazone

The diorganotin(IV) complexes derived from (E)-*N*'-[1-(5-bromo-2-hydroxyphenyl)ethylidene]-3-hydroxy-2-naphthohydrazide (H_2L1) and (E)-*N*'-[1-(5-chloro-2-hydroxyphenyl)ethylidene]-3-hydroxy-2-naphthohydrazide (H_2L2) ligands have been reported to possess excellent anticancer capabilities. The ligands still displayed good cytotoxic activities towards all of the tested cell lines, with an IC_{50} value below 8 μg mL^{-1} compared to some diorganotin(IV) complexes that have exceeded 30 μg mL^{-1}. The cytotoxic activities of the ligands are more or less good compared with the cytotoxicity of cisplatin which it IC_{50} value is 5 μg mL^{-1}. Cisplatin is the positive reference standard in the study. The trend of the cytotoxic activities among the diorganotin(IV) decreases in the following order: dibutyltin(IV) > dicyclohexyltin(IV) > dibenzyltin(IV) > di(*p*-chlorobenzyl)tin(IV) > di(*o*-chlorobenzyl)tin(IV) > diphenyltin(IV) derivatives. As seen here, the type of alkyl group attached to tin(IV) atom is crucial towards cytotoxic activities (Lee et al., 2013).

University of Malaya

2.3.2 Transition metal and other metal complexes with hydrazone ligands

The transition metal is an element whose atom has a partially filled *d* sub-shell, or those that can give rise to cations with an incomplete *d* sub-shell. Transition metal complexes are studied due to their fascinating properties, such as copper(II), nickel(II), cobalt(II), manganese(II) and vanadium(IV) oxide especially for its anticancer (Dhahagani et al., 2014; El-Tabl et al., 2015), cytotoxicity of brine shrimp bioassay (Bagihalli et al., 2008), antimicrobial (Mohamed et al., 2006), antibacterial (Devi et al., 2012) and antiviral activities and catalytic activity in the oxygenation of alkene (Kumar et al., 2009). Metal such as zinc(II) or cadmium(II) is not a transition metal because it forms only ions of +2 charge with fully filled 3d electrons. The metals are able to form positively charged ions in an aqueous solution that can bind with negatively charged biological molecules (Haas & Franz, 2009).

In 2015, new metal complexes are synthesized, such as copper(II), nickel(II), cobalt(II), manganese(II), zinc(II), cadmium(II), mercury(II), and iron(III) derived from 2-hydroxy-3-(hydroxyimino)-4-oxopentan-2-ylidene)benzohydrazide. The cytotoxic activity of the ligand and its metal complexes demonstrated potent cytotoxicity activity against the growth of human liver cancer (HepG2) cell lines compared to that of the standard drug Sorafenib (Nexavar). The copper complex reported the highest cytotoxicity activity, with an IC_{50} value of 2.24 μM (El-tabl et al., 2015).

Tweedy's chelation theory explained biological behavior seems affected by changes to the anion, coordination sites, and the nature of the metal ion. The cytotoxicity activity of the complexes could be due to the central metal atom, while chelation could help a complex cross a cell membrane (Tweedy, 1964). The cytotoxicity activity of the ligand and complexes are commonly compared, and in many cases, it was reported that metal chelates exhibit better biological activities compared to their ligands (Prasad et al., 2011).

University of Malaya

2.4 Metal complexes with *tris*(hydroxymethyl)aminomethane (TRIS) ligands

TRIS is probably the most common biochemical buffer used on its own, or in combination with other buffers. It has also been adopted as a ligand for the synthesis of chromatographic adsorbents. It is stable, unreactive, and compatible with most proteins and other biomolecules. It is also nontoxic and has medicinal properties (Bui et al., 2010; Nagaj et al., 2013). TRIS exhibited excellent catalytic activity (Sui et al., 2007), and it successfully treated a tumor-induced lactic acidosis (Sundaramurthy et al., 2016). TRIS alone has some substantial capabilities, and has been utilized in many applications.

TRIS contains a primary aliphatic amine nitrogen separated from the alkoxy or alcoholic functional groups by two carbon atoms as shown in Figure 2.6. It can lead to the formation of one or two chelate rings, composed of five members, each with geometries of trigonal bipyramidal formed by seven complexes as reported (Dotson, 1972).

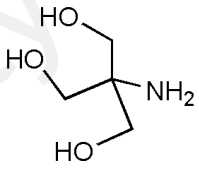

Figure 2.6: *Tris*(hydroxymethyl)aminomethane (TRIS)

Condensation with the carbonyl groups of ketones or aldehydes is possible due to the presence of the amino group, which leads to changes in its physicochemical and biological properties, making it an effective method for treating acidosis in acute lung injuries (Kallet et al., 2000). The ligand of TRIS produces brightly colored, air-stable, crystalline complexes with the first-row bi-and trivalent transition and representative metal salts from manganese to zinc (Dotson, 1972). Martinez et al., (2011) figured out that the structures of a series of Schiff bases generated from TRIS and salicylaldehydes holding different substituents were all enamine tautomers in the solid state. Example of TRIS ligand which was compound 20 as shown in Figure 2.7.

University of Malaya

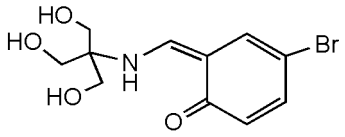

Figure 2.7: Compound 20 in solution exhibits an enamine structure

Wang (2002) synthesized oxovanadium derivatives, an example being V_2O_2{naphthalylidene[hydroxymethyl-*bis*(oxymethyl)]-aminomethane}$_2$ complex derived from the TRIS ligand. Toxicity tests were carried out by incubating transformed fibroblasts from mice with solutions of vanadium complexes for 12, 24, and 36 hours. The results reported that the toxicity increases with increasing exposure time of the cells, while it decreases with decreasing concentration. Also, most vanadium compounds are toxic at c(V) = 1 mM.

Odabasoglu et al., (2007) prepared several new substituted polyhydroxy azo-azomethine compounds from reacting TRIS with (E)-2-hydroxy-5-(phenyldiazenyl)benzaldehyde and its substituted derivatives. The derivative compounds were studied *in vitro* to determine their antimicrobial properties. The result showed that the compounds exhibited a strong antimicrobial activity against gram-positive bacteria, mold, and yeast.

In 2014, complexes of zinc with ligands were prepared *via* the reduction of Schiff bases derived from salicylaldehyde and TRIS. The structure was proposed as a model of the active site of the zinc enzyme *Aeromonas Proteolytica* aminopeptidase. This is because zinc(+2) was in a 5-coordinate sphere, one of the nitrogen atoms was bound to each zinc(+2) along with four oxygen atoms, and finally, there was an acetate ligand bridging two zinc ions (Abu-Sbeih & Abu-Yamin, 2014).

In 2015, diorganotin(IV) complexes with TRIS Schiff bases were synthesized and tested against three cancer cell lines namely colon, ovarian, and breast. The cytotoxicity

University of Malaya

activities of the diorganotin(IV) complexes of the dibutyltin(IV) and dicyclohexyltin(IV) derivatives were remarkable and exhibited excellent cytotoxic activities (Lee et al., 2015).

2.5 Anticancer drug administration

The anticancer drugs will be administered into the human body *via* several routes, such as injection, orally ingestion, and inhalation, among others. The drugs will be enhanced, and the side effects will be reduced by encapsulating it in drug carriers, such as niosome.

The purpose of a drug delivery system is to enhance or facilitate the action of therapeutic compounds. Ideally, the system is expected to deliver the drug to the site of action at designated rates, time, and volume to maximize the desired therapeutic response (Hillery et al., 2005).

Anticancer drugs are introduced into the body *via* several routes. They may be taken by mouth (orally) (Akbari & Javar, 2013), injected into muscles intramuscularly (IM) (Adiseshaiah et al., 2010), by injection into a vein intravenously (IV) (Dhand et al., 2014), an injection beneath the skin subcutaneously (SC) (Nair et al., 2008) as shown in Figure 2.8. Each route comes with its own specific purposes, advantages, and disadvantages.

Oral delivery of the drug is the most convenient, safest, least expensive, and most commonly used method (Hua, 2014). Many drugs can be administered orally in the form of liquids, tablets, capsules, and chewable tablets. Food and other drugs in the digestive tract may affect the rate at which the drug is absorbed when taken orally (Vasconcelos et al., 2007). This route meets its limitation when a person cannot consume medication orally, or when a drug must be administered quickly or in an exact or very high dosage, and when a drug is poorly or erratically absorbed from the digestive tract. This

University of Malaya

administration has several potential advantages, such as convenience and its much lower cost (Sharma & Saltz, 2000).

Examples of administration *via* injection include IV, IM, and SC (Jin et al., 2015). A needle is inserted directly into the vein for the IV route. The drug will be liquid, and the test subject will be given a single dose or a continuous infusion. The solution moves through a thin flexible tubing to a tube inserted in a vein, most often in the forearm *via* infusion with the help of an infusion pump. The IV infusion pumps offer hard-and soft-dose limits and safety practice guidelines to help keep the medication administration safe (Doyle & McCutcheon, 2016). The veins are relatively insensitive to irritation by irritant drugs at higher concentrations. This route may be unsuitable for an obese person, as inserting a needle into a vein would be difficult.

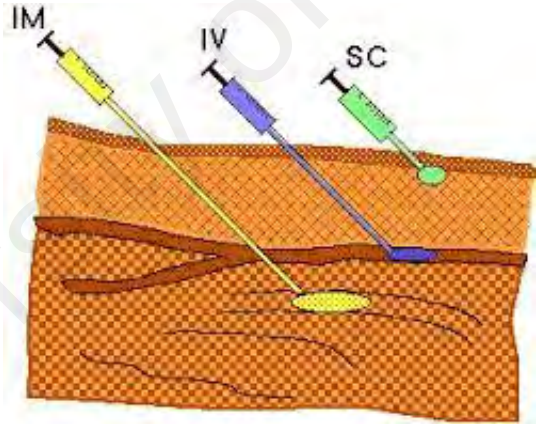

Figure 2.8: Insertion of needle for each type of parenteral such as IM, IV and SC (Bourne, 2001)

For the SC route, a needle is inserted into the fatty tissue just beneath the skin (Nair et al., 2008). This route is used for many protein drugs because if they were taken orally, the drugs would be eliminated in the digestive tract. The IM route is preferred over the SC route in the case of larger volumes of drugs is needed. The skeletal muscles also have fewer pain-sensing nerves compared to the subcutaneous tissue (Hunter, 2008).

University of Malaya

Among the three injection routes, IV is better at delivering a precise dose quickly and in a well-controlled manner throughout the body. Drugs are delivered immediately to the bloodstream and tend to take effect more quickly. Normally, anticancer agents do not always reliably differentiate between cancerous and normal cells. This certainly limits the maximum allowable dose of the drug. Moreover, administration of large quantities of drugs will result in its rapid elimination and widespread distribution into targeted organs and tissues, which is not economical, and the outcomes frequently show undesirable toxicity (Sinha et al., 2006). If the injection of the drug is repeated at the same site, it could damage the veins and skin, while also causing ulceration, swellings, and collapsed veins (Nair et al., 2008). In some cases, finding a vein will be difficult; the injector may choose dangerous sites, such as the femoral vein in the groin, or the fine blood vessels in the fingers or toes. A cancer drug is administered through injection to the targeted organ with the help of drug carrier, which is expected to enhance its effects. Drbohlavova et al., (2013) explained that the choice of a delivery route depends on a few factors such as i) patient acceptance, ii) properties of the drug including its solubility, iii) access to a disease location, or iv) effectiveness in dealing with specific diseases.

Administering anticancer drugs in its pure form would result in side effects, therefore, they are administered separately to allow large amounts to work in short periods of time. A drug carrier helps reduce the side effects of cancer treatment, as it allows for a sustained release of the drugs (Morsy, 2014). Many researchers are interested in nanoparticle vesicular systems, such as liposomes and niosomes. The drug encapsulation in nanocarriers provides better bioavailability, biocompatibility, and therefore potential use in pharmaceuticals (Drbohlavova et al., 2013). The vesicular formulations are expected to reduce toxicity and increase accumulation at target sites (Verma et al., 2010).

University of Malaya

2.5.1 Drug carriers

Drug carriers are compounds that act as a vehicle for drug molecules, allowing for targeted delivery, controlled release, and increased the efficiency of drug delivery. This is made possible *via* slight structural modifications (Gujral et al., 2013). There are many drug carriers that act as a buffer to reduce the toxic effects of medications in the human body. They consist of natural and synthetic compounds from a variety of sources, ranging from lipids to nanoparticles, including vesicles (De Jong & Borm, 2008). The active ingredient is not consumed in its pure form, instead, it is coated and used as fillers, which helps enhance its delivery. Drug carriers can also change the way a drug acts in the body, as it controls where the drug travels to and how it reacts once it arrives at a certain site. Encapsulation of a drug will prevent undesirable side effects and increase bioavailability and fraction of the drug accumulated in the pathological area of control (Torchilin, 2006).

The formation of colloidal drug carriers, such as niosome, liposome, and others involve surfactants. The surfactants consist of a positive cationic charge and negative anionic charge. The lack of charges means that the surfactants are nonionic, while surfactants with both cationic and anionic centers attached to the same molecules are called zwitterionic.

2.5.2 Types of surfactants

The surfactant or surface active agent is a chemical compound exhibiting surface activity when dissolved in a liquid (water). It lowers the surface tension or interfacial tension *via* preferred adsorption at the liquid or vapors surface or interfaces (Rosen & Kunjappu, 2012). There are two types of surfactants: natural biosurfactants produced by yeast or bacteria such as spingonmyeline, and synthetics surfactant, which is industrially produced, such as Tween-80 (Pei et al., 2010). There are several classes of surfactants, namely cationic, anionic, nonionic, and amphoteric.

University of Malaya

Generally, surfactants play a vital role in modern pharmaceutical biotechnology, since they are largely utilized in various drug dosage forms to control stability, wetting, and bioavailability, among other properties. In terms of biological significance, it is used for cell-to-cell adhesion or interaction, drug delivery system, digestion system, and synovial fluids (joint lubrication). The capacity of surfactants in solubilizing drugs depends on numerous factors, such as a chemical structure of the surfactant, chemical structure of the drug, temperature, pH, ionic strength, and surface charges (Lavasanifar et al., 2002; Torchilin, 2006). Surface charges are known to induce different effects. The positive surface charge could support better interactions with a cell membrane and internalization, but it is more toxic to cells (Rosen & Kunjappu, 2012). The neutral surface charge results in increased circulation time and the inhibition of plasma protein adsorption on the particle surface, while negative charges have weak cell adsorption of particles and lower toxicity.

(a) Cationic surfactants

Cationic dissociate in aqueous solution and act as a carrier of the surface-active properties. Cationic have the ability to adsorb on negatively charged surfaces such as hairs and fibers. Cationic surfactants are in general more expensive than anionic surfactants, and the former is only used in specific applications, such as those that require positive charges or bactericidal actions. Examples of the cationic surfactant include quaternary ammonium salts, amines with amide linkages, and polyoxyethylene alkyl, and alicyclic amines (Kronberg et al., 2014).

(b) Anionic surfactants

Anionics are compounds that also dissociate in solution into a negatively charged ion (anion), carrying the surface activity and a positively charged ion (cation), such as for

University of Malaya

instance carboxylates, sulfonates, alkylbenzene sulfonate, and sulfated natural oils and fats (Salager, 2002; Rosen & Kunjappu, 2012).

(c) Nonionic surfactants

The nonionic surfactant cannot dissociate into ions but are soluble in water due to the presence of polar groups. Example of nonionic includes ethoxylated aliphatic alcohol, Tween-80, carboxylic esters, polyethylene glycol esters, carboxylic amides, and polyoxyethylene fatty acid amides (Salager, 2002; Rosen & Kunjappu, 2012).

(d) Amphoteric surfactants

Those surfactants that change their charge with pH. They contain both acidic and basic hydrophilic moiety in their surfaces, such as n-cocamide ethyl-n-hydroxyethylglycine and a sodium salt (Salager, 2002; Rosen & Kunjappu, 2012).

2.5.3 Vesicular system

The main purpose of drug delivery systems is to efficiently deliver the essential amounts of drugs to the targeted site for a set period of time. There are several types of drug carriers, such as nanoparticles, microsphere, polymeric micelles, and vesicular. Meanwhile, the vesicular system are divided into niosome, liposomes, cubosomes, and hexosomes, which are used to improve the therapeutic index of both known and new drug molecules by encapsulating an active ingredient inside the vesicular structure (Jadhav et al., 2011). This research considers suitable preparation methods of niosomes.

2.5.3.1 Niosome

Niosomes are a nonionic surfactants vesicular system (example; alkyl ethers and alkyl esters). The inner structure of niosome is shown in Figure 2.9. They are unilamellar or multilamellar vesicles, depending on the preparation method used, obtained through hydration or synthetic nonionic surfactants, with or without the combination of other

University of Malaya

lipids or cholesterol. The size of niosomes is very small and microscopic, mostly in the nanometer region (Makeshwar & Wasankar, 2013). The vesicular systems of niosomes are similar to liposomes and can be used as carriers of hydrophilic and lipophilic drugs. The medication of niosome, as a novel drug delivery system, is encapsulated in a vesicle. The vesicle holds hydrophilic drugs within the space enclosed in the vesicle, while hydrophobic drugs are embedded within the bilayer itself (Verma et al., 2010). A niosome can be classified into three categories, such as a function of the number of bilayers, size, or the method of preparation. Niosomes, as a delivery material, has been studied for the delivery of anticancer, anti-inflammatory, antitubercular, and hormonal drugs, and oral vaccines (Manosroi et al., 2003).

Niosomes are made up of a variety of amphiphiles bearing sugar, polyoxyethylene, polyglycerol, polysorbate, or Tween (20, 40, 60, 80), sorbitans or Span (20, 40, 60, 80, 85), crown ether and amino acid hydrophilic head groups. These amphiphiles typically possess one to two hydrophobic alkyl, perfluoroalkyl, or steroidal groups (Kumar & Rajeshwarrao, 2011).

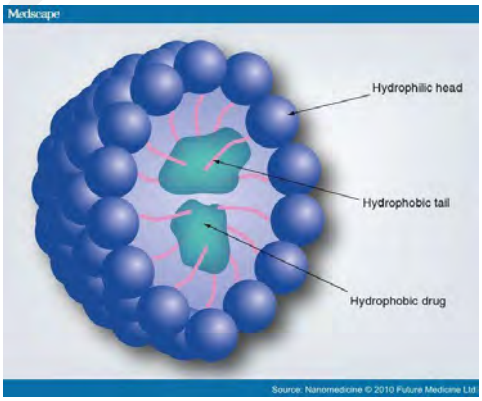

Figure 2.9: The inner structure of niosome (Bei et al., 2010)

2.5.3.2 Liposome

A liposome is composed of either synthetic or natural phospholipids (Dhamecha et al., 2009). It is a vesicular structure, consisting of hydrated lipid bilayers that can incorporate

University of Malaya

hydrophilic, hydrophobic, and amphiphilic compounds. A liposome is formed in a variety of sizes, as unilamellar or multilamellar construction. Its name is related to its structural building blocks, such as phospholipids, instead of its size. Liposome's size can vary from very small (0.025 μm) to large (2.5 μm) vesicles (Akbarzadeh et al., 2013). It is a tiny bubble (vesicle), made out of the same material as a cell's membrane. Liposomes are formed when thin lipid films or lipid cakes are hydrated and stacks of liquid crystalline bilayers become fluid and swell. During agitation, the hydrated lipid sheets detach and self-associate to form vesicles, which prevents water from interacting with the hydrocarbon core of the bilayer at the edges (Verma et al., 2010).

Liposomes can be used as carriers for numerous molecules in the cosmetic and pharmaceutical industries. Applications of the liposome include drugs, enzymes, and other biologically active molecules, which can also be used in antimicrobial, antifungal, and antiviral therapies. Liposomes can trap both hydrophobic and hydrophilic compounds, avoid decomposition of the entrapped combinations, and release the entrapped molecules at designated targets (Akbarzadeh et al., 2013). There are three types of the vesicles, which are multilamellar vesicle (MLV): > 500 nm, a large unilamellar vesicle (LUV): > 100 nm; and small unilamellar vesicle (SUV): 20 - 100 nm (Laouini et al., 2012).

2.5.3.3 Cubosome

Cubosomes are self-assembling cubic crystals of certain detergents with an intersecting network of water channels (Madni et al., 2014). According to Shinde et al., (2012) cubosomes are single crystal structures with visible unilamellar vesicles, bicontinuous cubic lamellar, and liquid crystalline phase particles. Cubosomes consist of honeycombed (cavernous) structures separating two internal aqueous channels and a large interfacial area. They exhibit different internal cubic structure and compositions with

University of Malaya

different drug-loading modalities. Cubosomes are nanoparticles with diameters of 10 - 500 nm. Some of its advantages include high drug payloads due to the high internal surface area and cubic crystalline structures, the biodegradability of lipids, and the ability to encapsulate hydrophobic, hydrophilic, and amphiphilic substances, a relatively simple preparation method, and the targeting and controlled release of bioactive agents. Several applications of cubosome include in melanoma (cancer) therapy and the cubic phases, which are more bioadhesives in nature, making them convenient for topical use, mucosal depositions, and the delivery of multiple drugs (Thadanki et al., 2011).

2.5.3.4 Hexosome

Hexosomes are submicron sized particles containing internally inverted type hexagonal liquid crystal-line phases (HII), which are dispersed in a continuous aqueous medium. Hexosomes (dispersed HII phases), due to their special structural properties, can be used as an alternative delivery vehicle for pharmaceuticals. Biologically active molecules can either be accommodated within the aqueous domains or can be directly coupled to the lipid hydrophobic moieties oriented radially outwards from the core of the water rods. These special properties of hexosomes render them usable for improving the solubility of poorly water-soluble drugs and transport therapeutic peptides and proteins *via* transdermal, oral, and parenteral routes (Hirlekar et al., 2010). Some of its advantages include its ability to solubilize, encapsulate, and transport active pharmaceutical ingredients, high drug loading, and its inherently enhanced stability (Revathi & Dhanaraju, 2014). Several therapeutic applications of hexosome are the transmucosal delivery of hormones, transdermal delivery of peptide, delivery of the anticancer agent, and parenteral sustained drug delivery system (Hirlekar et al., 2010).

University of Malaya

2.5.3.5 Niosome as a preferable drug carrier

The selection and types of drug carrier depend primarily on the type of drug, type of disease in which the system is being used, and the targeted area (Gujral et al., 2013).

For the active ingredient, which is hydrophobic drugs, in this case, it is embedded within the bilayer itself. The chemical stability and relatively low cost of the materials used to prepare niosomes made these vesicles more attractive than liposomes for industrial production, both in pharmaceutical and cosmetic applications (Stan et al., 2013). Other reasons include the fact that the prepared niosomes are assumed to be more chemically stable surfactants compared to that of phospholipids. The phospholipids in niosome are easily hydrolyzed due to the presence of ester bonds (Shinde et al., 2012). It has several advantages, such as its surfactants being biodegradable, biocompatible, and nonimmunogenic. It can also improve the performance of the drug molecules, and the vesicles can act as a depot to slowly release the drug *via* controlled release. Characteristics such as size and lamellarity of the vesicle can vary depending on the requirement, handling, and storage of surfactants, which do not require any special conditions and can be used for oral, parenteral, as well as topical applications (Makeshwar & Wasankar, 2013).

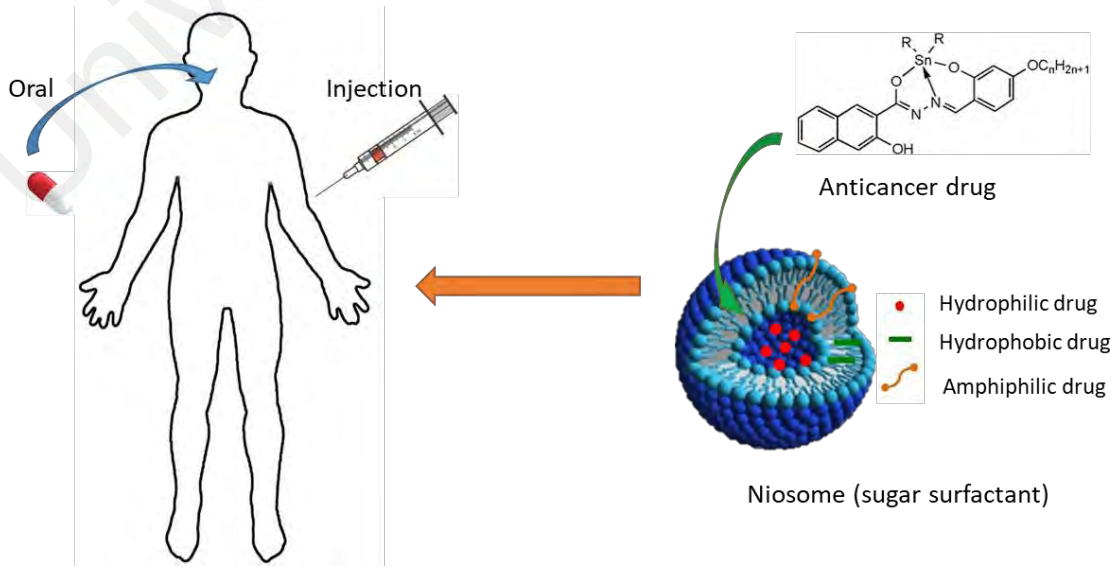

Figure 2.10: Graphical abstract of niosome in drug delivery

University of Malaya

A smaller drug carrier size is preferred for anticancer purposes, due to its slow drug release. Moreover, the anticancer drug is administered *via* IV injection, making a small size drug carrier vital. When administered *via* IV injection as shown in Figure 2.10, using niosomes to encapsulate the drugs help reduce toxicity without decreasing the drug's potency. Hence, the best approach in this work is to synthesize small vesicles *via* two methods which are the microencapsulation vesicle method will produce a vesicle that size below 300 nm and by using ethanol injection method it can reduce the size more to below 200 nm.

2.5.4 Factors affecting the characteristic of the drug carrier

There are several factors that affect drug carrier size and shapes, such as pH, temperatures, types of solvent, and methods of preparation. The drug solubility increases with increasing pH, due to the increase in the ionized form of the drug. The temperature of the hydration medium has a significant role in the formation of vesicles and their subsequent shapes and sizes. The temperature is supposedly always above the gel-to-liquid phase transition temperature of the system. Temperature affects the assembly of surfactants into vesicles and also induces changes in the vesicle's shape (Kumar & Rajeshwarrao, 2011). Entrapping drugs in vesicle increases its size, probably due to the interaction of a solute with the surfactant head groups, increasing the charge and mutual repulsion of the surfactant bilayers (Akhilesh et al., 2012).

The physical properties and structure of niosomes are affected by cholesterol where cholesterol increases its hydrodynamic diameter and entrapment efficiency (Akhilesh et al., 2012) due to its interaction with nonionic surfactants (Kumar & Rajeshwarrao, 2011). The size and shape of drug carriers determine whether or not a drug will interact with non-targeted organs and tissues (Liu, 2014). The size and charge of vesicles significantly affect the corresponding stability and drug encapsulation. Size and charge can be

University of Malaya

determined using a multifunctional zeta potential analyzer, where the size of the vesicles is the result of repulsion forces between the bilayers and entrapped drug (Kumar & Rajeshwarrao, 2011).

For example, the cationic niosomes will be larger due to the repulsion between the positive charges of the niosomes and the loaded drug. A smaller sized carrier, regardless of IV administration or direct injection, help avoid steric hindrance and can penetrate farther into the tumor to deliver their respective payloads. A net neutral charge on the carrier also allows it to penetrate up to three times farther than its charge bearing counterparts. A neutral charge improves the distribution of homogeneity within the tumor tissue (Liu, 2014). Accumulation in the lung will occur if particles are larger than 5 μm, due to the capillary filtration effect (Sato et al., 1996).

Besides having the advantage, some drug carrier also brings disadvantage to the host, namely Tween-80 which is believed to cause acute hepatitis and renal failure. While Cremophor EL will result in hypersensitivity reactions in human and animals. For IV administration, due to their surface activity, surfactant molecules can be hemolytic and have the potential to penetrate and disrupt biological membranes (Liu, 2008).

2.5.5 Preparation of drug carrier

Various methods to prepare drug carriers depends on its intended applications. The types of the method also play important roles in deciding the size and shape of the drug carrier, a number of bilayers, the lamellarity, the level of entrapment efficiency, and membrane permeability of the vesicle (Laouini et al., 2012; Akhilesh et al., 2012).

2.5.5.1 Microencapsulation vesicle (MCV) method

The MCV method has the advantage of being able to control the preparation conditions, such as the ambient temperature of each emulsification and the selection of the type of organic solvent. It can also produce niosomes with small particle sizes and

University of Malaya

efficiently encapsulate water-soluble material with good stability. A mixture of surfactants and drugs are dissolved in an organic solvent, then distilled water is added. The mixture is homogenized at 7000 rpm for 10 minutes to form a water-oil (w/o) emulsion. Then, the emulsion is stirred at 45 ^{o}C to form a water-oil-water (w/o/w) emulsion. Stirring will be continued for several hours until the organic solvent is evaporated (Nii & Ishii, 2005).

2.5.5.2 Ethanol injection method

A solution of the surfactant is dissolved using ethanol. The surfactant mixture in ethanol is injected through the 14-gauge needle into warm water containing the drug and stored at 60 ^{o}C. Niosomes in the form of the large unilamellar vesicle (LUV) are synthesized, and the diameter was 50 - 1000 μm (Jaafar-Maalej, 2010).

2.5.5.3 Sonication method

The aqueous phase is added into a mixture of surfactant and cholesterol in a glass vial. The mixture is probe-sonicated at 60 °C for 3 minutes using a sonicator to yield a small unilamellar vesicle (SUV) niosomes (Madhav et al., 2011).

2.5.5.4 Hydration of thin lipid film method

A mixture of phospholipid and cholesterol are dispersed in volatile organic solvents such as chloroform or diethyl ether. Then, the organic solvent is removed using a rotary evaporator at reduced pressure. Finally, by adding an aqueous buffer solution under agitation at a temperature above the lipid transition temperature, the dry lipidic film deposited on the flask wall is hydrated, leaving behind multilamellar vesicle (MLV) niosomes (Makeshwar & Wasankar, 2013).

University of Malaya

2.6 Characterization of vesicle

Characterizing niosome is needed to determine its viability for clinical applications, encompassing parameters such as encapsulation efficiency, size, polydispersity index (PDI), morphology, zeta potential, and release rate of the drug.

2.6.1 Entrapment efficiency

Entrapment efficiency (%EE) is defined as drug encapsulated in the bilayer of the drug vehicle (Yassin et al., 2010). After the niosomal dispersion is prepared, the unentrapped drug is separated by dialysis, centrifugation, or gel filtration, while the remaining entrapped drug in niosomes is determined by complete vesicle disruption using 50% n-propanol or 0.1% Triton X-100. Ultracentrifugation can also be used for the separation of the unentrapped drug, while the supernatant was removed and sediment washed twice with distilled water to remove any absorbed drug (Akhilesh et al., 2012). The resultant solution is analyzed by an assay method that is responsive to the drug. The loaded and free drug concentrations can be determined using a UV-Vis spectrophotometer (Mehta & Jindal, 2013) or high-performance liquid chromatography (HPLC) (Waddad et al., 2013), where the percentage of entrapment efficiency (%EE, amount of drug entrapped / total amount of drug) × 100 % (Makeshwar & Wasankar, 2013). Entrapment efficiency of niosomes is significantly affected by the pH of the hydration medium. At lower pH, niosome formulations should be examined using an optical microscope to confirm the presence of drug precipitates both before and after centrifugation and washing to determine the concentration of the drug (Kumar & Rajeshwarrao, 2011).

2.6.2 Size, shape and morphology

The size of the vesicle size falls between 20 nm - 50 μm. The structure of surfactant-based vesicles is visualized and established using freeze-fracture microscopy, while photon correlation spectroscopy was used to determine the average diameter of the vesicles. Volume dispersion of niosomes can be determined using a coulter counter

University of Malaya

(>1 μm) (Makeshwar & Wasankar, 2013). Vesicles in the submicron range can be detected using electron microscopy or dynamic light scattering (DLS) techniques. The former is used to study the morphology of the vesicles, while the latter is generally used to determine the size distribution, mean surface diameter, and mass distribution of niosomes. Electron microscopic analysis, such as transmission electron microscopy (TEM) or freeze-fracture techniques are used to determine the size of niosomes and the number of bilayers. Another instrument that can be used for this purpose includes scanning electron microscopy (SEM). Atomic force microscopy (AFM) and cryo-TEM can be used to determine the shape and surface properties of niosomes (Akhilesh et al., 2012).

2.6.3 Vesicle charge

The zeta potential can be used to estimate the storage stability of colloidal dispersions. Zeta potential values above 30 mV (positive or negative values) lead to more stable nanocapsule suspensions due to the absence of aggregation when there is repulsion between the particles (Torchilin, 2006). The zeta potential can be defined as the difference between the bulk solution (dispersing medium) and the surface of the hydrodynamic shear (slipping plane). It can be used to optimize the nanoparticle formulation for long-term stability (Sreelola & Sailaja, 2014). The vesicle surface charge is crucial towards the behavior of niosomes *in vivo* and *in vitro*. Basically, charged niosomes are more stable against aggregation and fusion compared to uncharged vesicles. The zeta potential of individual niosomes can be measured by microelectrophoresis to obtain an estimation of the surface potential. An alternative approach is to use pH-sensitive fluorophores. Dynamic light scattering (DLS) is frequently used to measure the zeta potential of niosomes (Kumar & Rajeshwarrao, 2011; Akhilesh et al., 2012).

University of Malaya

2.6.4 *In-vitro* release

An important factor that helps develop a successful formulation is drug release from a nanoparticle or a vesicular system. Numerous targeted and controlled release drug delivery systems have been developed for this purpose. Controlled release is one of the basic points of drug delivery, which aims to release a drug into a patient's body at a predetermined rate, or with specific release profiles at specific times (Torchilin, 2006). A method of *in-vitro* release rate study includes the use of dialysis tubing. A dialysis tube is washed and soaked in distilled water. The vesicle suspension is pipetted or injected into a bag made up of the tubing and sealed using threads. The bag containing the vesicles is placed in a 100 ml of buffer solution in a 100 ml beaker, which is constantly stirred at 25 °C or 37 °C. At various time intervals, the buffer is analyzed for drug content by a suitable assay method (Kumar & Rajeshwarrao, 2011).

University of Malaya

CHAPTER 3: EXPERIMENTAL

3.1 Materials

The materials used in this work are listed in **3.1.1**, which include chemicals that were commercially obtained, and **3.1.2**, which were the materials needed in anticancer study and materials for preparation and formulation of anticancer drugs. The details of the list of complexes and materials as well as how the complexes will be used later are explained in point **1A**, **1B** and **2**.

3.1.1 Materials for synthesis and characterization of new complexes

Reagent grade 2,4-dihydroxybenzaldehyde and 3-hydroxy-2-naphthoic hydrazide were obtained from Aldrich, *tris*(hydroxymethyl)aminomethane was obtained from TCI Mark, and triethylamine was purchased from Fluka. Chemicals 1-bromodecane, 1-bromododecane, and dimethyltin(IV) dichloride were purchased from Merck, while dibutyltin(IV) dichloride was obtained from Fluka. Magnesium sulfate and potassium iodide were obtained from Systerm, while potassium carbonate was obtained from Sigma. For metal salts, cobalt(II) acetate tetrahydrate was purchased from JT Baker, nickel(II) acetate tetrahydrate was purchased from Unilab, while cadmium(II) acetate dihydrate, copper(II) acetate monohydrate, and zinc(II) acetate dihydrate were procured from Fluka and Merck, respectively.

3.1.2 Materials for preparation of anticancer drugs and drug carrier

The materials used in this research are divided into 2 parts: 1) Materials for anticancer activities that have 2 different ligands such as (**A**), which consists of NAH ligands and its diorganotin(IV) complexes, and NAH metal complexes, (**B**), which are TRIS ligands and its diorganotin(IV) complexes. 2) Materials for formulation study that are obtained from previous research (Lee, 2010). This selection is taken to compare their IC_{50} values with the new complexes synthesized in current research for their anticancer activities.

University of Malaya

1A) The structures of NAH ligands and its diorganotin(IV) complexes were shown in Figure 3.1 and NAH metal complexes were shown in Figure 3.2. List of NAH ligands and its diorganotin(IV) complexes, as well as NAH metal complexes, are presented in Table 3.1 and 3.2, respectively.

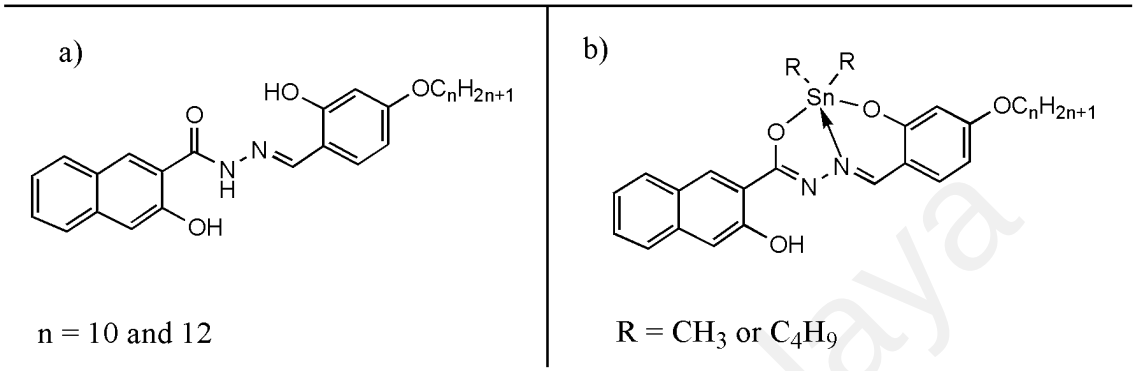

Figure 3.1: The general structure of (a) NAH ligands in keto form (more stable) and (b) its diorganotin(IV) complexes

Table 3.1: List of NAH ligands and its diorganotin(IV) complexes

Ligands/ Complexes	Empirical formula
n = 10; **NA**	$C_{28}H_{34}N_2O_4$
n = 12; **NB**	$C_{30}H_{38}N_2O_4$
R = Me, n = 10; **NA1**	$C_{30}H_{38}N_2O_4Sn$
R = Bu, n = 10; **NA2**	$C_{36}H_{50}N_2O_4Sn$
R = Me, n = 12; **NB1**	$C_{32}H_{42}N_2O_4Sn$
R = Bu, n = 12; **NB2**	$C_{38}H_{54}N_2O_4Sn$

University of Malaya

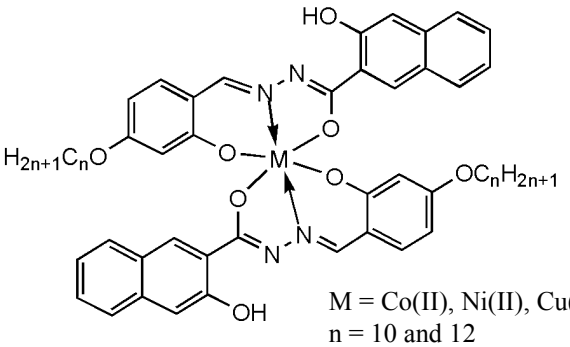

Figure 3.2: The general structure of NAH metal complexes

Table 3.2: List of NAH metal complexes

Complexes	Empirical formula
M = Co, n = 10; **CoNA**	$C_{56}H_{64}N_4O_8Co$
M = Ni, n = 10; **NiNA**	$C_{56}H_{64}N_4O_8Ni$
M = Cu, n = 10; **CuNA**	$C_{56}H_{64}N_4O_8Cu$
M = Zn, n = 10; **ZnNA**	$C_{56}H_{64}N_4O_8Zn$
M = Cd, n = 10; **CdNA**	$C_{56}H_{64}N_4O_8Cd$
M = Co, n = 12; **CoNB**	$C_{60}H_{72}N_4O_8Co$
M = Ni, n = 12; **NiNB**	$C_{60}H_{72}N_4O_8Ni$
M = Cu, n = 12; **CuNB**	$C_{60}H_{72}N_4O_8Cu$
M = Zn, n = 12; **ZnNB**	$C_{60}H_{72}N_4O_8Zn$
M = Cd, n = 12; **CdNB**	$C_{60}H_{72}N_4O_8Cd$

1B) The structures and the list of TRIS ligands and its diorganotin(IV) complexes are shown in Figure 3.3 and presented in Table 3.3 respectively.

a)

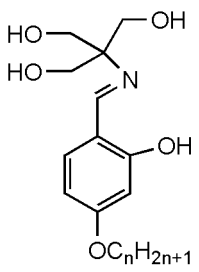

n = 10 and 12

b)

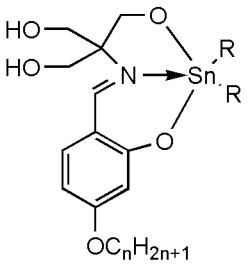

R = CH_3 or C_4H_9

Figure 3.3: The general structure of (a) TRIS ligand and (b) its diorganotin(IV) complexes

University of Malaya

Table 3.3 List of TRIS ligands and its diorganotin(IV) complexes

Ligands/ Complexes	Empirical formula
n = 10; **TA**	$C_{21}H_{35}NO_5$
n = 12; **TB**	$C_{23}H_{38}NO_5$
R = Me, n = 10; **TA1**	$C_{23}H_{39}NO_5Sn$
R = Bu, n = 10; **TA2**	$C_{29}H_{51}NO_5Sn$
R = Me, n = 12; **TB1**	$C_{25}H_{43}NO_5Sn$
R = Bu, n = 12; **TB2**	$C_{31}H_{55}NO_5Sn$

2) Materials used for formulation studies

The complexes used for formulation part are obtained from previous research (Lee, 2010) because as overall they showed better cytotoxicity compared with the current complexes in their anticancer activities. The structures of NAH and TRIS compounds are shown in Figure 3.4 and 3.5, respectively. The list of complexes are listed in Table 3.4 and 3.5. Glycolipid surfactant was synthesized in previous work (Hussen, 2010; Hussen, 2012), ethanol (95% purity) was purchased from J. Kollins Chemicals, and dichloromethane, (>99% purity) was procured from Merck.

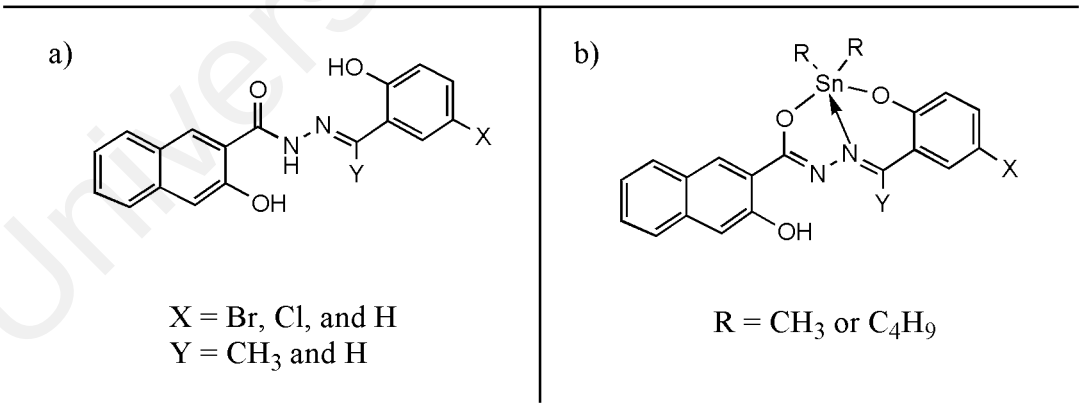

Figure 3.4: The general structure of (a) NAH ligands and (b) its diorganotin(IV) complexes from previous research (Lee et al., 2010)

University of Malaya

Table 3.4: List of NAH diorganotin(IV) complexes from previous research (Lee et al., 2010)

Complexes	Empirical formula
R = Me, X = Br, Y = H; **NC1**	$C_{20}H_{17}N_2O_3BrSn$
R = Bu, X = Br, Y = H; **NC2**	$C_{26}H_{29}N_2O_3BrSn$
R = Me, X = Cl, Y = H; **ND1**	$C_{20}H_{17}N_2O_3ClSn$
R = Bu, X = Cl, Y = H; **ND2**	$C_{26}H_{29}N_2O_3ClSn$
R = Me, X = Br, Y = CH_3; **NE1**	$C_{21}H_{19}N_2O_3BrSn$
R = Bu, X = Cl, Y = CH_3; **NF2**	$C_{27}H_{31}N_2O_3BrSn$

a)

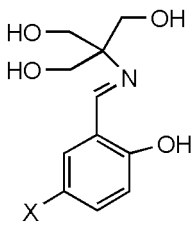

X = Cl and H

b)

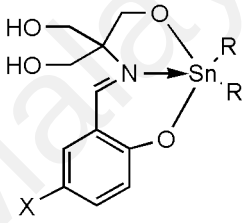

R = CH_3 or C_4H_9

Figure 3.5: The general structure of (a) TRIS ligand and (b) its diorganotin(IV) complexes from previous research (Lee et al., 2010)

Table 3.5: List of TRIS diorganotin(IV) complexes from previous research (Lee et al., 2010)

Complex	Empirical formula
R = Bu, X = Cl, **TC2**	$C_{19}H_{30}NO_5ClSn$

University of Malaya

3.2 Experimental methods

This subheading describes three different parts of the work. At the first part (**Part 1a**), the diorganotin(IV) complexes as potential anticancer drugs were synthesized through a condensation reaction. Then (**Part 1b**), all the samples prepared were analyzed using the Melt-Temp II, Infrared (IR) spectroscopy, Nuclear Magnetic Resonance (NMR) spectroscopy, Auto Magnetic Susceptibility Balance (for transition metal complexes), Single Crystal X-ray Diffraction (SCXRD) and elemental analyses to study their compounds characteristic. The next part (**Part 2),** the anticancer activities were studied to determine the IC_{50} values of ligands and its diorganotin(IV) complexes. In the last part (**Part 3**), niosome-encapsulated complex were studied using ultracentrifugation, ultraviolet-visible (UV-Vis) spectrophotometer, dynamic light scattering (DLS), field emission scanning electron microscopy (FESEM).

3.2.1 Part 1a: Preparation of compounds

3.2.1.1 Preparation of ligand precursor

(a) Preparation of 4-decyloxy-2-hydroxybenzaldehyde, SA

2,4-dihydroxybenzaldehyde (5.53 g, 40.00 mmol), potassium carbonate (5.53 g, 40.00 mmol), potassium iodide (6.64 g, 40.00 mmol) and 1-bromodecane (8.30 mL, 40.00 mmol) were mixed in 50 mL dimethylformamide (DMF). The mixture was heated under reflux for 4 hours by monitoring the thin layer chromatography (TLC) in hexane: ethyl acetate ratio of (8:2). The solution was then filtered while still hot to remove any insoluble solid. Diluted hydrochloric acid (HCl) was added to neutralize the warm solution, which was then extracted with diethyl ether. Subsequently, the combined organic fractions were dried over magnesium sulfate and evaporated to obtain a clear concentrated yellow liquid.

University of Malaya

(b) Preparation of 4-dodecyloxy-2-hydroxybenzaldehyde, SB

2,4-dihydroxybenzaldehyde (5.53 g, 40.00 mmol), potassium carbonate (5.53 g, 40.00 mmol), potassium iodide (6.64 g, 40.00 mmol), and 1-bromododecane (9.60 mL, 40.00 mmol) were mixed in 50 mL DMF. The mixture was then heated under reflux for 4 hours by monitoring the TLC in hexane: ethyl acetate ratio of (8:2). Thereafter, the solution was filtered while still hot to remove any insoluble solids. Diluted HCl acid was added to the solution and extracted with diethyl ether. The combined organic fractions were dried over magnesium sulfate and left to evaporate to obtain a clear concentrated yellow liquid.

3.2.1.2 Preparation of the ligands

(a) Preparation of N'-(4-decyloxy-2-oxidobenzylidene)-3-hydroxy-2-naphthohydrazide, NA

A solution of SA (0.23 g, 0.50 mmol) was added to 60 mL ethanolic solutions of 3-hydroxy-2-naphthoic hydrazide (0.20 g, 0.50 mmol) and was refluxed for 4 hours. The hot solution was filtered and a light yellow solid was obtained by cooling to room temperature.

(b) Preparation of N'-(4-dodecyloxy-2-oxidobenzylidene)-3-hydroxy-2-naphthohydrazide, NB

A solution of SB (0.25 g, 0.50 mmol) was added to 60 mL ethanolic solutions of 3-hydroxy-2-naphthoic hydrazide (0.20g, 0.50 mmol) and left to reflux for 4 hours. The hot solution was then filtered, and a light yellow solid was formed upon cooling to room temperature.

University of Malaya

(c) Preparation of [N'-(4-decyloxy-2-oxidobenzylidene)-2-(hydroxymethyl)-1,3-dihydroxypropane], TA

A solution of SA (1.39 g, 5.00 mmol) was added to 30 mL ethanolic solution of *tris*(hydroxymethyl)aminomethane (0.60 g, 5.00 mmol) and refluxed for 3 hours. The hot solution was then filtered, and a dark yellow thin flake was obtained upon cooling to room temperature. The solid was recrystallized with 1-propanol and ethanol. It was further washed with hexane in order to dry the wet solid.

d) Preparation of [N'-(4-dodecyloxy-2-oxidobenzylidene)-2-(hydroxymethyl)-1,3-dihydroxypropane], TB

A solution of SB (1.53 g, 5.00 mmol) was added to 30 mL ethanolic solutions of *tris*(hydroxymethyl)aminomethane (0.60 g, 5.00 mmol). The solution was reflux for 3 hours. Then, the hot solution was filtered, and a dark yellow thin flake was formed upon cooling the solution to room temperature. The solid was then recrystallized with 1-propanol and ethanol, and further condensed using hexane.

3.2.1.3 Preparation of diorganotin(IV) complexes

(a) Preparation of [N'-(4-decyloxy-2-oxidobenzylidene)-3-hydroxy-2-naphtho-hydrazidato]dimethyltin(IV), NA1

Compound NA (0.46 g, 1.00 mmol) and triethylamine (0.14 mL, 1.00 mmol) were heated in the mixture of ethyl acetate: dimethylformamide (10:1) under reflux for 1 hour. Dimethyltin(IV) dichloride (0.23 g, 1.00 mmol) was then added to a solution and the mixture was further refluxed for 5 hours. The mixture was filtered and the clear yellow solution was left to evaporate. The solid was recrystallized from a 2:1 mixture of chloroform: dimethylformamide. Yellow crystals were obtained by slow evaporation at room temperature.

University of Malaya

(b) Preparation of [N'-(4-decyloxy-2-oxidobenzylidene)-3-hydroxy-2-naphtho-hydrazidato]dibutyltin(IV), NA2

Compound NA (0.46 g, 1.00 mmol) and triethylamine (0.14 mL, 1.00 mmol) were heated in ethyl acetate: dimethylformamide at a ratio of (10:1) solvent mixture under reflux for 1 hour. Dibutyltin(IV) dichloride (0.32 g, 1.00 mmol) was then poured into the solution, and the mixture was refluxed for another 5 hours. The clear yellow solution was then filtered. It was left to evaporate, and the solid was recrystallized from a mixture of chloroform: dimethylformamide at a ratio of (2:1) to produce a yellow powder.

(c) Preparation of [N'-(4-dodecyloxy-2-oxidobenzylidene)-3-hydroxy-2-naphtho-hydrazidato]dimethyltin(IV), NB1

Compound NB (0.49 g, 1.00 mmol) and triethylamine (0.14 mL, 1.00 mmol) were added in the solvent mixture of ethyl acetate:dimethylformamide (3:1) under reflux for 1 hour. Dimethyltin(IV) dichloride (0.23 g, 1.00 mmol) was then added into the solution, and the mixture was further refluxed for 5 hours. The resulting clear yellow solution was then filtered and left to evaporate, resulting in a yellow powder.

(d) Preparation of [N'-(4-dodecyloxy-2-oxidobenzylidene)-3-hydroxy-2-naphtho-hydrazidato]dibutyltin(IV), NB2

Compound NB (0.49 g, 1.00 mmol) and triethylamine (0.14 mL, 1.00 mmol) were heated in a solvent mixture of ethanol:toluene:dimethylformamide (3:1:1) under reflux for 1 hour. Dibutyltin(IV) dichloride (0.323 g, 1.00 mmol) was added into the solution, and the mixture was further refluxed for 5 hours. The clear yellow solution was then filtered prior to being left to evaporate, resulting in a yellow powder.

University of Malaya

(e) Preparation of (2-{[1,1-bis(hydroxymethyl)-2-oxidoethyl]iminomethyl}-4-decyloxy-2-oxidobenzylidene)dimethyltin(IV), TA1

Compound TA (0.19 g, 0.50 mmol), and triethylamine (0.14 mL, 1.00 mmol) were mixed in a solvent mixture of ethanol: toluene: dimethylformamide at a ratio of (2:1:1) under reflux for 1 hour. Dimethyltin(IV) dichloride (0.11 g, 0.50 mmol) was then added to the solution, and the mixture was refluxed for another 3 hours. A clear orange solution was filtered and left to evaporate. A light brown powder was obtained after a few days.

(f) Preparation of (2-{[1,1-bis(hydroxymethyl)-2-oxidoethyl]iminomethyl}-4-decyloxy-2-oxidobenzylidene)dibutyltin(IV), TA2

Compound TA (0.19 g, 0.50 mmol), and triethylamine (0.14 mL, 1.00 mmol), were added in the solvent mixture of ethanol:toluene:dimethylformamide (2:1:1) under reflux for 1 hour. Dibutyltin(IV) dichloride (0.15 g, 0.50 mmol) was directly added into the solution, and the mixture was then refluxed for 4 hours. The clear orange solution was filtered, and the solution was left to evaporate. A black semi-solid was obtained even after a few days.

(g) Preparation of (2-{[1,1-bis(hydroxymethyl)-2-oxidoethyl]iminomethyl}-4-dodecyloxy-2-oxidobenzylidene)dimethyltin(IV), TB1

Compound TB (0.21 g, 0.50 mmol), and triethylamine (0.14 mL, 1.00 mmol), were mixed into a solvent mixture of ethanol:toluene:dimethylformamide (2:1:1) under reflux for 1 hour. Then, dimethyltin(IV) dichloride (0.11 g, 0.50 mmol) was directly added into the solution, and the mixture was refluxed for another 3 hours. The clear yellow solution was then filtered, and left to evaporate, resulting in a light brown powder.

University of Malaya

(h) Preparation of (2-{[1,1-bis(hydroxymethyl)-2-oxidoethyl]iminomethyl}-4-dodecyloxy-2-oxidobenzylidene)dibutyltin(IV), TB2

Compound TB (0.21 g, 1.00 mmol), and triethylamine (0.14 mL, 1.00 mmol), were added into the mixture solvent of ethanol:toluene:dimethylformamide (2:1:1) under reflux for 1 hour. Next, dibutyltin(IV) dichloride (0.15 g, 0.50 mmol) was poured into the solution, and the mixture was refluxed for another 4 hours. The clear yellow solution was filtered, and the solution was then left to evaporate, resulting in a black semi-solid.

3.2.1.4 Preparation of the metal complexes

(a) Preparation of bis[N'-(4-decyloxy-2-oxidobenzylidene)-3-hydroxy-2-naphtho-hydrazidato]cobalt(II), CoNA

Cobalt(II) acetate tetrahydrate (0.13 g, 0.50 mmol) was dissolved in 5 mL distilled water. Then, it was added to a mixture of ethyl acetate: dimethylformamide (3:1) solution of compound NA (0.46 g, 1.00 mmol). The mixture was then refluxed for 3 hours. A reddish brown precipitate was formed. A solid was obtained from filtration and dried (Kavitha et al., 2013). The solid was further recrystallized using 1,4-dioxane and 1-propanol.

(b) Preparation of bis[N'-(4-decyloxy-2-oxidobenzylidene)-3-hydroxy-2-naphtho-hydrazidato]nickel(II), NiNA

Nickel(II) acetate tetrahydrate (0.12 g, 0.50 mmol) was dissolved in 10 mL distilled water and poured into a mixture of ethyl acetate: dimethylformamide (3:1) solution of compound NA (0.46 g, 1.00 mmol). The mixture was then refluxed for 4 hours. A green yellowish precipitate was formed during the reflux. The mixture was filtered, and a yellow solid was obtained. The solid was further recrystallized using 1,4-dioxane and 1-propanol.

University of Malaya

(c) Preparation of bis[N'-(4-decyloxy-2-oxidobenzylidene)-3-hydroxy-2-naphtho-hydrazidato]copper(II), CuNA

Copper(II) acetate monohydrate (0.10 g, 0.50 mmol) was dissolved in 5 mL distilled water. Next, it was added to a mixture of ethyl acetate: dimethylformamide (3:1) solution of compound NA (0.46 g, 1.00 mmol). The solution mixture was refluxed for 3 hours. A green precipitate was formed, and a green solid was collected after filtration. 1,4-dioxane and 1-propanol were used to recrystallize the resulting solid.

(d) Preparation of bis[N'-(4-decyloxy-2-oxidobenzylidene)-3-hydroxy-2-naphtho-hydrazidato]zinc(II), ZnNA

Zinc(II) acetate dihydrate (0.11 g, 0.50 mmol) was dissolved in 10 mL ethanol and mixed into the solution of ethyl acetate: dimethylformamide (3:1) that contains compound NA (0.46 g, 1.00 mmol). The mixture was refluxed for 4 hours. A yellow precipitate was formed during the refluxing process, resulting in a solid, which was dried after filtration. The solid was then recrystallized using 1,4-dioxane and 1-propanol.

(e) Preparation of bis[N'-(4-decyloxy-2-oxidobenzylidene)-3-hydroxy-2-naphtho-hydrazidato]cadmium(II), CdNA

Cadmium(II) acetate dihydrate (0.13 g, 0.50 mmol) was dissolved in 10 mL ethanol and was added to a mixture of ethyl acetate: dimethylformamide (3:1) solution of compound NA (0.46 g, 1.00 mmol). The mixture was refluxed for 4 hours (Hussain et al., 2013). A yellowish precipitate was formed during the reflux, and a solid was collected after filtration. The resulting solid was further recrystallized using 1,4-dioxane and 1-propanol.

University of Malaya

(f) Preparation of bis[N'-(4-dodecyloxy-2-oxidobenzylidene)-3-hydroxy-2-naphtho-hydrazidato]cobalt(II), CoNB

Cobalt(II) acetate tetrahydrate (0.13 g, 0.50 mmol) was added to a mixture of dimethylformamide: ethanol (1:3) solutions of compound NB (0.49 g, 1.00 mmol). The mixture was refluxed for 3 hours. A reddish brown precipitate formed during the reflux. A solid was acquired after the solution was filtered. Thereafter, the solid was further recrystallized using 1,4-dioxane and 1-propanol.

(g) Preparation of bis[N'-(4-dodecyloxy-2-oxidobenzylidene)-3-hydroxy-2-naphtho-hydrazidato]nickel(II), NiNB

Nickel(II) acetate tetrahydrate (0.12 g, 0.50 mmol) was combined with a mixture of dimethylformamide: ethanol (1:3) solutions of compound NB (0.49 g, 1.00 mmol). The mixture was refluxed for 4 hours. A yellow greenish precipitate formed during the reflux and a solid was then obtained after it was filtered. The solid was recrystallized using 1,4-dioxane and 1-propanol.

(h) Preparation of bis[N'-(4-dodecyloxy-2-oxidobenzylidene)-3-hydroxy-2-naphtho-hydrazidato]copper(II), CuNB

Copper(II) acetate monohydrate (0.10 g, 0.50 mmol) was added to a mixture of dimethylformamide: ethanol (1:3) solutions of compound NB (0.49 g, 1.00 mmol). The mixture was then refluxed for 3 hours. A green precipitate formed during the refluxed process. The solid was then filtered and left to dry. The solid was then further recrystallized using 1,4-dioxane and 1-propanol.

(i) Preparation of bis[N'-(4-dodecyloxy-2-oxidobenzylidene)-3-hydroxy-2-naphtho-hydrazidato]zinc(II), ZnNB

Zinc(II) acetate dihydrate (0.11 g, 0.50 mmol) was added to a mixture of dimethylformamide: ethanol (1:3) solution of compound NB (0.49 g, 1.00 mmol). The

University of Malaya

mixture was refluxed for 4 hours. A yellow precipitate formed during the reflux process and subsequently a solid was obtained and dried after it was filtered. The solid was recrystallized using 1,4-dioxane and 1-propanol.

(j) Preparation of bis[N'-(4-dodecyloxy-2-oxidobenzylidene)-3-hydroxy-2-naphtho-hydrazidato]cadmium(II), CdNB

Cadmium(II) acetate dihydrate (0.13 g, 0.50 mmol) was combined with a mixture of toluene: dimethylformamide: ethanol (1:1:3) solutions of compound NB (0.49 g, 1.00 mmol). The mixture was refluxed for 3 hours. A yellowish precipitate was already formed during the reflux process and a solid was obtained after filtration. 1,4-dioxane and 1-propanol were used to recrystallize the solid.

3.2.2 Part 1b: Characterization of prepared compounds

3.2.2.1 Melting point

The melting point of all samples was determined using Melt-Temp II (Laboratory devices USA) melting point apparatus. The samples were packed into a melting point capillary tube. The heating rate was set to 2 ^{o}C per minutes.

3.2.2.2 ATR-IR spectroscopy

All spectra were run by applying the attenuated total reflectance (ATR) sampling technique. ATR-IR spectra were recorded in the region of 4000-400 cm^{-1} on a Perkin Elmer Spectrum 400 infrared (IR) spectrophotometer. The sample was in a solid form and was used as it is. A few amounts of sample were placed on top of the diamond surface of ATR and measurement was taken. The IR spectrum was collected with its peaks labeled.

3.2.2.3 NMR spectroscopy

The ^{1}H and ^{13}C NMR analysis for the ligands and diorganotin(IV) complexes were recorded using a JEOL ECA 400MHz System FT NMR spectrometer. All of the samples

University of Malaya

were dissolved in a deuterated DMSO at a very high temperature, except for NB, NA1, TA, TB, TA2, and TB2, which were dissolved in $CDCl_3$. The samples were then placed at a height of ~4 cm length of deuterated solvent in an NMR tube. The tube was placed in the sample holder of NMR instrument. NMR spectrum was obtained and labeled.

3.2.2.4 Magnetic susceptibility

Magnetic susceptibility was determined using a Sherwood Auto Magnetic Susceptibility Balance *via* the Gouy method at room temperature. The finely ground solid sample was placed into a clean tube to a length of at least 1.5 cm. The sample tube was then placed into a tube guide on the top of the balance, and its length and weight were recorded accordingly (Hanif & Chohan, 2013). The value of the mass magnetic susceptibility (χ_g) was obtained from the instrument. The molar susceptibility (χ_m) was calculated using:

$$\chi_m = \chi_g \times \mathrm{MW}$$

The molar susceptibility (χ_m) of diamagnetism of the constituent atom (χ_{dia}) was corrected using Pascal's constant, using the following equation:

$$\chi_m^{corr} = \chi_m - \chi_{dia}$$

Then, the effective dipole moment (μ_{eff}) was calculated using the following equation:

$$\mu_{eff} = 2.83\sqrt{T(\chi_m^{corr} - N\alpha)}$$

Where, T is the absolute temperature (298 K), and Nα is the temperature-independent paramagnetism.

3.2.2.5 Single crystal X-ray diffraction (SCXRD)

The NA1 complex was the only one among the diorganotin(IV) complexes that was successful recrystallized from DCM: DMF (1:1). A yellow crystal was formed after the filtrate undergoes a slow evaporation process. The NA1 crystal data from SCXRD was collected at 100 K on Oxford Supernova Dual diffractometer Mo (λ=0.71073 Å).

University of Malaya

Absorption correction was determined by a multi-scan method using CrysAlis Pro (Rigaku Oxford diffraction, 2015). The full matrix least-squares refinement against $|F^2|$ was done using SHELXS (Sheldrick, 2008). The program SHELXL2014/7 (Sheldrick, 2015) was also used throughout the study.

3.2.2.6 CHNS elemental analyzer

Elemental analyses were performed using a Thermofischer Scientific FlashSMART CHNS/O analyzer. In this technique, the percentage of carbon, hydrogen, and nitrogen are determined that lead to the determination of empirical formula of the complex from which molecular formula of the complex can be drawn. A few samples are selected such as NA1, NB1, NB2, and TA1 based on their purity and amount of samples stock. The samples are further purified by using ethanol and ethyl acetate. Then, they are left to dry in a desiccator for a few days. 3-5 mg of each sample is placed inside the tin foil and folded. The tin foil is placed on the autosampler and the sequence started to produce chromatogram.

3.2.3 Part 2: Anticancer studies

The cytotoxic activity of the prepared ligands and its diorganotin(IV) complexes were tested using the MTT dye reduction assay as described by Mosmann (Mosmann, 1983; Chew et al., 2014). The method is based on the reduction of the yellow tetrazolium salt MTT to a violet formazan being treated for 72 hours, with increasing concentration of the compounds *via* the mitochondrial succinate dehydrogenase in viable cells. The compounds were dissolved in DMSO and experiment was carried out in triplicate. The experiments were carried out using human colon carcinoma cell line (HT29) and hormone-dependent breast carcinoma cell line (MCF7). Cytotoxicity value of each sample was reported as IC_{50} value. Where, IC_{50} is the concentration of the concerned drug

University of Malaya

that will inhibit the concerned activity of a biological system (Nikolova-Mladenova et al., 2009).

3.2.4 Part 3: Formulation studies

The formulation studies include the determination of the percentage of encapsulation efficiency (%EE) and the percentage of drug loading of the complexes (%DL), the particle size measurement, morphology studies, and drug release study. %EE and %DL were determined for all seven complexes, but only one exemplary drug which is ND2 was selected for the determination of its size, morphology, and drug release study. ND2 was selected as the yield was high as well as it exhibited the highest cytotoxicity activity and the highest %EE and %DL compared to other diorganotin(IV) complexes. The diorganotin(IV) complexes from a previous research of Lee et al., (2012) and Lee et al., (2013) were used in the formulation part. These complexes have been identified for anticancer activities. The reason to use the previous research complexes is their IC_{50} values are better and more promising than the current research complexes for their anticancer activities. While the formulation part for new complexes synthesized in current research will be continued in the next future.

3.2.4.1 Preparation of the niosomes containing active ingredient

The material used to prepare the drug carriers or niosomes was own synthesized glycolipid. This glycolipid is proven in previous work to be able to produce vesicles in nano size (Mak et al., 2015). There are two methods were used to prepare the niosomes. Firstly, the microencapsulation vesicle (MCV) method in which 1 mM of nonionic glycolipid and 10 mM of diorganotin(IV) complexes were dissolved in 2 mL of dichloromethane. This was then followed by the addition of 3 mL of distilled water was added to the solution and mixed with a homogenizer at 7000 rpm for 10 minutes to form a w/o emulsion. Then, 2 mL of distilled water was added and stirred at 520 rpm at 45 °C to form a w/o/w emulsion. The stirring continued for 120 minutes to remove all

University of Malaya

dichloromethane from the suspension *via* evaporation and generate a drug-loaded niosome suspension (Nii & Ishii, 2007).

The second method is known as ethanolic injection method. The amount of surfactant and active ingredient are similar as prepared for the MCV method. The surfactant and active ingredient were dissolved in 5% of the ethanol based on the total volume of the formulation. The solution was then injected rapidly into bulk water through a 25 Ga bevel tip needle at room temperature (Mak et al., 2015).

3.2.4.2 Ultracentrifugation

The prepared vesicles were precooled in the refrigerator prior to being centrifuged using a refrigerated centrifuge Velocity 18R (Dynamica) at 15,000 rpm and 4 °C twice. Each centrifugation took 30 minutes, with 10 minutes gap to separate the free drug from the entrapped drug.

3.2.4.3 Ultraviolet-visible (UV-Vis) spectrophotometer

The clear supernatant after the centrifugation was collected and analyzed using a UV-Vis spectrophotometer (Shimadzu UV-2600) at the wavelength of the drugs, while the pellet obtained after centrifugation was lysed in ethanol and sonicated for 10 minutes. The drugs were analyzed by using UV-Vis spectrophotometer for its content at 268 nm as the maximum absorbance in water and at 264 nm in ethanol. The concentration of the drug, in both supernatant and pellet forms, were determined based on the calibration curve of the particular drug.

3.2.4.4 Encapsulation efficiency, %EE and Drug loading, %DL

The %EE of drug encapsulated in the bilayer of the drug vehicle was calculated by dividing the difference between the total amount of the drug used ($W_{\text{total drug used}}$) and the non-encapsulated drug in the supernatant ($W_{\text{free drug}}$) by the total amount of the drug usage.

University of Malaya

The %DL was obtained by dividing that difference by the total weight of the surfactant. The %EE and %DL of the drug can be calculated based on (Yassin et al., 2010):

$$\%EE = \frac{W_{\text{total drug used}} - W_{\text{free drug}}}{W_{\text{total drug used}}} X\ 100\%$$

$$\%DL = \frac{W_{\text{Total drug used}} - W_{\text{free drug}}}{(W_{\text{total drug used}} + W_{\text{total lipid}} - W_{\text{free drug}})} X\ 100\%$$

3.2.4.5 Dynamic light scattering (DLS)

The niosome-encapsulated ND2 and TC2 complexes were selected for this measurement as a comparison of different structures and the procedure was based on reported procedure with a few modifications (Alibolandi et al., 2015). The vesicle size and polydispersity index were measured using DLS (Zetasizer Nano ZS, Malvern, UK). The analysis was performed at a scattering angle of 173º and 25 ºC and an equilibrium time of 120 second. The measurements were conducted thrice. The dispersant used in this case was water, which has a refractive index of 1.33 and a viscosity (mPa.s) of 0.8872.

3.2.4.6 Field emission scanning electron microscopy (FESEM)

The morphology of niosome-encapsulated ND2 was determined using FESEM (Hitachi SU8220, Oxford Instruments). The niosome loaded with active ingredient was centrifuged to remove the non-encapsulated active ingredient. Then, the sediment was dried on a membrane and coated with platinum. Then the sample was loaded into the FESEM chamber and it was subsequently viewed under FESEM. The photomicrographs recorded at an acceleration voltage of 30 kV for imaging (Yassin et al., 2010).

3.2.4.7 *In vitro* drug release

Drug release from niosome-encapsulated ND2 was determined using the dialysis method with respect to the sink's conditions. The vesicle solution was placed into the dialysis bag and immersed in 100 mL of release medium (distilled water) in a glass bottle

University of Malaya

with cap, at 200 rpm magnetic stirring at 37 °C. At specific time intervals, 2 mL of medium was taken and replaced immediately with the same volume of fresh water into a glass bottle with cap (Haeri et al., 2014). The taken medium was analyzed using a spectrophotometer at the maximum wavelength absorbance. The concentration of the drug was estimated based on the calibration curve (Anbarasan et al., 2013), while the released drug was determined by the *in vitro* release profile, where the cumulative released percentage was plotted against the time of the drug release (Yew & Misran, 2015).

University of Malaya

CHAPTER 4: RESULT AND DISCUSSION

4.1 Part 1a: Preparation of compound and analytical data

A total of four hydrazone Schiff base ligands were synthesized from the reactions of 1:1 molar ratio of 3-hydroxy-2-naphthoic hydrazide (NAH) or TRIS ligands with 4-decyloxysalicylaldehyde and 4-dodecyloxysalicylaldehyde respectively. A general reaction scheme for the preparation of the ligand precursor and NAH ligands are shown in Scheme 4.1 and 4.2, respectively. The preparation of salicylaldehydes derivatives was based on a modified method (Mögele et al., 2009; Lai et al., 1997). The obtained compounds were used without purification to prepare the NAH ligands (Nath et al., 2010).

Scheme 4.1: The preparation of the substituted salicylaldehyde, ligand precursor

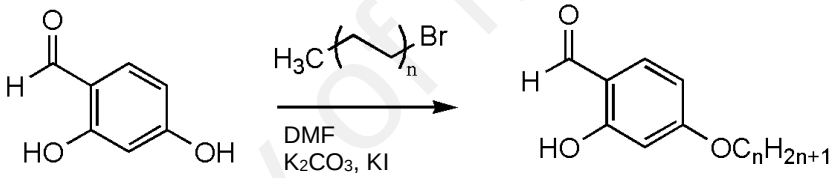

Where, n = 10 and 12

Scheme 4.2: The preparation of the NAH Schiff base ligands

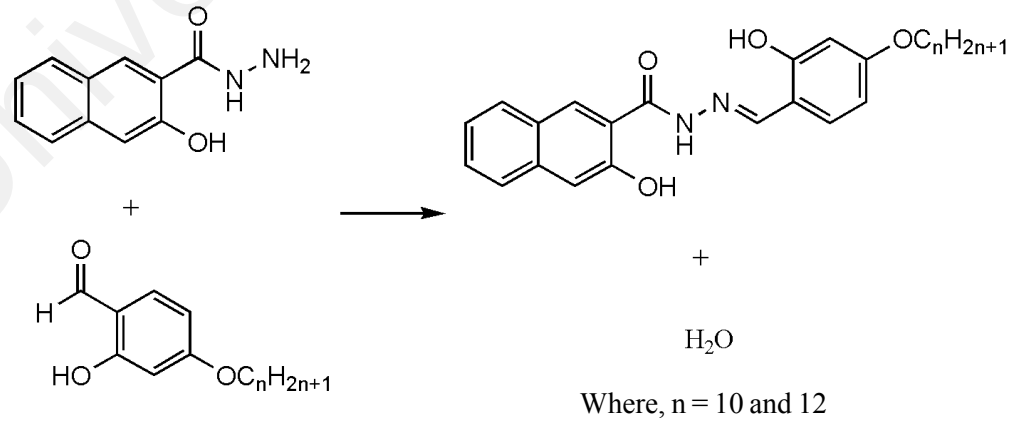

Where, n = 10 and 12

The NAH ligands were obtained in powder form and were further purified using ethyl acetate prior to being used to prepare diorganotin(IV) and metal complexes. The NAH

University of Malaya

Schiff base ligand has five potential donor sites which are two nitrogen atoms and three oxygens from hydroxy groups that can readily form coordination bonds with the diorganotin(IV) ion. The IR spectrum of the ligand showed that it was in keto form, due to the presence of a broad band combination with small sharp peak ν(OH) and ν(NH), respectively, in the 3050 - 3260 cm^{-1} region.

The hydrazone was able to coordinate with the metal atom, either in an enolic form [1] or in a ketonic form [2], as shown in Figure 4.1, which has been reported by Shaabani et al., (2014) and Deng et al., (2016). There were four potential sites of the enolized form, namely the azomethine nitrogen and three hydroxyl groups. The presence of several acidic hydroxyl groups that readily reacted with diorganotin(IV) dihalides in the presence of weak base became an important aspect of these Schiff base ligands.

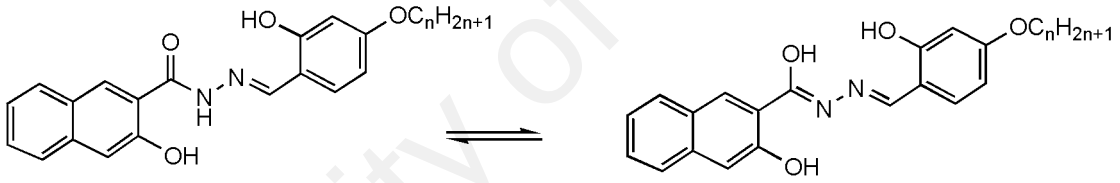

[1] [2]

Figure 4.1: Keto-enol tautomerism of the hydrazone NAH Schiff base ligand

The NAH diorganotin(IV) complexes were synthesized from dimethyltin(IV) or dibutyltin(IV) dichloride reacted with NAH ligands. The NAH ligands were also further reacted with metal salts, such as cobalt(II) acetate tetrahydrate, nickel(II) acetate tetrahydrate, copper(II) acetate monohydrate, zinc(II) acetate dehydrate and cadmium(II) acetate dihydrate to obtain NAH metal complexes. General reaction schemes for the preparation of these complexes are shown in Scheme 4.3 and Scheme 4.4.

University of Malaya

Scheme 4.3: The preparation of the NAH diorganotin(IV) complexes from diorganotin(IV) dichloride and the NAH ligand

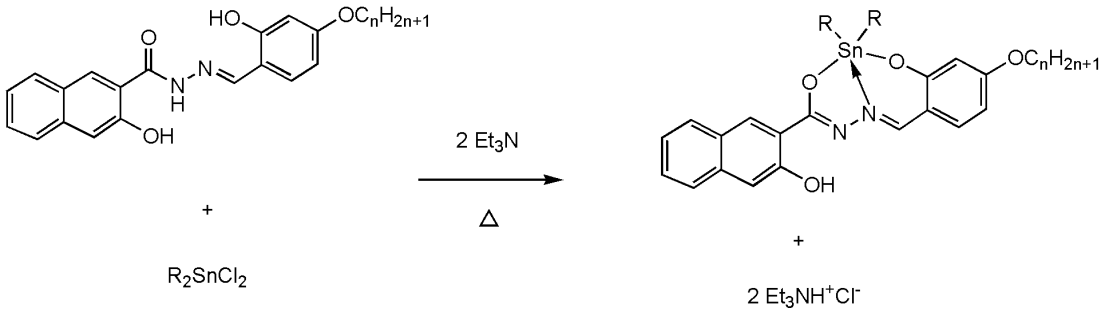

Where, n = 10 and 12 R= CH_3 or C_4H_9

Scheme 4.4: The preparation of the NAH metal complex

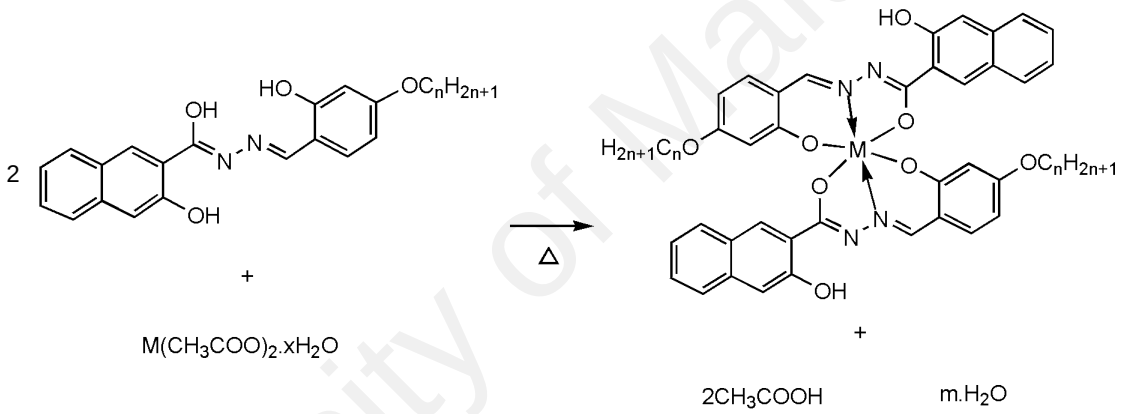

n = 10 and 12 x = 1, 2, 4
m = 2, 4, 6 M = Co(II), Ni(II), Cu(II), Zn(II), Cd(II)

The color of both ligands precursor 4-decyloxy-2-hydroxybenzaldehyde (SA) and 4-dodecyloxy-2-hydroxybenzaldehyde (SB) was a dark orange liquid. The color of the ligands was dark yellow, and its melting point is ranged between 222 - 228 ^oC for NAH ligands, as depicted in Table 4.1. Meanwhile, the color of four NAH diorganotin(IV) complexes was yellow, and its melting point are reported in wide range of 234 - 248 ^oC (Pawanoji et al., 2009; Lee et al., 2012; Hussain et al., 2013) where only 2 - 4 ^oC differences for each complex, as shown in Table 4.2. The differences in melting point range could be due to the present of impurities. As can be seen in the ^1H NMR spectrum of NA1 (Figure 4.11), small peaks at 1.25, 1.42 and 3.72 ppm for ethanol and 1.56 ppm

University of Malaya

for water residue peak are presented (Gottlieb et al., 1997; Babij et al., 2016). The differences of percentage CHN calculated value of complexes from found values as presented in Table 4.19 also indicated that the impurities are existed. The color of the NAH metal complexes varies from yellow, green and brown, with melting points of more than 300 ^{o}C as shown in Table 4.3.

Table 4.1: Analytical data for NAH ligands

Ligands	Molecular weight, g/mol	Color	Percentage yield, (%)	Melting point (^{o}C)
NA	462.581	Dark yellow	85	226 - 228
NB	490.634	Dark yellow	76	222 - 224

Table 4.2: Analytical data for NAH diorganotin(IV) complexes

Complexes	Molecular weight, g/mol	Color	Percentage yield, (%)	Melting point (^{o}C)
NA1	609.344	Yellow	93	234 - 236
NA2	693.503	Yellow	91	244 - 246
NB1	637.397	Yellow	54	240 - 244
NB2	721.556	Yellow	43	246 - 248

Table 4.3: Analytical data for NAH metal complexes

Complexes	Molecular Weight, g/mol	Color	Percentage Yield (%)	Melting Point (^{o}C)
CoNA	980.063	Brown	61	>300
NiNA	979.823	Yellow	63	>300
CuNA	984.675	Green	43	>300
ZnNA	986.519	Yellow	54	>300
CdNA	1033.540	Yellow	64	>300
CoNB	1036.169	Brown	63	>300
NiNB	1035. 929	Yellow	69	>300
CuNB	1040.782	Green	68	>300
ZnNB	1042.626	Yellow	61	>300
CdNB	1089.647	Yellow	72	>300

University of Malaya

While the TRIS Schiff base ligand has five potential coordination which are the imine nitrogen and four hydroxyl groups on the methylene group and on the substituted salicylaldehyde (Pandit et al., 2015). A general reaction scheme for the preparation of the TRIS ligands is shown in Scheme 4.5. The diorganotin(IV) complexes were synthesized by using such as dimethyltin(IV) and dibutyltin(IV) dichloride reacted with TRIS ligands. General reaction schemes for the preparation of the complexes is shown in Scheme 4.6.

Scheme 4.5: The preparation of the TRIS Schiff base ligands

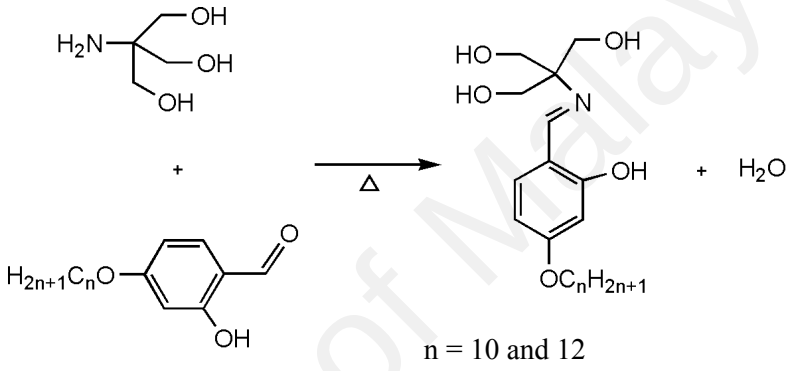

n = 10 and 12

Scheme 4.6: The preparation of the TRIS diorganotin(IV) complexes from diorganotin(IV) dichloride and the TRIS ligand

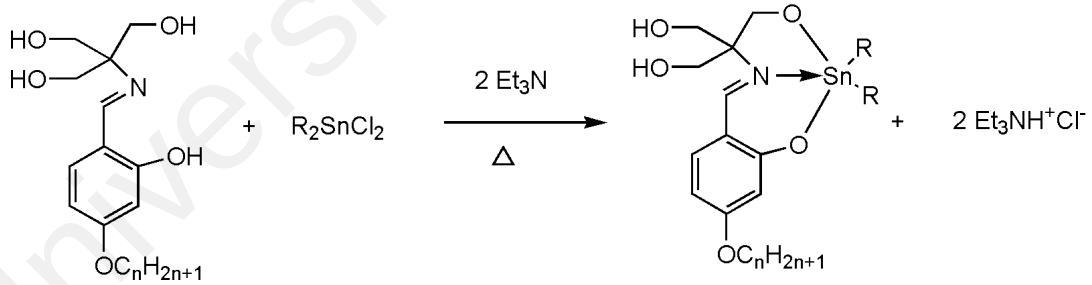

n = 10 and 12 R = CH_3 or C_4H_9

The color of TRIS ligands was dark yellow flakes, and their melting point is ranged between 110 - 124 ^oC, as shown in Table 4.4. The color of TRIS complexes was light brown solid for TA1 and TB1, and their melting point is ~154 - 165 ^oC, except for TA2 and TB2 which were black and in the form of semi-solid as shown in Table 4.5.

University of Malaya

Table 4.4: Analytical data for TRIS ligand

Ligands	Molecular weight, g/mol	Color	Percentage yield, (%)	Melting point (°C)
TA	381.506	Dark yellow	41	120 - 124
TB	409.559	Dark yellow	38	110 - 114

Table 4.5: Analytical data for TRIS diorganotin(IV) complexes

Complexes	Molecular weight, g/mol	Color	Percentage yield, (%)	Melting point (°C)
TA1	528.269	Light brown	45	164 - 165
TA2	612.429	Black	51	In semi-solid
TB1	556.323	Light brown	49	154 - 156
TB2	640.482	Black	52	In semi-solid

University of Malaya

4.2 Part 1b: Characterization of prepared compounds

This characterization part consist of Infrared (IR) spectroscopy, Nuclear Magnetic Resonance (NMR) spectroscopy, Auto Magnetic Susceptibility Balance (for transition metal complexes), Single Crystal X-ray Diffraction (SCXRD) and elemental analyses.

4.2.1 Infrared (IR) spectral data

Analysis of IR spectral data of NAH ligands and its diorganotin(IV) complexes, TRIS ligands and its diorganotin(IV) complexes, and lastly metal complexes.

4.2.1.1 The IR spectra of the NAH ligands and its diorganotin(IV) complexes

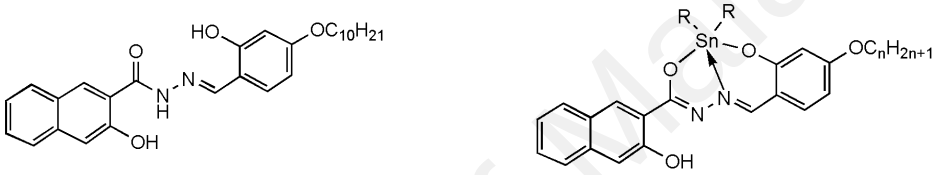

a) Ligand b) Complex

NA: n = 10, NB: n = 12

NA1: R = CH_3, n = 10, NA2: R = C_4H_9, n = 10
NB1: R = CH_3, n = 12, NB2: R = C_4H_9, n = 12

Figure 4.2: The structure of NAH a) ligand and b) diorganotin(IV) complex

Figure 4.2 shows the structure of the ligand and complex. In Figure 4.3, a strong broad peaks were observed at 3156 cm^{-1}, which could be attributed to ν(O-H). On the other hand, for the diorganotin(IV) complexes, a smaller broad band at ~3152 - 3187 cm^{-1} was detected, suggesting the presence of a hydroxyl functional group in its molecular structure.

University of Malaya

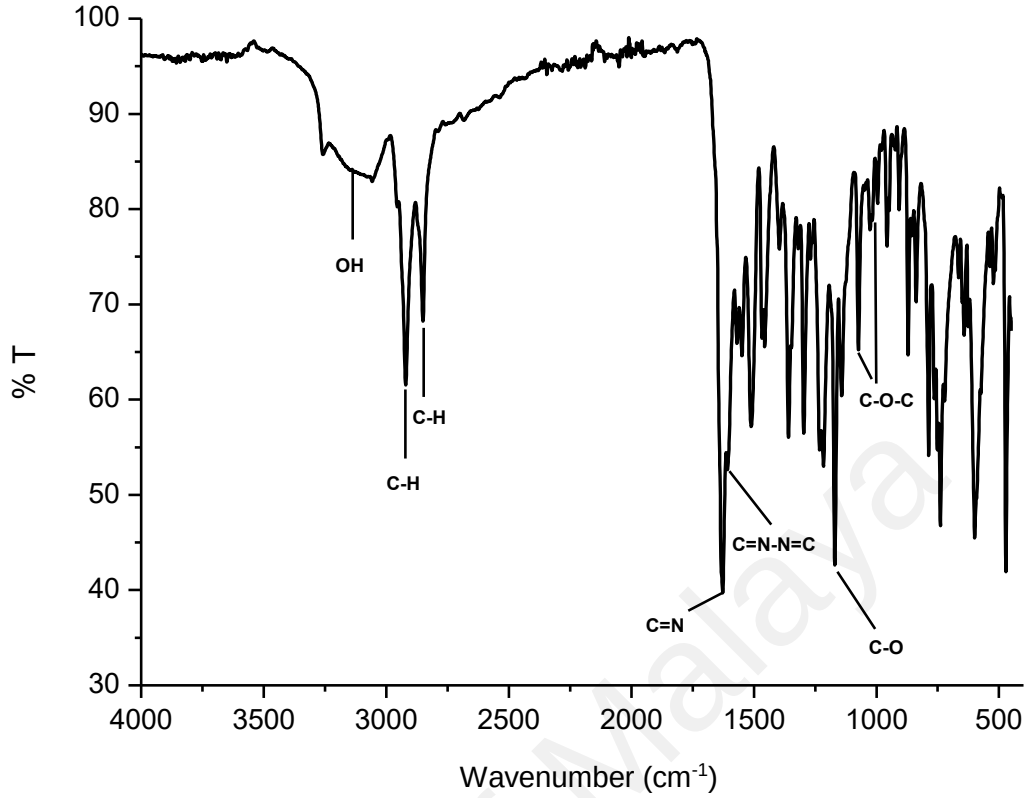

Figure 4.3: IR spectrum of NA

Two strong peaks at 2918 - 2921 cm^{-1} and 2847 - 2851 cm^{-1} were assigned to the asymmetric and symmetric stretching of ν(C-H) in both ligands and diorganotin(IV) complexes spectra (Figure 4.4), respectively. Two sharp bands at ~1626 - 1627 cm^{-1} region were attributed to ν(C=N), which was comparable to the values reported for Schiff base ligands (Lee et al., 2013; Kavitha et al., 2013). The diorganotin(IV) complexes showed strong absorption in the ~1624 - 1638 cm^{-1} and ~1597 - 1607 cm^{-1} region due to ν(C=N) and ν(C=N-N=C) stretching frequencies (Samanta et al., 2007; Hong et al., 2013b). The absence of ν(C=O) band in ligands spectra between than 1690-1740 cm^{-1} (Lampman et al., 2010) suggest that it was in an enolic form, while the medium-to-strong band of ~1169 - 1172 cm^{-1} indicates ν(C-O) asymmetrical stretching frequencies and ν(C-O-C) symmetrical stretching frequencies in the range of 1013 - 1074 cm^{-1} for both ligands and complexes, respectively. Meanwhile, the weak absorption bands at 679 - 775 cm^{-1} could be assigned to stretching vibrations of the Sn-O bond. The weak bands at 457

University of Malaya

- 489 cm^{-1} were assigned to Sn-N stretching frequency. In fact, both Sn-O and Sn-N stretching frequencies were in the range reported for derivatives of diorganotin(IV) complexes (Shujah et al., 2010; Shujah et al., 2011). The infrared stretching frequencies for NAH ligands and its diorganotin(IV) complexes are presented in Tables 4.6 and 4.7 respectively

Table 4.6: Infrared spectral data for NAH ligands

Ligands/ Wavenumber (cm^{-1})	**NA**	**NB**
ν(O-H)	3156b	3161b
ν (C=N)	1626s	1627s
ν (-C=N-N=C-)	1606s	1606s
ν (C-O)	1169m	1171m
ν (C-O-C)	1073m, 1025w	1072w, 1015w
$\nu(C\text{-}H)_{asym}$ / $\nu(C\text{-}H)_{sym}$	2921s, 2849s	2920s, 2848s

*b = broad, s = strong, m = medium, w = weak

Table 4.7: Infrared spectral data for NAH diorganotin(IV) complexes

Complexes/ Wavenumber (cm^{-1})	**NA1**	**NA2**	**NB1**	**NB2**
ν(O-H)	3162b	3187b	3152b	3156b
ν (C=N)	1633s	1624s	1638s	1627s
ν (-C=N-N=C-)	1597s	1607s	1607s	1607s
ν (C-O)	1169m	1169m	1169m	1172m
ν (C-O-C)	1073w, 1013w	1074m, 1026w	1054w, 1016w	1072w, 1018w
ν(Sn-O)	775w	679w	749w	747w
ν(Sn-N)	457w	470w	463w	489w
$\nu(C\text{-}H)_{asym}$ / $\nu(C\text{-}H)_{sym}$	2921s, 2850s	2918s, 2847s	2921s, 2851s	2919s, 2847s

*b = broad, s = strong, m = medium, w = weak

University of Malaya

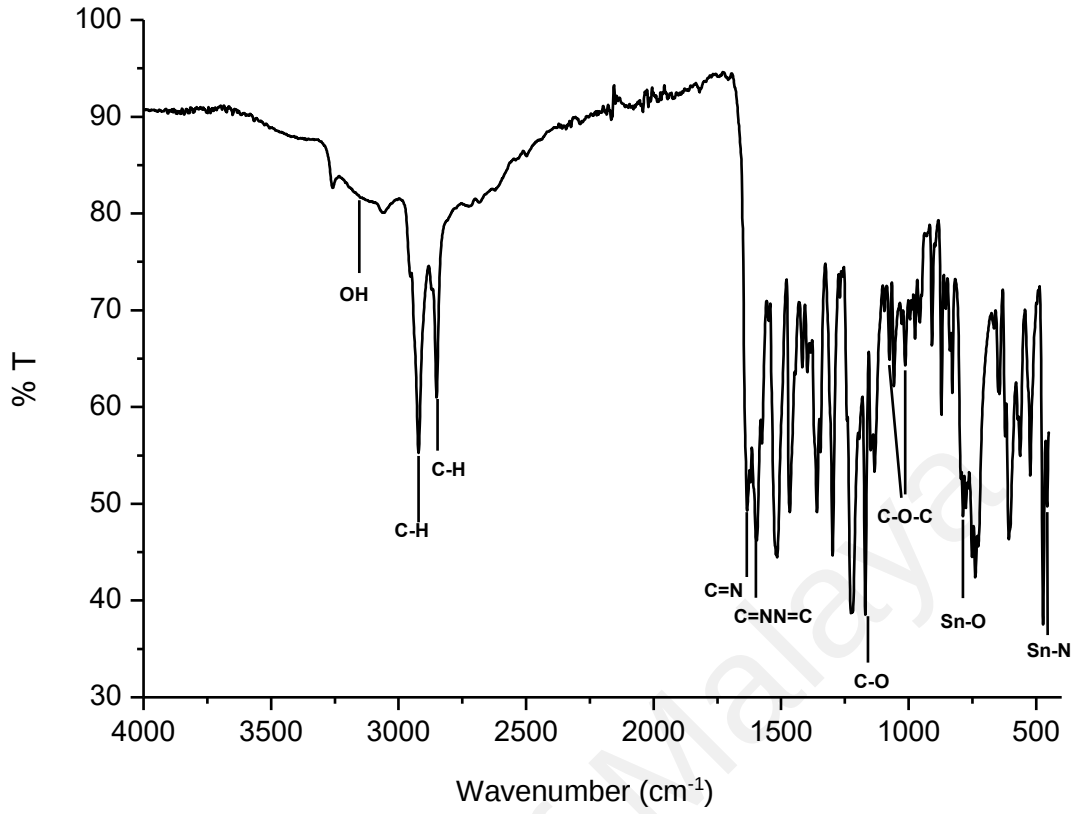

Figure 4.4: IR spectrum of NA1

4.2.1.2 The IR spectra of the TRIS ligands and its diorganotin(IV) complexes

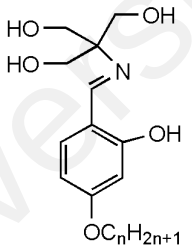

a) Ligand

TA: n = 10, TB: n = 12

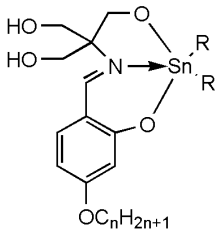

b) Complex

TA1: R = CH_3, n = 10, TA2: R = C_4H_9, n = 10
TB1: R = CH_3, n = 12, TB2: R = C_4H_9, n = 12

Figure 4.5: The structure of TRIS a) ligand and b) diorganotin(IV) complex

Figure 4.5 show the structure of ligand and complex. Two strong peaks at the range of 2920 - 2924 cm^{-1} and 2849 - 2855 cm^{-1} were assigned to asymmetric and symmetric stretching of ν(C-H) in both ligands (Figure 4.6) and diorganotin(IV) complexes spectra, respectively.

University of Malaya

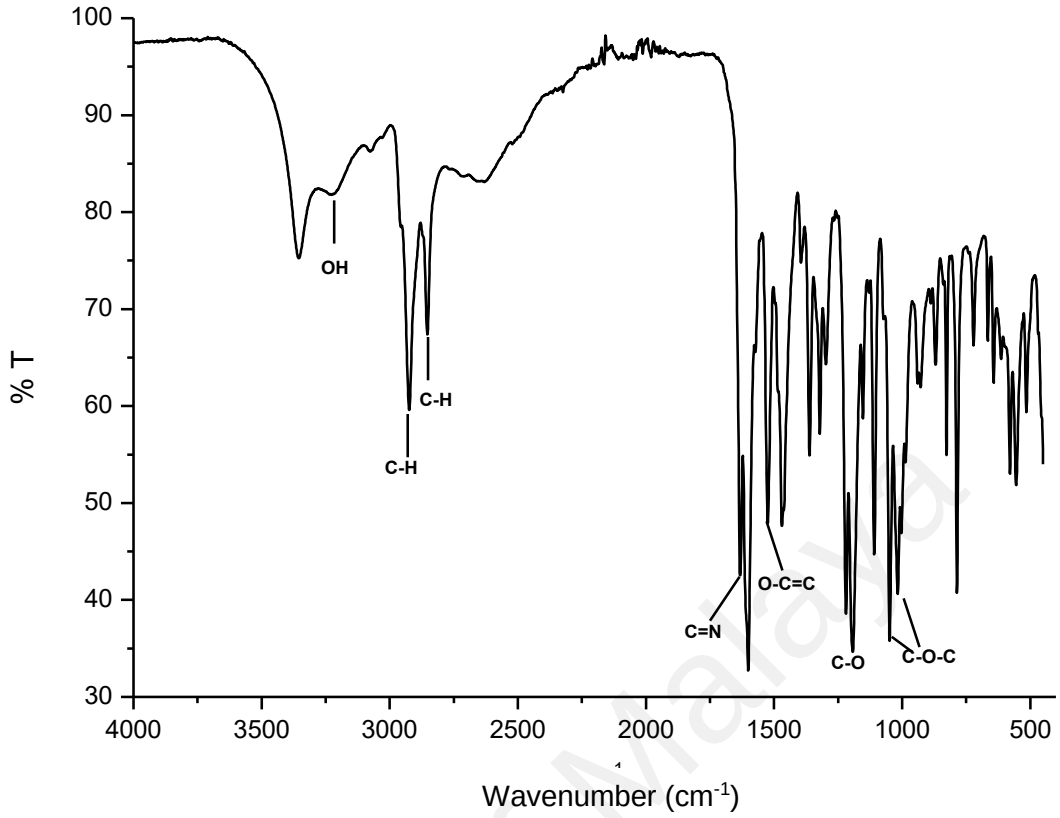

Figure 4.6: IR spectrum of TA

In diorganotin(IV) complexes spectrum (Figure 4.7), a broad band of alcoholic groups was observed at 3124 - 3220 cm^{-1} (Abu-Sbeih & Abu-Yamin, 2014), which suggest the involvement of only one of three OH groups in the coordination to the metal atom. The stretching vibrations of ν(C=N) azomethine bond in the ligands appeared as intense bands at 1631 - 1634 cm^{-1} (Abramenko et al., 2013). The ν(C=N) stretching frequencies for the diorganotin(IV) complexes were found in the region between 1599 and 1608 cm^{-1}, which is ~26 - 35 cm^{-1} lower than the ligands. The strong band of ν(O-C=C) at the region of 1524 - 1525 cm^{-1} increased to 1529 cm^{-1}, while the medium band at the range of 1187 - 1199 cm^{-1} indicated ν(C-O) asymmetrical stretching frequencies and ν(C-O-C) symmetrical stretching frequencies in the range of 1016 - 1078 cm^{-1} for the ligands and complexes, respectively. Moreover, the weak absorption bands at 748 - 757 cm^{-1} could be assigned to stretching vibrations of ν(Sn-O) bond, whereas the weak bands at 482 - 487 cm^{-1} were assigned to ν(Sn-N) stretching frequency (Lee et al., 2015; Yang et al.,

University of Malaya

2016). The characteristics of infrared stretching frequencies for TRIS ligands and its diorganotin(IV) complexes are presented in Tables 4.8 and 4.9 respectively.

Table 4.8: Infrared spectral data for TRIS ligands

Ligands/ Wavenumber (cm^{-1})	**TA**	**TB**
ν (O-H)	3230b	3233b
ν (C=N)	1631s	1634s
ν (-O-C=C)	1524s	1525s
ν (C-O)	1192m	1194m
ν (C-O-C)	1048s, 1017m	1047s, 1016m
$\nu(C\text{-}H)_{asym}$ / $\nu(C\text{-}H)_{sym}$	2923s, 2853s	2919s, 2851s

*b = broad, s = strong, m = medium, w = weak

Table 4.9: Infrared spectral data for TRIS diorganotin(IV) complexes

Complexes/ Wavenumber (cm^{-1})	**TA1**	**TA2**	**TB1**	**TB2**
ν(O-H)	3124b	3220b	3177b	3213b
ν (C=N)	1599s	1607s	1599s	1606s
ν (-O-C=C)	1529m	1529w	1529m	1529w
ν (C-O)	1199w	1190w	1187w	1190m
ν (C-O-C)	1066m, 1037m	1078w, 1020w	1067m, 1038m	1078w, 1020w
ν(Sn-O)	756w	748w	757w	749w
ν(Sn-N)	484w	485w	487w	482w
$\nu(C\text{-}H)_{asym}$ / $\nu(C\text{-}H)_{sym}$	2920s, 2849s	2923s, 2854s	2920s, 2849s	2924s, 2855s

*b = broad, s = strong, m = medium, w = weak

University of Malaya

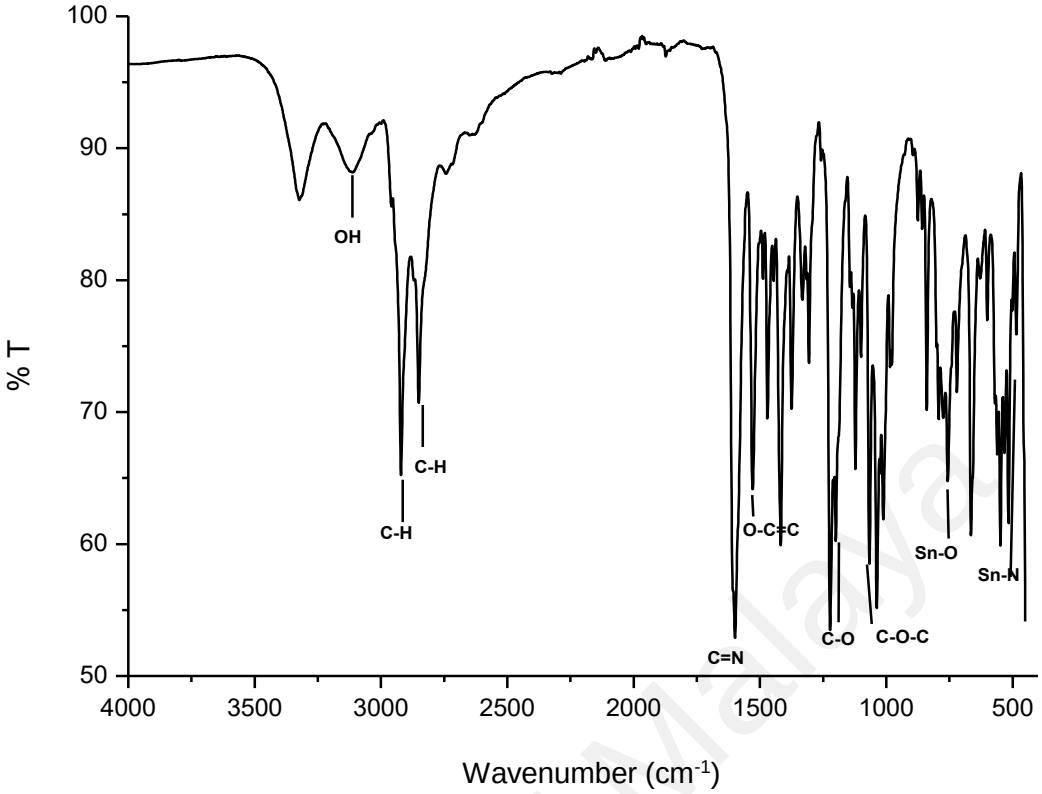

Figure 4.7: IR spectrum of TA1

University of Malaya

4.2.1.3 The IR spectra of the NAH ligands and its metal complexes

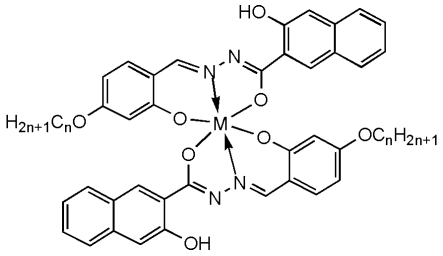

CoNA/ NB: n = 10/ 12
NiNA/ NB: n = 10/ 12
CuNA/ NB: n = 10/ 12
ZnNA/ NB: n = 10/ 12
CdNA/ NB: n = 10/ 12

Figure 4.8: The structure of NAH metal complexes

Figure 4.8 show the structure of metal complexes. Figure 4.9 shows the spectrum of CoNA. The weak band of ν(C-O-C) symmetrical stretching frequencies is observed in the range 1027 - 1086 cm^{-1} for the metal complexes.

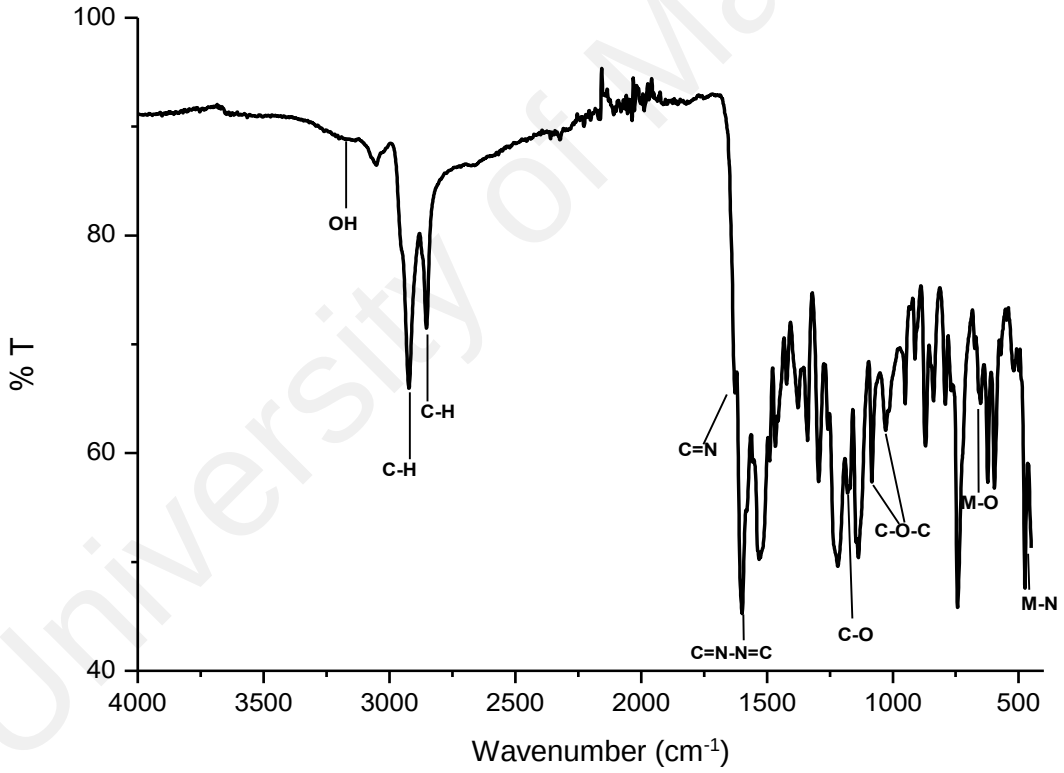

Figure 4.9: IR spectrum of CoNA

A broad band was ascribed to ν(OH) and ν(NH) bands in the 3155 - 3187 cm^{-1} region of the spectra of the ligand, as well as complexes due to the ligand and water molecules being associated with the complexes (Pawanoji & Mehta, 2009). The band due to ν(C=N) at 1626 - 1627 cm^{-1} in the free ligand shifts to a higher frequency on complexation suggests coordination *via* the azomethine group. The metal complexes show strong

University of Malaya

absorption in 1599 - 1608 and 1626 - 1634 cm^{-1} region due to ν(C=N-N=C) and ν(C=N) stretching frequencies (Thilagavathi et al., 2010; Miao, 2012; Saif et al., 2016), confirming the coordination of C=N group to the metal ion for all the prepared complexes. The ligand exhibits ν(C-O) stretching vibration at 1169 - 1171 cm^{-1}, while in the metal complexes, ν(C-O) absorption band appears at 1168 - 1180 cm^{-1}, which were compared to the corresponding (C-O) vibration of the reported free ligand (Kavitha & Lakshmi, 2015). The new bands in the range 640 - 674 cm^{-1} and 483 - 499 cm^{-1} region in all of the complexes were assigned to ν(M-O) and ν(M-N) stretching vibrations, respectively. The ν(M-O) and ν(M-N) stretching frequencies of these metal complexes were slightly higher than the reported values due to electron donating group, which was an alkoxy long chain attached to the ligand (Pawanoji & Mehta, 2009; Saif et al., 2016). The IR spectroscopy range was limited to only 4000 - 450 cm^{-1} only, thus, it was not confidently assigned to the peak of M-O and M-N stretching bonds. The characteristics of the infrared stretching frequencies for metal complexes are presented in Tables 4.10.

Table 4.10: Infrared spectral data for NAH metal complexes

Complexes/ Wavenumber (cm^{-1})	(O-H)	ν(C=N)	(-C=N-N=C-)	(C-O)	(C-O-C)	(M-O)	(M-N)
CoNA	3166b	1626s	1608s	1180w	1084m, 1027w	674w	499w
NiNA	3157b	1629s	1603s	1172m	1081w, 1028w	640w	488w
CuNA	3156b	1630s	1608s	1172m	1068m, 1029w	638w	497w
ZnNA	3155b	1628s	1600s	1179m	1086w, 1029w	674w	483w
CdNA	3156b	1629s	1601s	1169w	1078m, 1031w	651w	494w
CoNB	3168b	1627w	1602w	1170m	1082m, 1029w	652w	492w
NiNB	3160b	1630w	1603w	1168w	1082m, 1029w	651w	489w
CuNB	3187b	1634w	1608w	1170m	1066m, 1032w	650w	496w
ZnNB	3155b	1628w	1599s	1169s	1086m, 1032w	651w	486w
CdNB	3160b	1633w	1601m	1169sh	1078m, 1031w	651w	495w

*b = broad, s = strong, m = medium, w = weak

University of Malaya

4.2.2 Nuclear Magnetic Resonance (NMR) spectral data

Most of the prepared ligands and diorganotin(IV) complexes were dissolved in deuterated DMSO, except for NA1, TA, TB, TA2, and TB2, which were dissolved in deuterated $CDCl_3$. Solvent residue peak for DMSO and $CDCl_3$ are as reported (Gottlieb, et al., 1997; Babij et al., 2016). Meanwhile, the NMR experiment could not be carried out for metal complexes, due to solubility issues such that most of the solid do not dissolve well in several deuterated solvents.

4.2.2.1 The ^{1}H and ^{13}C NMR spectra of the NAH ligands and its diorganotin(IV) complexes

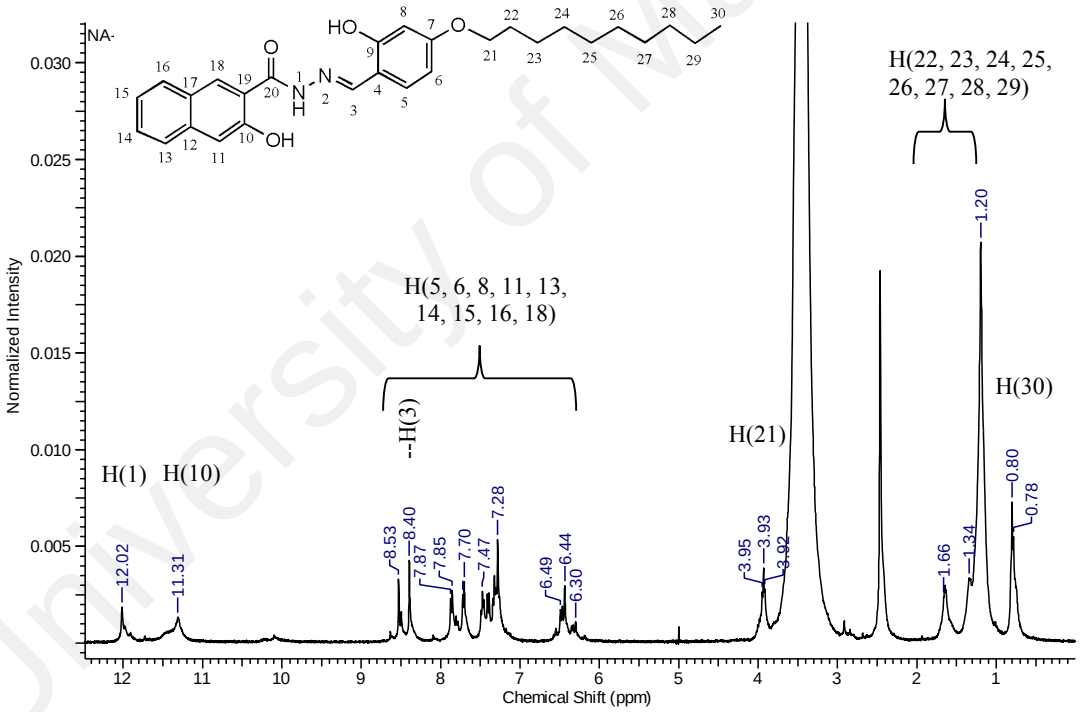

Figure 4.10: ^{1}H-NMR spectrum of NA

In Figure 4.10 shows ^{1}H NMR spectra of NA, the methylene protons, H(22, 23, 24, 25, 26, 27, 28, 29 and 30, 31) appeared as multiplets in the range of 1.20 - 1.74 ppm similar range as in the diorganotin(IV) complexes. The methyl protons, H(30 or 32) of the ligands and its diorganotin(IV) complexes were in the range of 0.78 - 0.89 ppm (Pavia et al., 2014). Meanwhile, the methylene protons for long alkoxy chain, H(21) appeared

University of Malaya

as a triplet in the range of 3.91 - 3.99 ppm. The chemical shift in the range of 6.18 - 7.94 ppm and 8.39 - 8.85 ppm are assigned to the aromatic protons, H(5, 6, 8, 11, 13, 14, 15, 16, 18) of the ligands and diorganotin complexes. The methine protons of the azomethine group, -N=C(H)-, H(3), occurred as a single peak at 8.40 and 8.24 for ligands, while 8.41 and 8.54 ppm for diorganotin(IV) complexes, making it comparable to the reported values (Samanta et al., 2007). In the diorganotin(IV) complexes spectra (Figure 4.13), the decrease in the integration value of the hydroxy protons signal suggests that tin(IV) atom is bonded to one of the oxygen atoms of the Schiff base ligand *via* the replacement of one of its phenolic protons. The hydroxyl, H(10) in the ligands appeared in the range of 11.31 - 11.32 ppm, while the small signal present in the region between 11.47 - 11.69 ppm in the diorganotin(IV) complexes showed that phenoxy proton on the naphthalene ring did not bind to tin(IV) atom. In the ^{1}H NMR spectra of the ligands, a singlet at 12.02 ppm is assigned to the NH proton H(1) (Lee et al., 2013). However, the signal disappeared in the spectra of the complexes (Figure 4.11) due to the engagement of the imine nitrogen atoms in complexation. ^{1}H NMR chemical shifts are listed in Tables 4.11 and 4.12, respectively.

Table 4.11: ^{1}H NMR chemical shifts for the NAH ligands

Ligands/ δ (ppm)	**NA**	**NB**
H(5, 6, 8, 11, 13, 14, 15, 16, 18)	6.30-6.48 (m, 3H) 7.28-7.49 (m, 3H) 7.70-7.72, d (1H, *J* = 8.4) 7.85-7.87, d (1H, *J* = 8.0) 8.53 (s, 1H)	6.38- 6.52 (m, 3H) 7.08-7.11, d (1H, *J* = 8.8) 7.44-7.51 (m, 2H) 7.65-7.60, d (1H, *J* = 9.2) 7.71-7.77 (m, 1H) 8.39 (s, 1H)
H(3)	8.40 (s, 1H)	8.24 (s, 1H)
H(10)	11.31 (s, 1H)	11.32 (s, 1H)
H(1)	12.02 (s, 1H)	12.08 (s, 1H)
H(21)	3.91-3.94, t (2H, *J* = 6.4)	3.93-3.97, t (2H, *J* = 6.8)
H(30 or 32)	0.78-0.81, t (3H, *J* = 6.4)	0.83-0.87, t (3H, *J* = 6.8)
H(22, 23, 24, 25, 26, 27, 28, 29 and 30, 31)	1.20-1.66 (m, 16H)	1.22-1.74 (m, 20H)

University of Malaya

Table 4.12: ^{1}H NMR chemical shifts for the NAH diorganotin(IV) complexes

Complexes/ δ (ppm)	NA1	NA2	NB1	NB2
H(5, 6, 8, 11, 13, 14, 15, 16, 18)	6.22-6.38 (m, 2H) 7.40-7.44 (m, 4H) 7.65-7.67, d (1H, *J* = 8) 7.78-7.80, d (1H, *J* = 8) 8.55 (s, 1H)	6.45-6.50 (m, 2H) 7.30-7.50 (m, 4H) 7.71-7.73, d (1H, *J* = 8) 7.86-7.88, d (1H, *J* = 8) 8.57 (s, 1H)	6.18-6.35 (m, 2H) 7.27-7.47 (m, 4H) 7.72-7.74, d (1H, *J* = 8.4) 7.92-7.94, d (1H, *J* = 8) 8.85 (s, 1H)	6.45-6.50 (m, 2H) 7.31-7.50 (m, 4H) 7.72-7.74, d (1H, *J* = 8.4) 7.86-7.88, d (1H, *J* = 8) 8.54 (s, 1H)
H(3)	8.45 (s, 1H)	8.45 (s, 1H)	8.45 (s, 1H)	8.41 (s, 1H)
H(10)	11.69 (s, 1H)	11.49 (s, 1H)	11.47 (s, 1H)	11.47 (s, 1H)
H(21)	3.94-3.97, t (2H, *J* = 6.4)	3.92-3.95, t (2H, *J* = 6.4)	3.96-3.99, t (2H, *J* = 6.4)	3.93-3.96, t (2H, *J* = 6.4)
H(30 or 32)	0.85-0.89, t (3H, *J* = 7.2)	0.81-0.83, t (3H, *J* = 7.2)	0.83-0.87, t (3H, *J* = 7.2)	0.80-0.84, t (3H, *J* = 7.2)
H(22, 23, 24, 25, 26, 27, 28, 29 and 30, 31)	1.26-1.78 (m, 16H)	1.20-1.69 (m, 16H)	1.24-1.70 (m, 20H)	1.24-1.66 (m, 16H)
Sn-R (R = CH_3 : NA1 & NB1, R = $CH_2CH_2CH_2CH_3$: NA2 & NB2)	0.79 (s, 6H)	0.79-1.88 (m, 18H)	0.77 (s, 6H)	0.79-2.02 (m, 18H)

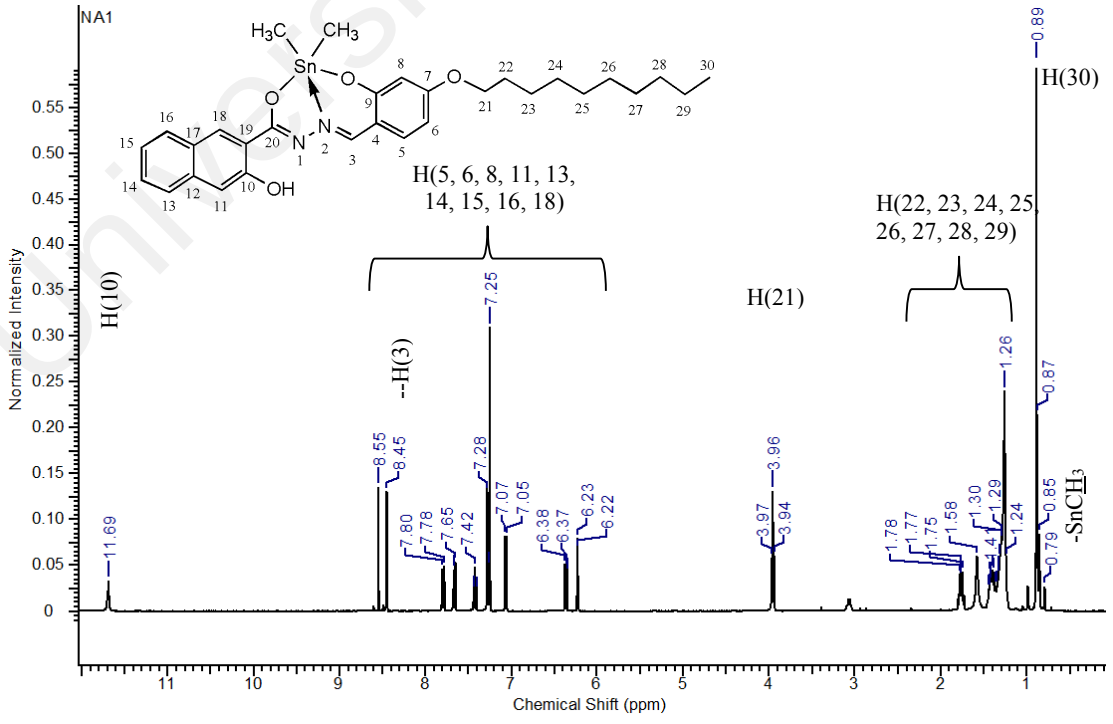

Figure 4.11: ^{1}H-NMR spectrum of NA1

University of Malaya

The ^{13}C NMR spectra of ligand is shown in Figure 4.12. C(7) is attached to the electron donating groups substituents with lone pairs, they activate the aromatic ring by increasing the electron density on the ring through a resonance donating effect. The chemical shift of the C(7) for the Schiff base ligands and the diorganotin(IV) complexes appeared in the range 154.25 - 160.03 ppm.

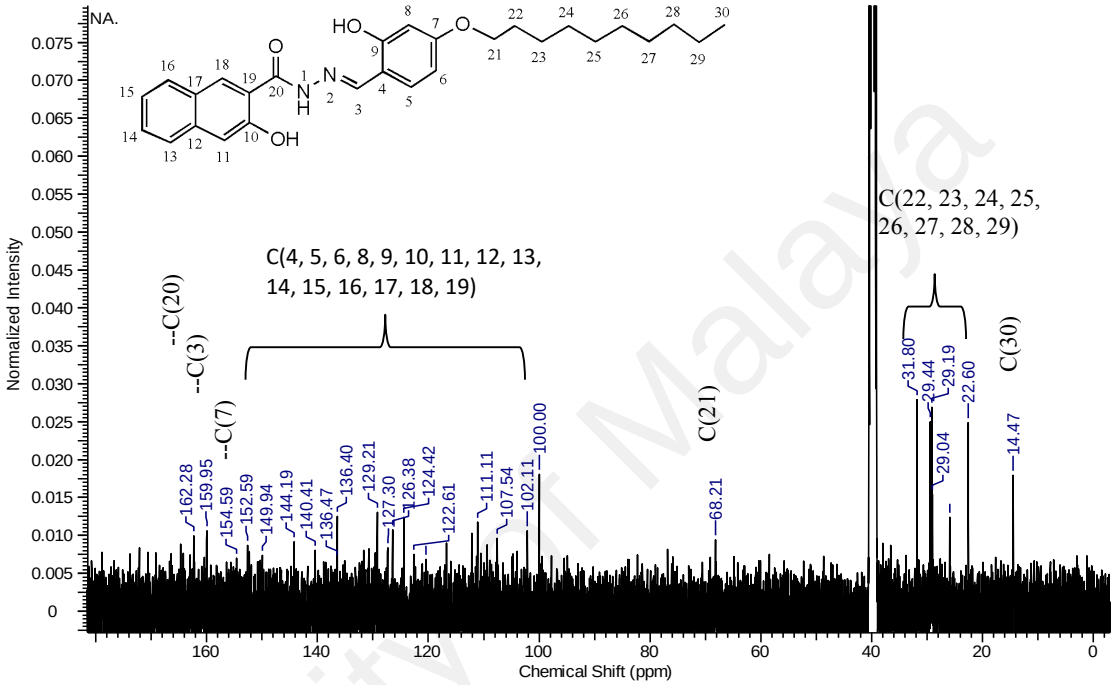

Figure 4.12: ^{13}C-NMR spectrum of NA

While the chemical shift for C(3) of the ligands (NA and NB) and complexes (NA1, NA2, NB1 and NB2) were in the range 156.24 - 162.26 ppm. The carbonyl carbon C(20), was more deshielded than C(3), where its chemical shift was in the region at 162.28 - 165.60 ppm. The methyl carbon of long alkoxy chain C(30 and 32) appeared in the region at 14.17 - 14.49 ppm for both ligands and its diorganotin(IV) complexes. There are new signals appeared in the complexes spectrum (Figure 4.13) at 6.84, 8.83, 9.05, 10.50, 14.44, 14.48, 22.61, 22.62, 29.08 and 31.21 ppm indicated that for the alkyl group substituent of tin(IV). The signal of the methylene carbons of long alkoxy chain C(22, 23, 24, 26, 27, 28, 29 and 30, 31) for the Schiff base ligands and its diorganotin(IV) complexes appeared in the region at 22.60 - 31.98 ppm, with some of the peaks

University of Malaya

overlapping with each other. The aromatic carbons C (4, 5, 6, 8, 9, 10, 11, 12, 13, 14, 15, 16, 17, 18, 19) were found in the range of 101.86 - 160.03 ppm for both ligands and complexes (Majumder et al., 2017). The structure of the ligands and its diorganotin complexes are shown in Figure 4.16. The ^{13}C NMR chemical shifts for NAH ligands and its diorganotin(IV) complexes are listed in Tables 4.13.

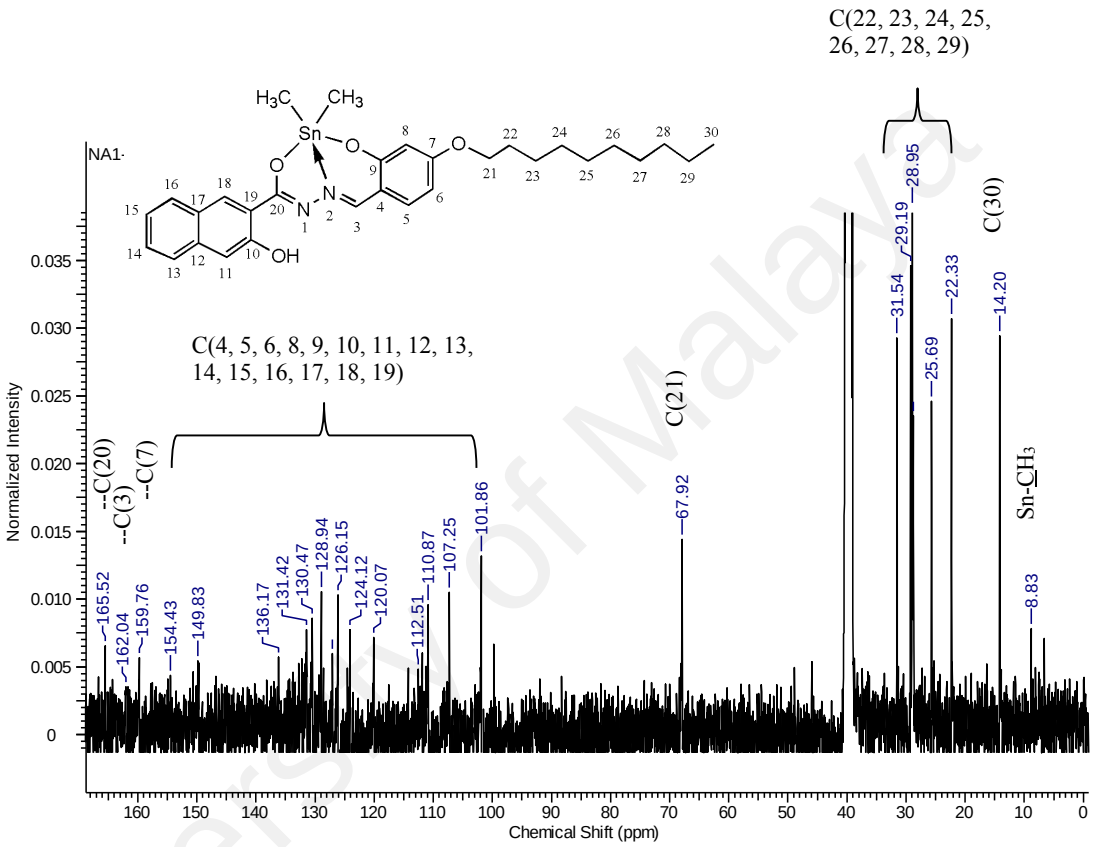

Figure 4.13: ^{13}C-NMR spectrum of NA1

University of Malaya

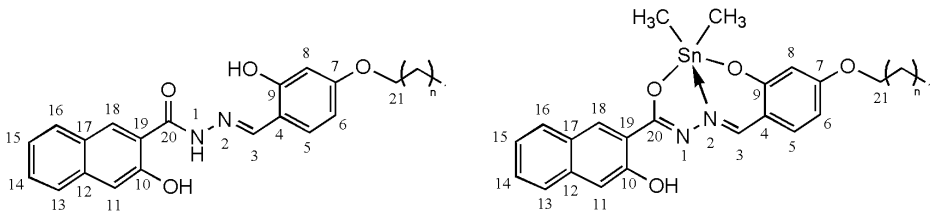

a) b)

NA: n = 8, NB: n = 10 NA1: R = CH_3, n = 8, NA2: R = C_4H_9, n = 8
NB1: R = CH_3, n = 10, NB2: R = C_4H_9, n = 10

Figure 4.14: The structure of NAH a) ligand and b) diorganotin(IV) complex

Table 4.13: ^{13}C NMR chemical shifts for NAH compounds

Compound/ δ (ppm)	**NA**	**NA1**	**NA2**	**NB**	**NB1**	**NB2**
C(3)	159.95	162.04	162.26	156.24	161.06	162.24
C(7)	154.60	159.95	160.03	154.25	155.66	159.98
C (4, 5, 6, 8, 9, 10, 11, 12, 13, 14, 15, 16, 17, 18, 19)	102.11 107.54 111.11 112.10 120.40 124.42 126.38 127.30 127.35 129.21 130.74 131.68 136.40 149.90 152.59	101.86 107.25 110.87 112.51 120.07 124.12 126.15 126.20 127.03 128.94 130.47 131.42 136.17 149.83 154.43	102.10 107.47 111.14 112.10 120.12 124.33 126.36 127.27 128.81 129.19 130.71 131.68 136.45 149.99 154.77	102.59 106.19 111.00 111.99 120.00 123.96 125.99 126.51 128.83 129.36 131.50 132.21 135.50 145.04 151.70	102.00 107.52 110.30 111.45 119.18 123.81 126.27 127.26 128.30 129.17 130.23 136.37 136.83 148.14 154.63	102.09 107.52 111.09 112.10 120.39 124.36 126.38 127.27 128.81 129.19 130.70 131.63 136.39 149.87 154.63
C(20)	162.28	165.52	163.90	162.70	165.6	163.87
C(21)	68.21	67.92	68.17	59.58	68.11	68.17
C(22, 23, 24, 26, 27, 28, 29 and 30, 31)	22.60 25.96 29.04 29.19 29.23 29.44 29.49 31.80	22.33 25.69 28.80 28.95 28.95 29.19 29.19 31.54	22.61 25.98 29.08 29.23 29.26 29.47 29.52 31.82	22.75 25.34 29.01 29.20 29.43 29.75 29.75 30.99 31.30 31.98	22.62 25.95 29.01 29.23 29.48 29.53 31.22 31.22 31.82	22.54 22.62 25.99 29.06 29.23 29.50 29.53 30.99 31.21 31.82
C(30 and 32); $\underline{C}H_3$	14.47	14.20	14.44	14.17	14.49	14.48
Sn-R (R = CH_3 : NA1 & NB1, R = $CH_2CH_2CH_2CH_3$: NA2 & NB2)	None	8.83	9.05 14.44 29.08 22.61	None	6.84	10.50 14.48 31.21 22.62

University of Malaya

4.2.2.2 The ^{1}H and ^{13}C NMR spectra of the TRIS ligands and its diorganotin(IV) complexes

In the ^{1}H NMR spectra of TA (Figure 4.15), the methyl protons for long alkoxy chain H(21 and 23) were presented as triplets in the range of 0.84 - 0.88 ppm, while in the diorganotin(IV) complexes (Figure 4.16), the range was 0.79 - 0.92 ppm.

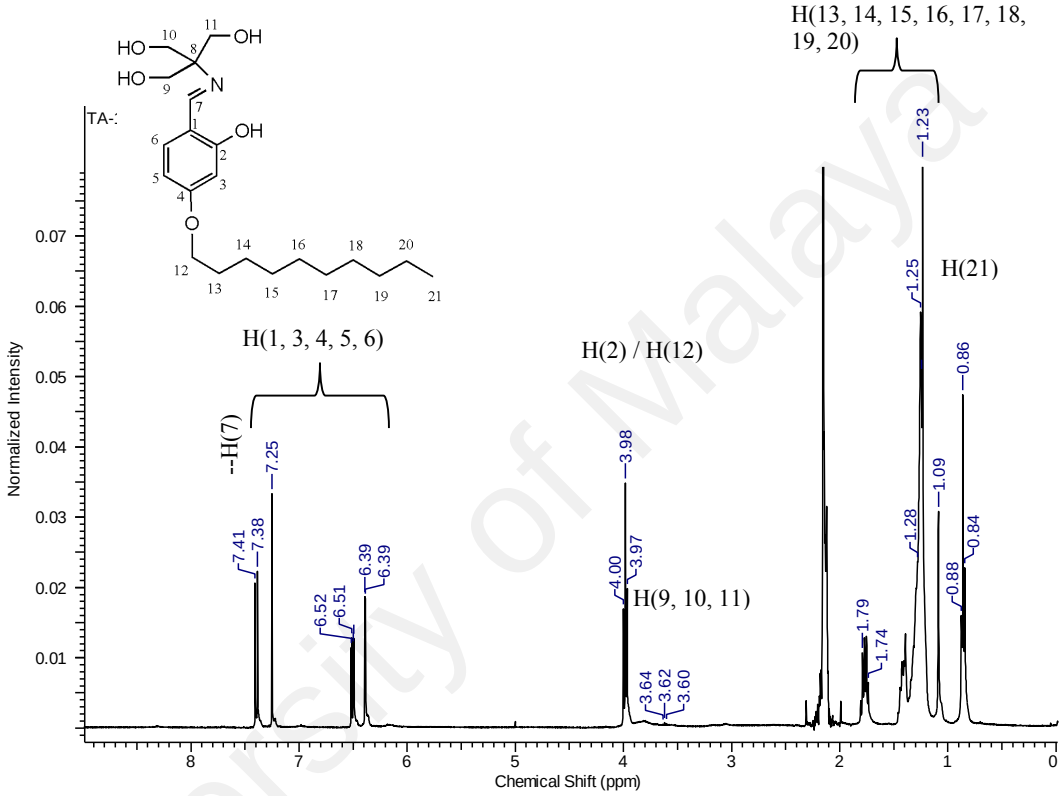

Figure 4.15: ^{1}H-NMR spectrum of TA

The methylene protons for long alkoxy chain H(13, 14, 15, 16, 17, 18, 19, 20 and 21, 22) of the ligands and complexes appeared as multiplets in the range from 1.20 - 1.68 ppm. While the signal for the methylene protons attached to hydroxyl H(9, 10, 11) was in the range of 3.56 - 3.91 ppm. The signal for methylene of alkoxy long chain H(12) appeared between 3.87 - 4.00 ppm (Sui et al., 2007). The ^{1}H NMR chemical shifts of the hydroxyl protons H(2) in the ligands were found to be 3.98 - 3.99 ppm, while for the diorganotin(IV) complexes, the chemical shifts were slightly downfield in the region of 4.03 - 4.93 ppm as the oxygen was bonded to tin(IV) atom. The integration value of the

University of Malaya

hydroxyl protons signal was decreasing for the diorganotin(IV) complexes, due to one oxygen atom of the Schiff base ligand being bonded to the tin(IV) atom *via* the replacement of one of the phenolic proton. When these synthesized ligands reacted with diorganotin(IV) ions, the ligands get deprotonated from one phenolic proton and one hydroxyl proton thus diorganotin(IV) complex is formed. Furthermore, the multiplet peaks at 6.02 - 7.41 ppm were assigned to the aromatic protons H(1, 3, 4, 5, 6) of the ligands and the diorganotin(IV) complexes. Meanwhile, a single peak at 7.41 ppm was assigned to the methine protons of the azomethine carbon H(7) of the ligand, and the signals were shifted downfield in the diorganotin(IV) complexes at the region 8.29-8.30 ppm. The value of azomethine proton observed was slightly lower from those reported for the Schiff base ligands (Sui et al., 2007). ^{1}H NMR chemical shifts are listed in Tables 4.14 and 4.15, respectively.

Table 4.14: ^{1}H NMR chemical shifts for TRIS ligands

Ligands/ δ (ppm)	**TA**	**TB**
H(1, 2, 3, 4, 5, 6)	6.39, d (1H, *J* = 2.4), 6.49-6.52, dd (1H, *J* = 9.2, 2.4) 7.38 (s, 1H)	6.39-6.40, d (1H, *J* = 2.4) 6.50-6.52, dd (1H, *J* = 8.4, 2.4) 7.39, s (1H)
H(7)	7.41 (s, 1H)	7.41 (s, 1H)
H(2)	3.98 (s, 3H)	3.99 (s, 3H)
H(12)	3.97-4.00 (m, 6H)	3.97-4.00 (m, 6H)
H(9, 10, 11)	3.60-3.64 (m, 2H)	3.61-3.64 (m, 2H)
H(21 and 23)	0.84-0.88, t (3H, *J* = 6.8)	0.84-0.88, t (3H, *J* = 6.8)
H(13, 14, 15, 16, 17, 18, 19, 20 and 21, 22)	1.23-1.81 (m, 18H)	1.24-1.79 (m, 20H)

University of Malaya

Table 4.15: ^{1}H NMR chemical shifts for TRIS diorganotin(IV) complexes

Complexes/ δ (ppm)	TA1	TA2	TB1	TB2
H(1, 2, 3, 4, 5, 6)	6.02-6.03,d (1H, *J* = 4.0) 6.17-6.19, dd (1H, *J* = 8.8, 2.1) 7.15-7.17, d (1H, *J* = 8.0)	6.38, d (1H, *J* = 2.0) 6.48-6.50 (m, 1H) 7.38-7.40 dd (1H, *J* = 7.2, 1.2)	6.02, d (1H, *J* = 2.4) 6.17-6.20, dd (1H, *J* = 8.8, 2.4) 7.16-7.18, d (1H, *J* = 8.8)	6.40, d (1H, *J* = 2) 6.50-6.53, dd (1H, *J* = 6.8, 2.0) 7.39-7.41, d (1H, *J* =8.0)
H(7)	8.29 (s, 1H)	8.30 (s, 1H)	8.29 (s, 1H)	8.30 (s, 1H)
H(2)	4.93 (s, 2H)	4.03 (s, 2H)	4.34 (s, 2H)	4.18 (s, 2H)
H(12)	3.87-3.99 (m, 6H)	3.96-3.99 (m, 6H)	3.96-3.99 (m, 6H)	3.95-3.97 (m, 6H)
H(9, 10, 11)	3.56-3.66 (m, 2H)	3.60-3.62 (m, 2H)	3.87-3.91 (m, 2H)	3.65-3.67 (m, 2H)
H(21 and 23)	0.79-0.83, t (3H, *J* = 8.0)	0.90-0.92, t (3H, *J* = 6.0)	0.79-0.83, t (3H, *J* = 8.0)	0.89-0.91, t (3H, *J* = 8.0)
H(13, 14, 15, 16, 17, 18, 19, 20 and 21, 22)	1.20-1.64 (m, 16H)	1.24-1.65 (m, 20H)	1.20-1.68 (m, 16H)	1.28-1.48 (m, 20H)
Sn-R (R = CH_3 : TA1 & TB1, R = $CH_2CH_2CH_2CH_3$: TA2 & TB2)	0.36 (s, 6H)	0.84-1.81 (m, 18H)	0.37 (s, 6H)	0.92-1.81 (m, 18H)

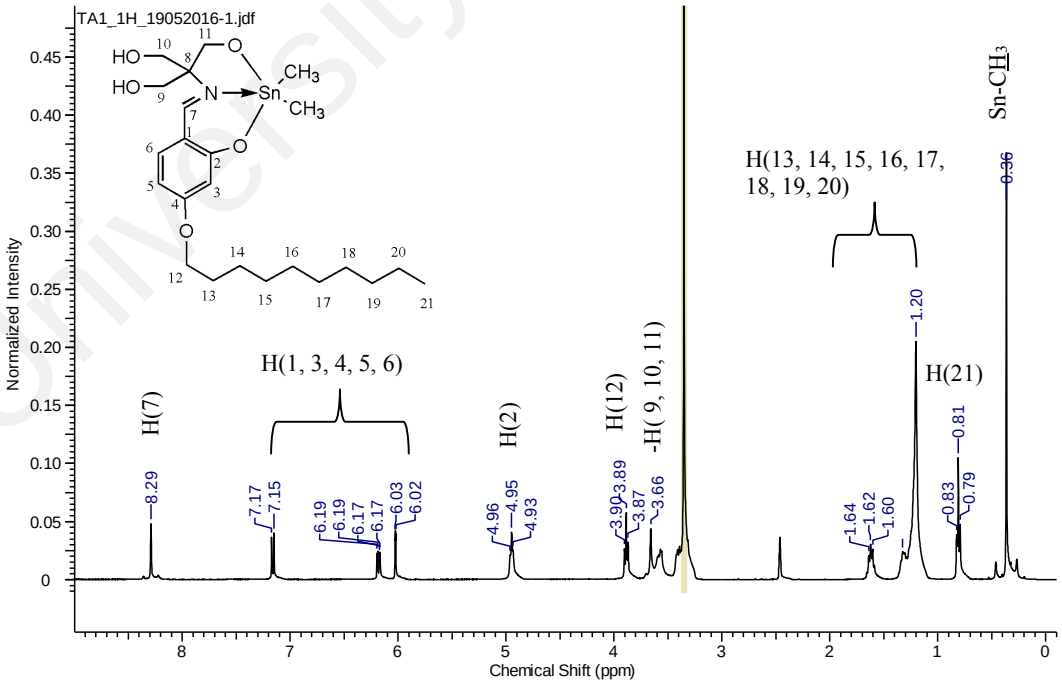

Figure 4.16: ^{1}H-NMR spectrum of TA1

University of Malaya

In the ^{13}C NMR spectrum of Schiff base ligands (Figure 4.17), signals of the azomethine carbons C(7) appeared at 166.57 ppm while in the diorganotin(IV) complexes it appeared at 166.56, 166.57 and 171.34 ppm.

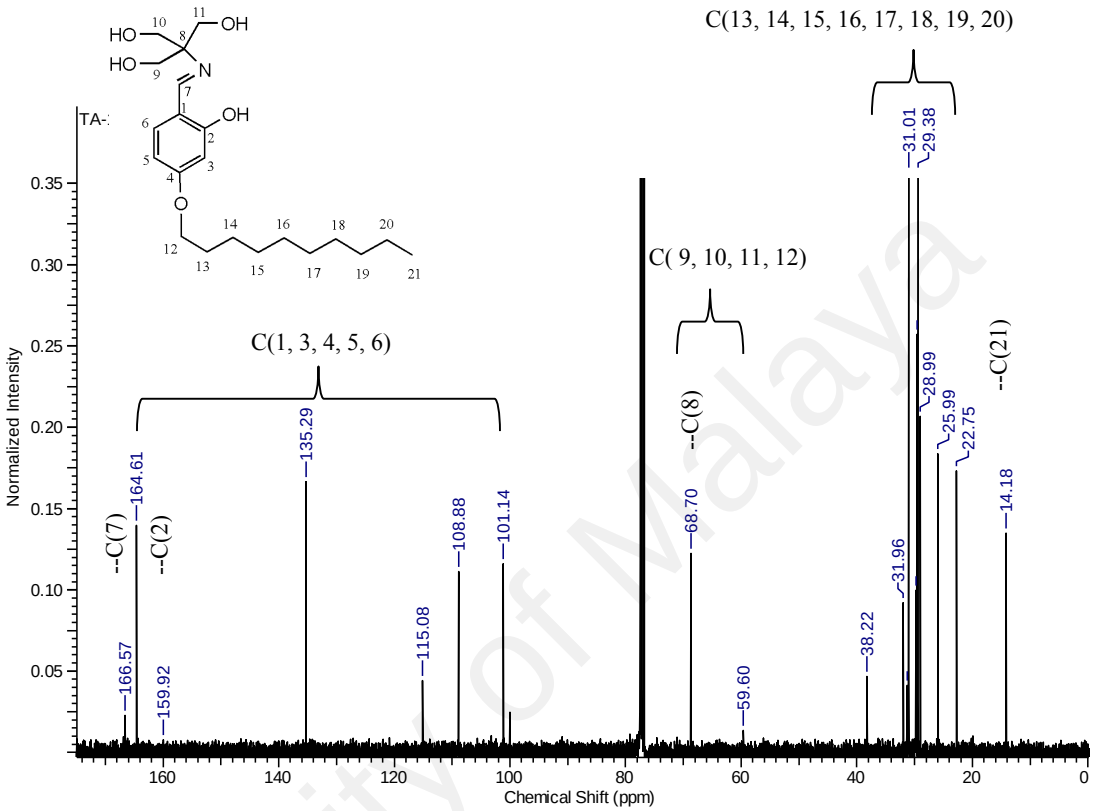

Figure 4.17: ^{13}C- NMR spectrum of TA

In addition, ^{13}C NMR spectra for TA1 complexes (Figure 4.18) displayed a significant downfield shift for the carbon resonances in comparison to the free ligands. C(2) is shifted to higher frequency in the complexes, 165.52, 162.66, 163.60 and 163.85 ppm for TA1, TA2, TB1 and TB2 respectively compared to the ligands 159.92 (TA) and 158.81 (TB) ppm, this is indicative that the phenolic hydrogen has been replaced by the tin(IV) atom (Mu et al., 2014). The chemical shift value for C(9, 10, 11) was found at 59.60 ppm for the ligands, while for the diorganotin(IV) complexes, its chemical shift value range was slightly wider, between 59.59 and 67.07 ppm, due to the influence of the interaction between the methylene oxygen with the tin(IV) atom. The aromatic carbons C (1, 3, 4, 5, 6) were assigned in the region at 101.14 - 164.61 ppm for Schiff base ligands and slightly

University of Malaya

downfield at 101.11 - 171.27 ppm for diorganotin(IV) complexes. The signals for the quarternary carbon C(8) were observed between 67.07 - 68.70 ppm in both ligands and diorganotin(IV) complexes. There is a new signal appeared in the complexes spectrum at 1.02 and 1.06 ppm for TA1 and TB1 respectively indicated the carbon of Sn-CH_3. These new signals at 13.66, 13.70, 18.97, 18.97, 26.57, 26.71, 27.20 and 27.35 ppm indicated for carbon bonded to Sn-$CH_2CH_2CH_2CH_3$ in TA2 and TB2 (Dey et al., 2011). While the ^{13}C NMR chemical shifts for TRIS ligands and its diorganotin(IV) complexes are listed in Tables 4.16. The structure of the ligands and its diorganotin complexes are shown in Figure 4.19.

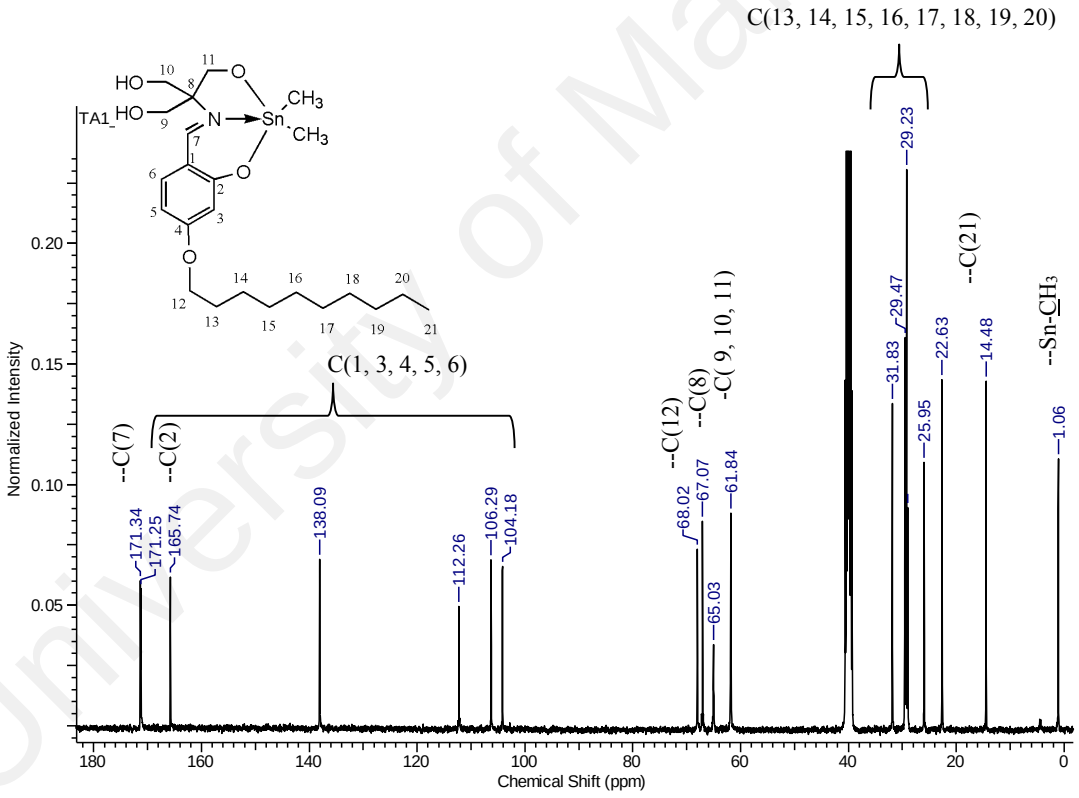

Figure 4.18: ^{13}C-NMR spectrum of TA1

University of Malaya

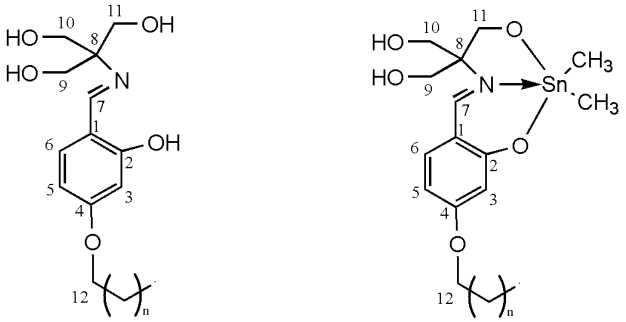

a) b)

TA: n = 8, TB: n = 10 TA1: R = CH_3, n = 8 , TA2: R = C_4H_9, n = 8
TB1: R = CH_3, n = 10, TB2: R = C_4H_9, n = 10

Figure 4.19: The structure of TRIS a) ligand and b) diorganotin(IV) complex

Table 4.16: ^{13}C NMR chemical shifts for TRIS compounds

Compound/ δ (ppm)	**TA**	**TA1**	**TA2**	**TB**	**TB1**	**TB2**
C(2)	159.92	165.74	162.66	158.27	163.60	163.85
C(7)	166.57	171.34	166.56	166.57	171.31	166.57
C(8)	68.70	67.07	68.69	68.70	68.04	68.70
C (9, 10, 11, 12)	59.60 68.70	61.84 65.03 68.02	51.58 62.76 68.69	59.60 68.70	67.07 68.04 68.52	62.86 63.21 59.59 68.70
C (1, 3, 4, 5, 6)	101.14 108.88 115.08 135.29 164.61	104.18 106.29 112.06 138.09 171.27	101.11 108.87 115.06 135.30 164.59	101.14 108.88 115.08 135.29 164.61	101.64 108.26 116.56 138.09 165.75	101.12 108.91 115.07 135.30 164.62
C (13, 14, 15, 16, 17, 18, 19, 20 and 21, 22)	22.75 25.99 28.99 29.38 29.61 29.78 31.01 31.96	22.63 25.95 29.01 29.23 29.23 29.47 29.51 31.83	22.75 25.98 28.98 29.38 29.60 29.77 31.52 31.95	22.77 25.99 28.99 29.38 29.61 29.70 29.72 29.78 31.01 31.99	22.61 25.89 25.93 28.92 28.99 29.23 29.48 29.53 31.19 31.81	22.79 25.99 26.71 28.99 29.43 29.62 29.71 29.79 31.32 32.00
C(21 and 23)	14.18	14.48	14.19	14.19	14.45	14.22
Sn-R : CH_3 and $CH_2CH_2CH_2CH_3$ (CH_3 : TA1 & TB1, and $CH_2CH_2CH_2CH_3$: TA2 & TB2)	None	1.06	13.70 18.97 27.35 26.71	None	1.02	13.66 18.97 27.20 26.57

University of Malaya

4.2.3 Magnetic susceptibility of the NAH transition metal complexes

(a) Bis[N'-(4-decyloxy-2-oxidobenzylidene)-3-hydroxy-2-naphthohydrazidato]-cobalt(II), CoNA

The value was calculated using the formula: $\mu_{eff} = 2.83[T(\chi_m^{corr} - N\alpha)]^{½}$, and the following data: Mw = 980.081 g mol^{-1}, $\chi_g = 4.78 \times 10^{-6}$ cm^3 g^{-1}, $\chi_m = 4.68 \times 10^{-3}$ cm^3 mol^{-1}, $\chi_{dia} = -1.72 \times 10^{-4}$ cm^3 mol^{-1}, and $\chi_m^{corr} = 4.86 \times 10^{-3}$ cm^3 mol^{-1}. Moments in the range of 4.7 - 5.2 B.M. and 2.0 - 2.2 B.M. are expected for high spin and low spin octahedral complexes respectively. However, a magnetic moment of 3.40 B.M. was observed for this CoNA complex at 298 K due a reasoned reported before which is a combination of spin equilibrium (spin-crossover) between the high spin and low spin octahedral geometries (Osowole et al., 2016). The magnetic moment observed was lower than the reported value which is in the range of 4.34 - 4.62 B.M. (Hanif & Chohan, 2013).

(b) Bis[N'-(4-dodecyloxy-2-oxidobenzylidene)-3-hydroxy-2-naphtho-hydrazidato]-nickel(II), NiNB

The value of μ_{eff}, calculated from the values of Mw = 1035.849 g mol^{-1}, $\chi_g = 6.43 \times 10^{-6}$ cm^3 g^{-1}, $\chi_m = 6.49 \times 10^{-3}$ cm^3 mol^{-1}, $\chi_{dia} = -1.72 \times 10^{-4}$ cm^3 mol^{-1}, and $\chi_m^{corr} = 6.67 \times 10^{-3}$ cm^3 mol^{-1} was 3.99 B.M. at 298 K which seems to agree with reported values of 3.80 - 4.02 B.M. (Mohamed et al., 2006). The moments in the range of 2.8 - 3.5 B.M were reported for high spin octahedral Ni(II) while low spin octahedral Ni(II) complexes were diamagnetic (Al-Shaheen et al., 2012; Osowole et al., 2016). The observed moment was a combined spin equilibrium (spin-crossover) between the high spin and low spin octahedral geometries.

University of Malaya

(c) Bis[N'-(4-dodecyloxy-2-oxidobenzylidene)-3-hydroxy-2-naphtho-hydrazidato]-copper(II), CuNB

The value of μ_{eff} was calculated using the same formula mentioned above at 298 K from the values of Mw = 1040.802 g mol^{-1}, $\chi_g = 2.14 \times 10^{-6}$ cm^3 g^{-1}, $\chi_m = 2.17 \times 10^{-3}$ cm^3 mol^{-1}, $\chi_{dia} = -1.72 \times 10^{-4}$ cm^3 mol^{-1}, and $\chi_m^{corr} = 2.34 \times 10^{-3}$ cm^3 mol^{-1} (Al-Ne'aimi, 2012). The magnetic moment value of 2.37 B.M. falls within the range normally observed for octahedral Cu(II) complexes (Mohamed et al., 2009). Mononuclear copper(II) complexes usually are observed in the range of 1.9 - 2.2 B.M. moment, regardless of stereochemistry, due to the orbital contribution and spin-orbit coupling moment is expectedly higher than the spin only moment (Osowole et al., 2016).

(d) The diamagnetic transition metal complexes of Zn(II) and Cd(II)

The Zn(II) and Cd(II) complexes were found to be diamagnetic in nature as expected for d^{10} configuration (Sunitha et al., 2012; Kumar et al., 2014).

4.2.4 Single crystal X-ray diffraction (SCXRD) study

The NA1 complex has a molecular formula of $Sn(CH_3)_2(C_{28}H_{32}N_2O_4)$. Crystal NA1 crystallized in monoclinic crystal system with *I2*/a space group as shown in Figure 4.20.

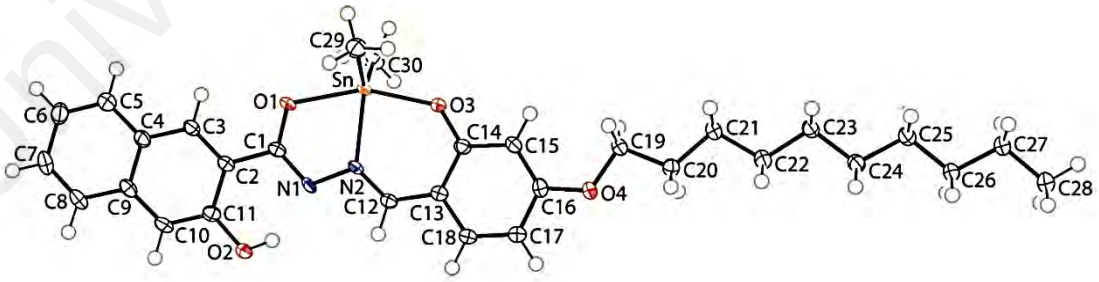

Figure 4.20: The molecular structure of NA1

The tin(IV) atom displays a distorted C_2NO_2 between ideal trigonal bipyramidal and square pyramidal. The bond angle of O(1) —Sn—O(3) is 157.14°, which it deviated from the ideal angle of 180°, thus showing the distorted trigonal bipyramidal geometry of the

University of Malaya

structure (Yang et al., 2016; Zafarian et al., 2017). The Schiff base coordinates to the tin(IV) atom as a tridentate ligand *via* the hydrazinyl-N atom, the hydroxyl O atom and the carbonyl O atom with the Sn—N(2) distance is 2.1503 (16) Å, Sn–O(1) bond lengths is 2.1600 (15) Å and Sn—O(3) bond length is 2.0984 (15) Å (Hong et al., 2013a). Other bond lengths such as Sn—C(29) and Sn—C(30) are 2.112 (2) Å and 2.106 (2) Å, respectively (Yang et al., 2016). All the bond distances are in good agreement with other previously known hydrazone diorganotin(IV) complexes in the literatures. Selected bond distances and angles are listed in Table 4.17.

Table 4.17: Selected bond lengths (Å) and bond angles (°) for NA1 crystal

Sn—O1	2.1600 (15)
Sn—O3	2.0984 (15)
Sn—N2	2.1503 (16)
Sn—C29	2.112 (2)
Sn—C30	2.106 (2)
O1—Sn—O3	157.14 (6)
O1—Sn—N2	73.16 (6)

The packing diagram of NA1 (Figure 4.21) showing an intramolecular hydroxyl-O-H···N(hydrazinyl) hydrogen bond, O(2)-H(2)O...N(1) 2.580 (2) is in close agreement with values reported in literature (Wang et al., 2014). The crystallographic details of NA1 crsytal is listed in Table 4.18.

University of Malaya

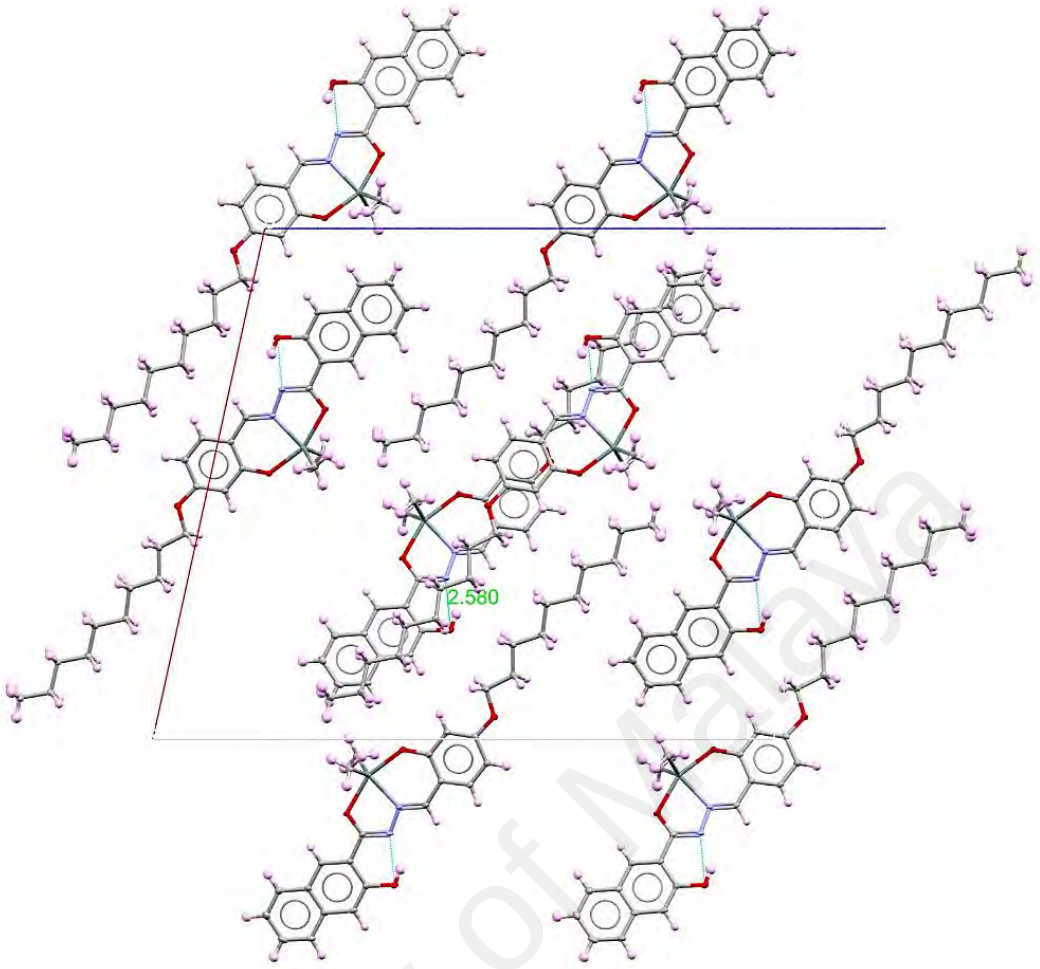

Figure 4.21: Packing diagram of NA1 showing hydrogen bonds interactions (2.580)

University of Malaya

Table 4.18: Crystallographic and refinement details for NA1 complex[1]

Empirical formula	$C_{30}H_{38}N_2O_4Sn$
Formula weight	609.31
Temperature/K	100
Crystal system	Monoclinic
Space group	*I*2/*a*
a / Å	25.2622 (9)
b / Å	7.4543 (2)
c / Å	29.9819 (11)
α / °	90.00
β / °	102.349 (4)
γ / °	90.00
Volume / Å^3	5515.3 (3)
Z	8
μ / mm^{-1}	0.96
Radiation	Mo *Kα,* λ = 0.71073 Å
Crystal size / mm	0.26 × 0.21 × 0.09
Absorption coeficient, (mm^{-1}), F(000)	2512
T_{min}, T_{max}	0.756, 1.000
No. of measured, independent and observed I > 2σ(I) reflections	38191, 7182, 6371
R_{int}	0.038
(sin $\theta/\lambda)_{max}$ (Å^{-1})	0.696
R *[*F^2 > *2σ(*F^2*)]*, wR*(*F^2*)*, S	0.031, 0.076, 1.01
Data/restraints/parameters	7182/1/340
$\Delta\rho_{max}$, $\Delta\rho_{min}$ (e Å^{-3})	0.80, -1.32
(Δ/σ)max	0.006

[1] Computer programs: QMol (Gans & Shalloway, 2001), DIAMOND (Brandenburg, 2006), SHELXS (Sheldrick, 2008), publCIF (Westrip, 2010), ORTEP-3 for Windows (Farrugia, 2012), SHELXL2014 (Sheldrick, 2015) and CrysAlis PRO (Rigaku Oxford Diffraction, 2015).

University of Malaya

4.2.5 CHNS elemental analysis

Elemental analysis were done to several compounds only. Even though, the found values have more than +/- 0.40 % difference than the calculated values, but the range was not too far. The differences of percentage CHN calculated value of complexes from found values were probably influenced by the presence of solvent residue or impurities in the compounds (Sainorudin et al., 2015). Type of solvents such as water, DMF, ethyl acetate, and ethanol. For example, a trace of ethanol and water can be spotted in the NA1 ^{1}H NMR spectrum as shown in Figure 4.11. A small peak at 1.25, 1.42 and 3.72 ppm for ethanol and 1.56 ppm for water residue peak (Gottlieb et al., 1997; Babij et al., 2016). Data for elemental analysis for C, H, and N are shown in Table 4.19.

Table 4.19: Elemental analysis of diorganotin(IV) complexes

Complexes	Element% Anal. Calc (Found)			Differences %		
	C	H	N	C	H	N
NA1	59.13 (60.20)	6.29 (7.17)	4.60 (4.21)	-1.07	-0.88	0.39
NB1	60.30 (59.09)	6.64 (7.63)	4.39 (5.38)	1.21	-0.72	-0.99
NB2	63.25 (63.92)	7.54 (7.67)	3.88 (3.99)	-0.67	-0.13	-0.11
TA1	52.29 (51.75)	7.44 (7.33)	2.65 (2.25)	0.54	0.11	0.4

4.3 Part 2: Anticancer studies

4.3.1 Cytotoxicity activities of NAH ligands and its diorganotin(IV) complexes

By using the MTT assay, cytotoxic activity of NAH Schiff base ligands and its diorganotin(IV) complexes were summarized in Table 4.20. Cisplatin was used as positive control, and the IC_{50} values of HT29 and MCF7 were taken from Lee et al., (2013).

All NA series reported good cytotoxic activities for HT29 cell lines in the range of 0.17 - 1.62 μg mL^{-1}. For NA series, the effect of carbon chain length on the substituent of the complexes was clearly seen that the ligand have better anticancer activity than the dimethyltin(IV) and dibutyltin(IV) complexes against HT29. Nevertheless, the series

University of Malaya

demonstrated poor cytotoxic activity against MCF7 cell line. Meanwhile, for NB series, all compounds displayed very weak cytotoxic activity in both tested cell lines, except for NB2 against MCF7 which was 0.25 μg mL^{-1}.

In short, among this diorganotin(IV) complexes, NA1 showed the lowest IC_{50} value equivalent with excellent cytotoxicity activities when tested *in vitro* across two human cancer cell lines, indicating its high potential as an anticancer drug. Overall, the NA series were more selective towards HT29 cancer cell line, while the NB series were more selective towards MCF7 cancer cell line. The results also indicate that different type of alkyl groups attached to the organotin(IV) moiety has different effects on anticancer activity (Hong et al., 2013a). Many organotin(IV) compounds dibutyltin(IV) derivatives reported have displayed both higher activity and lower toxicity (Singh & Singh, 2014). The degree of toxicity for alkyl group substituted organotin(IV) complexes varies with the certain organism tested (Carraher & Roner, 2014).

Table 4.20: Cytotoxic activities of NAH ligands and its diorganotin(IV) complexes

Compounds	IC_{50} (μg mL^{-1})*	
	HT29	MCF7
Cisplatin (Lee et al., 2013)	5.0± 0	2.4±0.6
NA	0.17 ± 0.03	10.51 ± 0.37
NA1	0.29 ± 0.03	8.35 ± 0.87
NA2	1.62 ± 0.61	>30
NB	10.54 ± 1.34	9.23 ± 0.912
NB1	>30	9.82 ± 0.76
NB2	>30	0.25 ± 0.02

*IC_{50} values (μg mL^{-1}) = inhibition concentration at 50%, i.e., concentration to reduce growth of cancer cells by 50%.

University of Malaya

4.3.2 Cytotoxicity activities of TRIS ligands and its diorganotin(IV) complexes

The results of cytotoxic activity of TRIS ligands and diorganotin(IV) complexes on HT29 and MCF7 cell lines were analyzed using mean of cell viability and expressed as IC_{50} values are shown in Table 4.21. Cisplatin was used as positive control and its IC_{50} values of HT29 and MCF7 were taken from Lee et al., (2015).

The results showed that the ligands and complexes resulted in good cytotoxic activities for both cells at 2.34 - 5.70 μg mL^{-1}. Also, complexes TA2 and TB2 reported better cytotoxic activity than TA1 and TB1 towards HT29 and MCF7 cell lines. Generally, the dibutyltin(IV) derivatives of TA and TB series were more cytotoxic than dimethyltin(IV) against both cell lines. Furthermore, TA2 and TB2 (n = 10) which have a longer chain of carbon on the ligand as substituent showed better cytotoxicity activity than TA1 and TB1 (n = 12).

The end results indicated that majority of all the compounds react selectively towards HT29 cells, the longer carbon chain length on the ligand as substituent gives better anticancer activities and different type of alkyl groups attached to the organotin(IV) moiety result in different effects of anticancer activity (Hong et al., 2014).

Table 4.21: Cytotoxic activities of TRIS ligands and its diorganotin(IV) complexes

Compounds	IC_{50} (μg mL^{-1})	
	HT29	MCF7
Cisplatin (Lee et al., 2013)	5.0 ± 0	2.4 ± 0.6
TA	5.17 ± 0.66	5.70 ± 0.52
TA1	10.04 ± 0.70	0.74 ± 0.14
TA2	0.98 ± 0.51	2.24 ± 0.16
TB	2.34 ± 0.32	5.26 ± 0.35
TB1	3.98 ± 0.57	6.32 ± 0.71
TB2	0.56 ± 0.20	2.07 ± 0.39

University of Malaya

4.4 Part 3: Formulation studies of diorganotin(IV) complexes from previous research conducted by Lee (2010)

The diorganotin(IV) complexes from a previous research were used in the formulation part (Lee et al., 2012; Lee et al., 2013). The general structure of the complexes is shown in Figure 4.22, while its names are listed in Table 4.22.

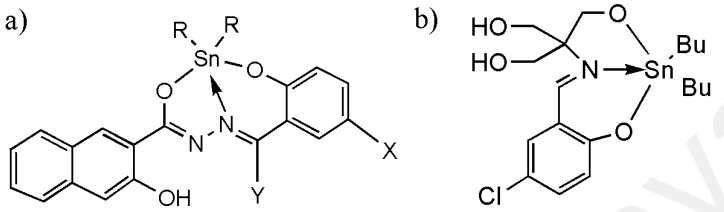

Figure 4.22: General structures of (a) NAH diorganotin(IV) complexes and (b) TC2 diorganotin(IV) complexes

Table 4.22: List of anticancer drugs of NAH and TRIS diorganotin(IV) complexes

Diorganotin(IV) complexes	Molecular weight, g/mol
R = Me, X = Br, Y = H; **NC1**	531.967
R = Bu, X = Br, Y = H; **NC2**	616.127
R = Me, X = Cl, Y = H; **ND1**	487.516
R = Bu, X = Cl, Y = H; **ND2**	571.678
R = Me, X = Br, Y = CH_3; **NE1**	545.994
R = Bu, X = Cl, Y = CH_3; **NF2**	585.590
R = Bu, X = Cl; **TC2**	678.500

4.4.1 Preparation of niosome-encapsulated diorganotin(IV) complexes

The microencapsulation vesicle (MCV) method is reported to produce homogenous particle size with a high encapsulation efficiency and good stability. Frequently, the outcome is influenced by the preparation conditions, such as a type of organic solvent, intensity, and the time of mechanical agitation in each emulsification (Ohshima & Makino, 2014). By using MCV method, the formulation of niosome-encapsulated ND2 with 10 mM concentration produces a particle size of 278 ± 25 nm if agitated overnight. Two hours agitation yields three peaks which are 724 ± 289 nm, 207 ± 52 nm and

University of Malaya

5370 ± 329 nm with the fraction of 87%, 11%, and 2% respectively. In addition, the particle size can be reduced down to 128 ± 13 nm with ethanol injection method.

4.4.2 Percentages of drug encapsulation efficiency, %EE and drug loading, %DL

The general structures of diorganotin(IV) complexes of NC to NF series and TC2 are shown in the Figure 4.23. The percentage of encapsulation efficiency, %EE and drug loading, %DL were calculated and tabulated in Table 4.23.

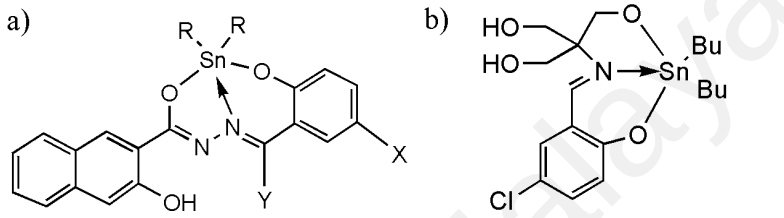

Figure 4.23: General structure of the diorganotin(IV) complexes where (a) is the structure for NC-NF series while (b) is the structure for TC2

Table 4.23: %EE, %DL and IC_{50} (µg mL^{-1}) values of (HT29) and (MCF7) of diorganotin(IV) complexes and common drugs

Complexes	%EE	%DL	HT29	MCF7
R=Me, X=Br, Y=H, **NC1**	99	88	5.0 ± 0.0	17 ± 3.6
R=Bu, X=Br, Y=H, **NC2**	>99	89	6.7 ± 0.6	5.3 ± 0.6
R=Me, X=Cl, Y=H, **ND1**	97	86	6.0 ± 0.0	71 ± 4.6
R=Bu, X=Cl, Y=H, **ND2**	>99	89	2.3 ± 1.2	8.5 ± 0.5
R=Me, X=Br, Y=CH_3, **NE1**	80	85	0.9 ± 0.1	0.62 ± 0.01
R=Bu, X=Br, Y= CH_3, **NF2**	>99	88	0.7 ± 0.0	0.69 ± 0.01
R=Bu, X=Cl, **TC2**	99	87	8.2 ± 0.2	2.2 ± 1.2
5-Fluorouracil	55	4	2.6 ± 0.4	12.03 ± 1.49
	(Fan et al., 2014)		(Flis & Splawinski, 2009)	(Li et al., 2013)
Paclitaxel	80	31	0.061± 0.001	7.0 ±9.2
	(Joshi et al., 2014)		(Dagar et al., 2012)	(Sain et al., 2006)

University of Malaya

The trend in NC and ND series showed that bigger molecular weight of the diorganotin(IV) complexes would result in higher loading efficiency. That could be due to the saturation of the media with diorganotin(IV) complexes that forces the drug to be encapsulated into niosomes (Mokhtar et al., 2008). Furthermore, the encapsulation efficiency and drug loading were found to be in the range of 80 - 99% and 86 - 89%, respectively. Moreover, both values for %EE and %DL of the synthesized diorganotin(IV) complexes were higher than the common drugs, such as 5-fluorouracil and paclitaxel. The diorganotin(IV) complexes were hydrophobic drugs that have poor solubility in water. Despite the formulations for hydrophobic drugs are normally uneasy, it has the advantage of providing a higher percentage of encapsulation efficiency as reported in Mehta and Jindal (2013) where all the hydrophobic drugs showed %EE more than 90%.

Paclitaxel is a hydrophobic drug and %EE reported as 80%. The synthesized diorganotin(IV) complexes showing higher %EE compared to paclitaxel because their molecular structures are smaller. Paclitaxel has a molecular weight of 853.906 g/mol while the molecular weight of the synthesized diorganotin(IV) complexes are in a range of 487.516 to 637.781 g/mol. NC2, ND2, and NF2 showed the highest encapsulation efficiencies with values are about 99%. The reason for the high encapsulation efficiencies for hydrophobic drugs is they do not leak due to diffusion (Nii & Ishii, 2005). Moreover, the chain length of the glycolipid surfactant could also affect the encapsulation efficiency of the drug. The glycolipid used in this formulation is a branched chain, containing a total of 16 carbons and the longer chain part is with 10 carbons. The longer the chain length, the higher the encapsulation efficiency (Kumar & Rajeshwarrao, 2011). Furthermore, the series of NC, ND, NE, and NF contained more ring in their structures than the TC series; yet the entrapment efficiency for the TC2 complex was almost similar, at 99%.

University of Malaya

4.4.3 Particle size and zeta potential measurements

DLS was used to measure particle size and zeta potential of drug loaded niosomes. Two complexes, ND2 and TC2 were used as prototypical drugs for the encapsulation and characterization. The size distribution and its percentage, polydispersity index (PDI) and their zeta potential are displayed in Table 4.24**.**

Table 4.24: The size and zeta potential of selected complexes

Complex, concentration	Method	PDI	Size, nm	%	Zeta potential, mV
No	MCV	0.2	278±25	100	-
No	Ethanol injection	0.3	97±1	100	-
ND2, 10 mM	Ethanol injection	0.3	128±13	100	-25±2
ND2, 10 mM	MCV (agitated overnight)		278±25	100	-
ND2, 10 mM	MCV	0.4	724±289 207±52 5370±329	75 23 2	-33±5
ND2, 25 mM	MCV (fresh)	0.3	627±257 164 ±37 5327±376	87 11 2	Not measured
	MCV (after 3 days)	0.2	402±200 4316±1023	97 3	Not measured
ND2, 50 mM	MCV (fresh)	0.3	431±112 113±16	92 8	Not measured
	MCV (after 3 days)	0.2	400±215 5227±458	>99 <1	Not measured
TC2, 10 mM	MVC (fresh)	0.2	269±96 4744±753	95 5	-36±5
	MCV (after 3 days)	0.2	296±132 4816±717	99 1	Not measured

The particle size measured with the light scattering is presented as a size in diameter and goes along with the PDI. PDI is the square of the light scattering polydispersity. This is used to describe the degree of "non-uniformity" of a distribution. For a perfectly uniform sample, the PDI would be 0.0. If the PDI values are between 0.1 - 0.25, indicating a narrow size distribution, while a PDI greater than 0.5 was related to a broad distribution

University of Malaya

(Lobato et al., 2013; Wu et al., 2013). In this research, the PDI is in a range of 0.2 to 0.4. Ethanol injection method enables to produce nanosize carriers.

Another physical property that obtained from the light scattering measurement is the zeta potential. A zeta potential measurement enables to predict the stability of a colloidal formulation. The high magnitude of zeta potentials indicates strong repulsive interactions of the carriers with the encapsulated drugs, which stabilize a colloidal dispersion, while low zeta potential indicates instability in terms of coagulation or flocculation. Zeta potentials value in a range between 0 mV to ±5 mV refers to rapid coagulation or flocculation. While a range of 10 mV to 30 mV, positive or negative, indicates developing instability. Reasonable stability is the value in between 30 mV and 40 mV, whereas good stability requires a range from 40 mV to 60 mV. Zeta potentials exceeding 60 mV are related with tremendous dispersion stability (Greenwood & Kendall, 1999; Hanaor et al., 2012; Hussen & Heidelberg, 2016). The zeta potentials ND2 were of -25±2 mV and -33±5 mV based on two different methods and environment. The 5% ethanol v/v is suspected to be the reason why the outcome from ethanolic injection method showing slightly low value. The formulation of TC2 gives -36.2 mV.

Overall, drug formulation with diorganotin(IV) complexes was reasonably stable. The zeta potential could be related to surfactant type or encapsulation efficiencies that might affect the zeta potential values according to what has been reported (Bayindir & Yuksel, 2009). In this case, the ethanol acting as a co-surfactant hence influenced the stability of the formulation. However, the benefit to use ethanol injection method is the particle size was much smaller with lower PDI.

4.4.4 Niosome morphology

Only the morphology of niosome-encapsulated ND2 was studied as an example in this work due to its higher percentage of encapsulation efficiency and a higher percentage of

University of Malaya

drug loading among other complexes. The concentration of the niosome-encapsulated diorganotin(IV) complex is 10 mM and was prepared using MCV method. The photomicrograph is shown in Figure 4.24.

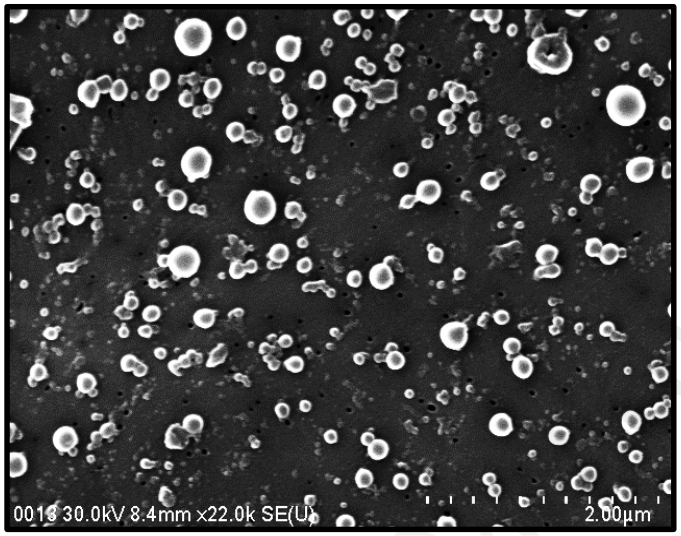

Figure 4.24: The photomicrograph of ND2 niosome

The photomicrograph confirmed that the drug carriers are niosome because they were spherical in shape as reported for vesicles (Mehta & Jindal, 2013; Anbarasan et al., 2013). The photomicrograph also is in agreement with the DLS measurement. Based on the DLS measurement, there are varies in size where the biggest niosomes are about 2%. Furthermore, a few niosomes in micro size are spotted and there are more particles below 1000 nm as well.

4.4.5 *In vitro* release study

The *in vitro* release study of the niosome-encapsulated ND2 was conducted. The niosome-encapsulated diorganotin(IV) complexes were freshly prepared using MCV method and was examined for more than 100 days. The release profiles of ND2 is shown in Figure 4.25.

University of Malaya

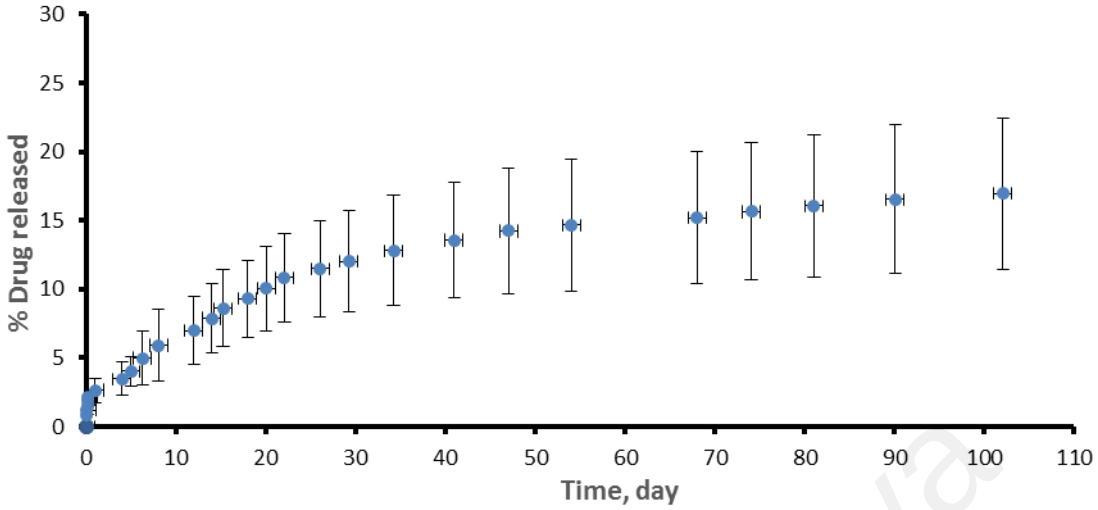

Figure 4.25: *In vitro* release profile of ND2 formulation in 102 days, data represents mean, n=2

It was observed that the release rate of ND2-niosomes sharply increased to 2.6% in 24 hours. The release was significant up to about day 50, the R^2 value was obtained 0.986 in Higuchi plot, 0.799 in the first order, and that 0.939 in zero order. This shows the best fit with higher correlation was found with the Higuchi's equation thus, ND2 release exhibits a linear relationship against the square-root of time. The entrapped ND2 was still releasing but slowly even until the last day it was observed. Even though the ND2 complex is suitable for colon cancer treatment, oral delivery is not suitable for the drug administration. Oral administration is designed for immediate release of drug for rapid absorption. As an anticancer drug, intravenous administration is one of the suitable way to manage the niosome-encapsulated ND2. Moreover, based on the release study, this formulation can achieve a prolonged therapeutic effect by continuously releasing medication over an extended period of time after administration of a single dosage. Common anticancer drugs for treating colon and breast such as paclitaxel and 5-fluorouracil are administered through an intravenous injection (Saville et al., 1995).

University of Malaya

CHAPTER 5: CONCLUSION

A total of eighteen compounds were synthesized and characterized in this work but several compounds were used in the niosomal formulation and anticancer activities. These compounds comprised of four Schiff base ligands derived from either NAH or TRIS ligand, four NAH and four TRIS diorganotin(IV) complexes, and ten other metal complexes. The compounds were characterized using IR, ^{1}H, and ^{13}C NMR spectroscopies and elemental analysis. In ^{1}H NMR and IR studies, the observations indicated that -C=N-N=C- hydrazone bond in the aliphatic free ligands could undergo keto-enol tautomerism. In TRIS diorganotin(IV) complexes spectrum, ν(C=N) bands are all shifted to lower wavenumbers compared to the free ligand due to coordination of the metal to the imine nitrogen. The magnetic susceptibility analysis showed that the transition metal complexes were octahedral geometry and paramagnetic, except for Cd(II) and Zn(II), which were diamagnetic and not transition metal. Single crystal structures were solved for one compound only. The SCXRD studies showed the distorted features of a C_2NO_2 coordination geometry falling in between the ideal trigonal bipyramidal and square pyramidal for the NA1 crystal. The space group of a NA1 crystal is *I2*/a, and it was crystallized in a monoclinic crystal system.

In terms of anticancer properties, it was proven by cytotoxic activity that the most promising diorganotin(IV) complexes were NA1 and TB2. The IC_{50} value of NA1 were 0.29 ± 0.03 μg mL^{-1} for HT29 and 8.35 ± 0.87 μg mL^{-1} for MCF7, while for TB2 against HT29 and MCF7, the IC_{50} values were 0.56 ± 0.20 μg mL^{-1} and 2.07 ± 0.39 μg mL^{-1}, respectively. Both showed the highest cytotoxicity activity when tested *in vitro* across both human cancer cell lines, indicating its significant potential for both HT29 and MCF7 anticancer drugs. In terms of the overall activities, the diorganotin(IV) complexes were selectively more on colon cancer cell line. Even though, as stated in Chapter 1 the focuses of this research is to design the anticancer drugs for breast cancer, only NB2 and TA1

University of Malaya

showing excellent IC_{50} values for MCF7 which were 0.25 ± 0.02 and 0.74 ± 0.14 respectively. It was evident that the anticancer activities of the complexes were strongly dependent on their respective substituents. Considering, the serious side effects and upcoming resistance of clinical reference drugs, these several new compounds are more useful candidates for the development of novel therapeutic agents to treat cancer.

The encapsulation efficiency of the niosome-encapsulated NAH diorganotin(IV) complexes was in a range of between 80 to 99%. The study on the niosome-encapsulated ND2 confirmed that it is in a spherical shape and their sizes were within the desired range for intravenous injection administration route, which was about 100 nm prepared by ethanolic injection method. The drug formulation is reasonable stable based on the zeta potential value. Niosome-encapsulated ND2 complex showed a slow drug release profile for 102 days. Therefore, niosome-encapsulated diorganotin(IV) complex is a good candidate for sustain and control release for longer periods of time.

For future work, the structures for the rest of complexes studied in this work need to be ascertained by X-ray crystallography of single crystals and CHN analysis. The anticancer activities of other metal complexes also can be pursued to determine whether they will exhibit good cytotoxicity. The formulation of the new compounds in this work has yet to be studied besides the compounds obtained from the previous work. Therefore, efforts to determine the percentage of encapsulation efficiency and drug loading, size, morphology and also drug release of the compounds will be continued. This is important in order to increases the compounds chances of succeeding in *in vitro* assay, clinical trials and ultimately to be used as therapeutic drugs. Furthermore, for future study, one of it could be to find out what is the required level of drug within the desired (or therapeutic) range.

University of Malaya

REFERENCES

Abramenko, V. L., Churakov, A. V, Sergienko, V. S., Mikhailov, Y. N., and Surazhskaya, M. D. (2013). Inner complex compounds of dioxomolybdenum(VI) with *o*-oxyazomethines, derivatives of substituted salicylaldehydes and *tris*(hydroxymethyl)aminomethane. Crystal structures of two complexes [MoO(L)]•CH_3OH; L= Z substituted salicylalimines Z = 3-NO_2 and 3-OCH_3. *Russian Journal of Coordination Chemistry*, *39*(8), 553-559.

Abu-Dief, A. M. and Mohamed I. M. A. (2015). A review on versatile applications of transition metal complexes incorporating Schiff bases. *Journal of Basic and Applied Sciences*, *4*, 119-133.

Abu-Sbeih, A. K. and Abu-Yamin, A. A. (2014). Reduced Schiff base zinc complexes as proposed models of the active site of the dinuclear zinc enzyme A. Aminopeptidase. *Journal of Chemical and Pharmaceutical Research*, *6*(7), 162-171.

Ahlawat, A., and Asijaa, S. (2016). Synthesis, characterization of organotin(IV) complexes of Schiff base ligands and evaluation of their biological activities against pathogenic bacteria and fungi. *International Journal of Chemical and Physical Sciences*, 5(4), 34-43.

Ahmad, M. S., Hussain, M., Hanif, M., Ali, S., and Mirza, B. (2007). Synthesis, chemical characterization and biological screening for cytotoxicity and antitumor activity of organotin(IV) derivatives of 3,4-methylenedioxy-6-nitrophenylpropenoic acid. *Molecules*, *12*, 2348-2363.

Akbarzadeh, A., Rezaei-Sadabady, R., Davaran, S., Joo, S. W., Zarghami, N., Hanifehpour, Y., Samiei, M., Kouhi, M., and Nejati-Koshki, K. (2013). Liposome: Classification, preparation, and applications. *Nanoscale Research Letters*, *8*, 102-110.

Akhilesh, D., Bini, K. B., and Kamath, J. V. (2012). Review on Span-60 based non-ionic surfactant vesicles (Niosomes) as novel drug delivery. *International Journal of Research in Pharmaceutical and Biomedical Sciences*, *3*(1), 6-12.

Albayrak, C., Odabasoglu, M., Buyukgungor, O., and Lonnecke, P. (2004). 5-(2-Chlorophenyldiazenyl)salicylaldehyde and 4-(2-chlorophenyldiazenyl)-2-{[*tris*(hydroxymethyl)methyl]aminomethylene}cyclohexa-3,5-dien-1(2*H*)-one. *Acta Crystallographica Section C: Crystal Structure Communications*, *60*(5), o318-o320.

University of Malaya

Alibolandi, M., Sadeghi, F., Abnous, K., Atyabi, F., Ramezani, M., and Hadizadeh, F. (2015). The chemotherapeutic potential of doxorubicin-loaded PEG-b-PLGA nanopolymersomes in mouse breast cancer model. *European Journal Pharmaceutics and Biopharmaceutics*, *94*, 521-531.

Al-Ne'aimi Mohammed, M. (2012). Synthesis and characterization of *bis*-acylhydrazone derivatives as tetradentate ligands and their dinuclear metal(II) complexes. *Periodica Polytechnica, Chemical Engineering*, *56*(2), 83-90.

Al-Shaheen, A. J., Sallomi, I. J., and Al-Sabaawi, S. A. (2012). Preparation, characterization of acid hydrazide Schiff base complexes of nickel(II) and their biological activity. *National Journal of Chemistry*, *48*, 482-492.

Anbarasan, B., Rekha, S., Elango, K., Shriya, B., and Ramaprabhu, S. (2013). Optimization of the formulation and *in-vitro* evaluation of capecitabine niosomes for the treatment of colon cancer. *International Journal of Pharmaceutical Sciences and Research*, *4*(4), 1504-1513.

Andresen, T. L., Jensen, S. S., and Jørgensen, K. (2005). Advanced strategies in liposomal cancer therapy: problems and prospects of active and tumor specific drug release. *Progress in Lipid Research*, *44*(1), 68-97.

Arjmand, F., Parveen, S., Tabassum, S., and Pettinari, C. (2014). Organotin antitumor compounds: their present status in drug development and future perspectives. *Inorganica Chimica Acta*, *423*, 26-37.

Arnott, J. A., and Planey, S. L. (2012). The influence of lipophilicity in drug discovery and design. *Expert Opinion on Drug Discovery*, *7*(10), 863-875.

Aryal, S., Hu, C. M. J., Fu, V., and Zhang, L. (2012). Nanoparticle drug delivery enhances the cytotoxicity of hydrophobic-hydrophilic drug conjugates. *Journal of Materials Chemistry*, *22*(3), 994-999.

Babij, N. R., McCusker, E. O., Whiteker, G. T., Canturk, B., Choy, N., Creemer, L. C., Amicis, C. V. D., Hewlett, N. M., Johnson, P. L. Knobelsdorf, J. A., Li, F., Lorsbach, B. A., Nugent,B. M., Ryan,S. J., Smith, M. R., and Yang, Q. (2016). NMR chemical shifts of trace impurities: industrially preferred solvents used in process and green chemistry. *Organic Process Research & Development*, *20*(3), 661-667.

Bagheri, A., Chu, B. S., and Yaakob, H. (2014). Niosomal drug delivery systems: Formulation, preparation and applications. *World Applied Sciences Journal*, *32*(8), 1671-1685.

University of Malaya

Bagihalli, G. B., Avaji, P. G., Patil, S. A., and Badami, P. S. (2008). Synthesis, spectral characterization, *in vitro* antibacterial, antifungal and cytotoxic activities of Co(II), Ni(II) and Cu(II) complexes with 1,2,4-triazole Schiff bases. *European Journal of Medicinal Chemistry*, *43*(12), 2639-2649.

Bayindir, Z. S., and Yuksel, N. (2009). Characterization of niosomes prepared with various nonionic surfactants for paclitaxel oral delivery. *Pharmaceutical Technology*, *99*(4), 2049-2060.

Bei, D., Meng, J., and Youan, B.-B. C. (2010). Engineering nanomedicines for improved melanoma therapy: progress and promises. *Nanomedicine, 5*(9), 1385-99.

Bhat, M., Murali M, Belagali, S. L., and Amruthesh. K. N. (2014). Synthesis, characterization and biological activities of hydrazide Schiff's Bases. *International Journal of Chemical and Physical Sciences*, *3(*6), 82-90.

Bikas, R., Farzaneh-Bonab, H., Noshiranzadeh, N., Aygün, M., Emami, M., and Lis, T. (2018). Coumarin-naphthohydrazone ligand with a rare coordination mode to form Mn (II) and Co (II) 1-D coordination polymers: synthesis, characterization, and crystal structure. *Journal of Coordination Chemistry*, 1-20.

Bourne, D. W. (2001). *Routes of drug administration. Intravenous*. Retrieved 2 June 2015, from https://www.boomer.org/c/p1/Ch07/Ch0704.html

Brandenburg, K. (2006). *Diamond*. Crystal Impact GbR, Bonn, Germany.

Bui, N. T. H., Verhage, J. J., and Irgum, K. (2010). *Tris*(hydroxymethyl)aminomethane-functionalized silica particles and their application for hydrophilic interaction chromatography. *Journal of Separation Science*, *33*(19), 2965-2976.

Carraher Jr, C. E., & Roner, M. R. (2014). Organotin polymers as anticancer and antiviral agents. *Journal of Organometallic Chemistry*, *751*, 67-82.

Chew, S. T, Lo, K. M., Lee, S. K., Heng, M. P., Teoh, W. Y., Sim, K. S., and Tan, K. W. (2014). Copper complexes with phosphonium containing hydrazone ligand: Topoisomerase inhibition and cytotoxicity study. *European Journal of Medicinal Chemistry*, *76*, 397-407.

Chohan, Z. H., Sumrra, S. H., Youssoufi, M. H., and Hadda, T. B. (2010). Metal based biologically active compounds: Design, synthesis, and antibacterial/ antifungal/ cytotoxic properties of triazole-derived Schiff bases and their oxovanadium(IV) complexes. *European Journal of Medicinal Chemistry*, *45*(7), 2739-2747.

University of Malaya

Corvo, M. L., Mendo, A. S., Figueiredo, S., Gaspar, R., Larguinho, M., da Silva, M. F. C. G., Baptista, P. V., and Fernandes, A. R. (2016). Liposomes as delivery system of a Sn(IV) complex for cancer therapy. *Pharmaceutical Research*, *33*(6), 1351-8.

Dagar, A., Kuzmis, A., Rubinstein, I., Sekosan, M., and Onyuksel, H. (2012). VIP-targeted cytotoxic nanomedicine for breast cancer. *Drug Delivery and Translational Research*, *2*(6), 454-462.

Das, S., Das, M. K., Mazumder, P. M., Das, S., and Basu, S. P. (2009). Cytotoxic activity of methanolic extract of Berberis aristata DC on colon cancer. *Global Journal of Pharmacology*, *3*(3), 137-140.

De Jong, W. H., and Borm, P. J. (2008). Drug delivery and nanoparticles: Applications and hazards. *International Journal of Nanomedicine*, *3*(2), 133-149.

Deng, J., Gou, Y., Chen, W., Fu, X., and Deng, H. (2016). The Cu/ligand stoichiometry effect on the coordination behavior of aroyl hydrazone with copper(II): Structure, anticancer activity and anticancer mechanism. *Bioorganic & Medicinal Chemistry*, *24*(10), 2190-2198.

Devi, J., Batra, N., and Malhotra, R. (2012). Ligational behavior of Schiff bases towards transition metal ion and metalation effect on their antibacterial activity. *Spectrochimica Acta - Part A: Molecular and Biomolecular Spectroscopy*, *97*, 397-405.

Dhahagani, K., Kumar, S. M., Chakkaravarthi, G., Anitha, K., Rajesh, J., Ramu, A., and Rajagopal, G. (2014). Synthesis and spectral characterization of Schiff base complexes of Cu(II), Co(II), Zn(II) and VO(IV) containing 4-(4-aminophenyl) morpholine derivatives: Antimicrobial evaluation and anticancer studies. *Spectrochimica Acta Part A: Molecular and Biomolecular Spectroscopy*, *117*, 87-94.

Dhamecha, D. L., Rathi, A. A., Saifee, M., Lahoti, S. R., and Hassan D. M. G. (2009). Drug vehicle based approaches of penetration enhancement. *International Journal of Pharmacy and Pharmaceutical Sciences*, *1*(1), 24-46.

Dhand, C., Prabhakaran, M. P., Beuerman, R. W., Lakshminarayanan, R., Dwivedi, N., and Ramakrishna, S. (2014). Role of size of drug delivery carriers for pulmonary and intravenous administration with emphasis on cancer therapeutics and lung-targeted drug delivery. *Royal Society of Chemistry Advances*, *4*(62), 32673-32689.

University of Malaya

Doğan, H. N., Duran, A., and Rollas, S. (2005). Synthesis and preliminary anticancer activity of new 1H-4, 5-dihydro-3-(3-hydroxy-2-naphthyl)-4-substituted-1, 2, 4-triazole-3-thiones. *Indian Journal of Chemistry Setion B*, *44*, 2301-7.

Dotson, R. L. (1972). Characterization and studies of some four, five and six coordinate transition and representative metal complexes of *tris*(hydroxymethyl)-aminomethane. *Journal Inorganic and Nuclear Chemistry, 34*, 3131-3138.

Doyle, G. R., and McCutcheon, J. A. (2016). *Clinical Procedures for Safer Patient Care*. Campus Manitoba.

Drbohlavova, J., Chomoucka, J., Adam, V., Ryvolova, M., Eckschlager, T., Hubalek, J., and Kizek, R. (2013). Nanocarriers for anticancer drugs - new trends in nanomedicine. *Current Drug Metabolism*, *14*(5), 547-564.

Dutta, S., Bendre, R., Padhye, S., Ahmed, F., and Sarkar, F. (2005). Synthesis, antioxidant properties and antiproliferative activities of tetrameric copper and copper-zinc metal complexes of catecholamine Schiff base ligand. *Synthesis and Reactivity in Inorganic, Metal-Organic, and Nano-Metal Chemistry*, *35*(1), 3-10.

El-tabl, A. S., Abd El-Waheed, M. M., Wahba, M. A., and Abou El-fadl, N. A. E. (2015). Synthesis, characterization, and anticancer activity of new metal complexes derived from 2-hydroxy-3-(hydroxyimino)-4-oxopentan-2-ylidene)-benzohydrazide. *Bioinorganic Chemistry and Applications, 2015,* 1-14.

Fan, Y. L., Fan, B. Y., Li, Q., Di, H. X., Meng, X. Y., and Ling, N. (2014). Preparation of 5-fluorouracil-loaded nanoparticles and study of interaction with gastric cancer cells. *Asian Pacific Journal of Cancer Prevention*, *15*(18), 7611-7615.

Farrugia, L. J. (2012).). WinGX and ORTEP for Windows: an update. *Journal of Applied Crystallography*. *45*(4), 849-854.

Flis, S., and Spławiński, J. (2009). Inhibitory effects of 5-fluorouracil and oxaliplatin on human colorectal cancer cell survival are synergistically enhanced by sulindac sulfide. *Anticancer Research*, *29*(1), 435-441.

Gans, J. D., and Shalloway, D. (2001). Qmol: a program for molecular visualization on Windows-based PCs. *Journal of Molecular Graphics and Modelling*, *19*(6), 557-559.

University of Malaya

Garza-Ortiz, A., Camacho-Camacho, C., Sainz-Espuñes, T., Rojas-Oviedo, I., Gutiérrez-Lucas, L. R., Gutierrez Carrillo, A., and Vera Ramirez, M. A. (2013). Novel organotin(IV) Schiff base complexes with histidine derivatives: Synthesis, characterization, and biological activity. *Bioinorganic Chemistry and Applications*, *2013*.

Geral, C., Angelova, A., and Lesieur, S. (2013). From molecular to nanotechnology strategies for delivery of neurotrophins: Emphasis on brain-derived neurotrophic factor (BDNF). *Pharmaceutics*, *5*(1), 127-167.

Gottlieb, H. E., Kotlyar, V., and Nudelman, A. (1997). NMR chemical shifts of common laboratory solvents as trace impurities. *The Journal of Organic Chemistry*, *62*(21), 7512-7515.

Greenwood, R., and Kendall, K. (1999). Selection of suitable dispersants for aqueous suspensions of zirconia and titania powders using acoustophoresis. *Journal of the European Ceramic Society*, *19*(4), 479-488.

Gujral, S. S., and Khatri, S. (2013). A review on basic concept of drug targeting and drug carrier system. *International Journal of Advances in Pharmacy, Biology and Chemistry*, *2*(1), 2277-4688.

Haas, K. L., and Franz, K. J. (2009). Application of metal coordination chemistry to explore and manipulate cell biology. *Chemical Reviews*, 109, 4921-4960.

Hadjikakou, S. K., and Hadjiliadis, N. (2009). Antiproliferative and anti-tumor activity of organotin compounds. *Coordination Chemistry Reviews*, *253*(1-2), 235-249.

Haeri, A., Alinaghiana, B., Daeihamed, M., and Dadashzadeh, S. (2014). Preparation and characterization of stable nanoliposomal formulation of fluoxetine as a potential adjuvant therapy for drug-resistant tumors. *Iranian Journal of Pharmaceutical Research*, *13*, 3-14.

Hanaor, D., Michelazzi, M., Leonelli, C., and Sorrell, C. C. (2012). The effects of carboxylic acids on the aqueous dispersion and electrophoretic deposition of ZrO_2. *Journal of the European Ceramic Society*, *32*(1), 235-244.

Hanif, M., and Chohan, Z. H. (2013). Design, spectral characterization and biological studies of transition metal(II) complexes with triazole Schiff bases. *Spectrochimica Acta Part A: Molecular and Biomolecular Spectroscopy*, *104*, 468-476.

University of Malaya

Harewood, G. R. (2007). *Synthesis, characterization and structure elucidation of some salicylaldimine-based ligands and their corresponding metal complexes*. (Ph.D. thesis) . University of the West Indies. Jamaica.

Hillery, A. M., Lloyd, A. W., and Swarbrick, J. (Eds.). (2005). *Drug delivery and targeting: for pharmacists and pharmaceutical scientists*. London: CRC Press.

Hirlekar, R., Jain, S., Patel, M., Garse, H., and Kadam, V. (2010). Hexosomes: a novel drug delivery system. *Current Drug Delivery*, *7*(1), 28-35.

Hong, M., Yin, H., Zhang, X., Li, C., Yue, C., and Cheng, S. (2013a). Di- and tri-organotin(IV) complexes with 2-hydroxy-1-naphthaldehyde-5-chloro-2-hydroxybenzoylhydrazone: Synthesis, characterization and *in vitro* antitumor activities. *Journal of Organometallic Chemistry, 724*, 23-31.

Hong, M. Yin, H. D., Zhang, Y. W., Jiang, J., and Li, C. (2013b). Coordination geometry of monomeric, dimeric and polymeric organotin(IV) compounds constructed from 5-bromopyridine-2-carboxylic acid and mono-, di- or tri-organotin precursors. *Journal of Molecular Structure*, *1036*, 244-251.

Hong, M., Geng, H., Niu, M., Wang, F., Li, D., Liu, J., and Yin, H. (2014). Organotin(IV) complexes derived from Schiff base N'-[(1E)-(2-hydroxy-3-methoxyphenyl)methylidene]pyridine-4-carbohydrazone: Synthesis, *in vitro* cytotoxicities and DNA/BSA interaction. *European Journal of Medicinal Chemistry*, *86*, 550-561.

Hua, S. (2014). Orally administered liposomal formulations for colon targeted drug delivery. *Frontier in Pharmacology*, *5*, 1-4.

Hunter, J. (2008). Intramuscular injection techniques. *Nursing Standard*, *22*(24), 35-40.

Hussain, M., Shafiq, Z., Nawaz, M. H., Shad, M. A., Nawaz, H., Yaqub, M., and Ahmad, H. B. (2013). Synthesis, characterization and biological evaluation of some novel hydrazide Schiff's bases and their metal complexes. *Asian Journal of Chemistry*, *25*(5), 2268-2672.

Hussen, R. S. D. (2010). *Preparation and evaluation of vesicles based on non-ionic branched chain glycolipids*. (Ph.D thesis). Universiti Malaya, Kuala Lumpur, Malaysia.

University of Malaya

Hussen, R. S. D. (2012). *Niosomes from chain-branched glycolipids for drug delivery. Synthesis, formulation and evaluation. United Kingdom*: Lambert Academic Publishing.

Hussen, R. S. D., and Heidelberg, T. (2016). Drug carriers in cancer therapy: Administration, formulation and characterization. *International Journal of Pharma Research and Review*, *5*(4), 37-45.

Islam, M. B., Islam, M. S., Rabbi, M. A., Rahman, M. M., Islam, M. J., and Hossain, M. (2013). Synthesis and ^{1}H NMR spectroscopic characterization of long alkoxy chains bearing Schiff base ligand. *Bangladesh Research Publications Journal*, *8*(3), 250-259.

Jaafar-Maalej, C., Diab, R., Andrieu, V., Elaissari, A., and Fessi, H. (2010). Ethanol injection method for hydrophilic and lipophilic drug-loaded liposome preparation. *Journal of Liposome Research*, *20*(3), 228-243.

Jadhav, S. M., Morey, P., Karpe, M. M., and Kadam, V. (2012). Novel vesicular system: An overview. *Journal of Applied Pharmaceutical Science*, *2*(1), 193-202.

Jayarajan, R., Vasuki, G., and Rao, P. S. (2010). Synthesis and antimicrobial studies of tridentate Schiff base ligands with pyrazolone moiety and their metal complexes. *Organic Chemistry International*, *2010*, 165-170.

Joshi, N., Shirsath, N., Singh, A., Joshi, K. S., and Banerjee, R. (2014). Endogenous lung surfactant inspired pH responsive nanovesicle aerosols: pulmonary compatible and site-specific drug delivery in lung metastases. *Scientific Reports*, *4*, 7085-7093.

Jin, J. F., Zhu, L. L., Chen, M., Xu, H. M., Wang, H. F., Feng, X. Q., Zhu, X. P., and Zhou, Q. (2015). The optimal choice of medication administration route regarding intravenous, intramuscular, and subcutaneous injection. *Patient Preference and Adherence*, *9*, 923-942.

Kallet, R. H., Jasmer, R. M., Luce, J. M., Lin, L. H., and Marks, J. D. (2000). The treatment of acidosis in acute lung injury with *tris*(hydroxymethyl)aminomethane (THAM). *American Journal of Respiratory and Critical Care Medicine*, *161*, 1149-1153.

Kaluderovic, G. N., & Paschke, R. (2011). Anticancer metallotherapeutics in preclinical development. *Current Medicinal Chemistry*, *18*(31), 4738-4752.

University of Malaya

Kang, W., Wu, X., and Huang, J. (2009). Synthesis, crystal structure and biological activities of four novel tetranuclear diorganotin(IV) carboxylates. *Journal of Organometallic Chemistry*, *694*(15), 2402-2408.

Kavitha, P., Chary, M. R., Singavarapu, B. V. V. A., and Reddy, K. L. (2013). Synthesis, characterization, biological activity and DNA cleavage studies of tridentate Schiff bases and their Co(II) complexes. *Journal of Saudi Chemical Society*, *20*(1), 69-80.

Kavitha, N., and Lakshmi, P. V. A. (2015). Synthesis, characterization and thermogravimetric analysis of Co(II), Ni(II), Cu(II) and Zn(II) complexes supported by ONNO tetradentate Schiff base ligand derived from hydrazino benzoxazine. *Journal of Saudi Chemical Society, 21*, S457-S466. .

Kemula, W., Brachaczek, W., and Hulanicki, A. (1962). Potentiometric investigation of metal-*tris*(hydroxymethyl)aminomethane complexes. *Theory and Structure of Complex Compounds*, 605-610.

Koch B, Baul, T. S. B., and Chatterjee, A. (2008). Structure-activity relationships for thiol reactivity and rat or human hepatocyte toxicity induced by substituted *p*-benzoquinone compounds. *Journal of Applied Toxicology*, *28*(4), 430-438.

Kronberg, B., Holmberg, K., and Lindman, B. (2014). Types of surfactants, their synthesis, and applications. *Surface Chemistry of Surfactants and Polymers*, 1-47.

Kumar, G. P., and Rajeshwarrao, P. (2011). Nonionic surfactant vesicular systems for effective drug delivery-an overview. *Acta Pharmaceutica Sinica B*, *1*(4), 208-219.

Kumar Naik, K. H., Selvaraj, S., and Naik, N. (2014). Metal complexes of ONO donor Schiff base ligand as a new class of bioactive compounds: Synthesis, characterization and biological evolution. *Spectrochimica Acta-Part A: Molecular and Biomolecular Spectroscopy, 131*, 599-605.

Kumar, S., Dhar, D. N., and Saxena, P. N. (2009). Applications of metal complexes of Schiff bases - a review. *Journal of Scientific and Industrial Research*, *68*(3), 181-187.

Lai, C. K., Chen, F. G., Ku, Y. J., Tsai, C.H., and Lin, R. (1997). Formation of disordered hexagonal arrangements in *bis*(β,δ-triketonato)copper(II) complexes. *Journal of Chemical Society, Dalton Trans*, (24), 4683-4688.

University of Malaya

Lampman, G. M., Pavia, D. L., Kriz, G. S., and Vyvyan, J. A. (2010). *Spectroscopy* (4th ed.). Bellingham, Washington: Cengage Learning.

Laouini, A., Jaafar-Maalej, C., Limayem-Blouza, I., Sfar, S., Charcosset, C., and Fessi, H. (2012). Preparation, characterization and applications of liposomes: state of the art. *Journal of Colloid Science and Biotechnology*, *1*(2), 147-168.

Lavasanifar, A., Samuel, J., and Kwon, G. S. (2002). Poly(ethylene oxide)-block-poly(L-amino acid) micelles for drug delivery. *Advanced Drug Delivery Reviews*, *54*(2), 169-190.

Lee, S. M. (2010). *Synthesis, structures and bioinorganic aspects of organotin(IV) derivatives*. (Ph.D. thesis) . Universiti of Malaya. Kuala Lumpur, Malaysia.

Lee, S. M., Mohd Ali, H., Sim, K. S., Abdul Malek, S. N., and Lo, K. M. (2012). Synthesis, structural characterization and *in vitro* cytotoxicity of diorganotin complexes with Schiff base ligands derived from 3-hydroxy-2-naphthoylhydrazide. *Applied Organometallic Chemistry*, *26*(6), 310-319.

Lee, S. M., Mohd. Ali, H., Sim, K. S., Abdul Malek, S. N., and Lo, K. M. (2013). Synthesis, characterization and biological activity of diorganotin complexes with ONO terdentate Schiff base. *Inorganica Chimica Acta*, *406*, 272-278.

Lee, S. M., Sim, K. S., and Lo, K. M. (2015). Synthesis, characterization and biological studies of diorganotin(IV) complexes with *tris*(hydroxymethyl)aminomethane Schiff bases. *Inorganica Chimica Acta*, *429*, 195-208.

Li, X., Kong, X., Kong, X., Wang, Y., Yan, S., and Yang, Q. (2013). 53BP1 sensitizes breast cancer cells to 5-fluorouracil. *Plos One*, *8*(9), e74928.

Liu, R. (Ed.). (2008). *Water Insoluble Drug Formulation*. (2nd ed.). London: CRC Press.

Liu, W., Li, H., Zhao, B., Shin, D., Lian, S., and Miao, J. (2009). Synthesis of novel ribavirin hydrazone derivatives and anti-proliferative activity against A549 lung cancer cells. *Carbohydrate Research*, *344*(11), 1270-1275.

Liu, W. (2014). Controlled anticancer drug delivery. *Austin Journal Biomedical Engineering*, *1*(1), 1004-1013.

University of Malaya

Lobato, K. B. S., Paese, K., Forgearini, J. C., Guterres, S. S., Jablonski, A., and de Oliveira Rios, A. (2013). Characterisation and stability evaluation of bixin nanocapsules. *Food Chemistry*, *141*(4), 3906-3912.

Madhav, N. V. S., and Saini, A. (2011). Niosomes: A novel drug delivery system. *International Journal of Research in Pharmacy and Chemistry*, *1*(3), 498-511.

Madni, A., Sarfraz, M., Rehman, M., Ahmad, M., Akhtar, N., Ahmad, S., Tahir, N., Ijaz, S., Al-Kassas, R., and Löbenberg, R. (2014). Liposomal drug delivery: A versatile platform for challenging clinical Applications. *Journal Pharmacy & Pharmaceutical Science, 17*(3), 401-426.

Majumder, S., Pasayat, S., Roy, S., Dash, S. P., Dhaka, S., Maurya, Reichelt, M., Reuters, H., and Dinda, R. (2018). Dioxidomolybdenum (VI) complexes bearing sterically constrained aroylazine ligands: Synthesis, structural investigation and catalytic evaluation. *Inorganica Chimica Acta*, *469*, 366-378.

Makeshwar, K. B., and Wasankar, S. R. (2013). Niosome: A novel drug delivery system. *Asian Journal Pharmaceutical Research*, *3*(1), 16-20.

Mak, O. W., Seman, N., Harun, N. H., Syahila, R., Hussen, D., Rodzi, N. M., and Heidelberg, T. (2015). Nanovesicles based on mixtures of a biantennary glycolipid with ionic co-surfactants. *Journal of Surfactants and Detergents*, *18*(6), 973-980.

Manosroi, A., Wongtrakul, P., Manosroi, J., Sakai, H., Sugawara, F., Yuasa, M., and Abe, M. (2003). Characterization of vesicles prepared with various non-ionic surfactants mixed with cholesterol. *Colloids and Surfaces*, *30*(1), 129-138.

Marianecci, C., Rinaldi, F., Esposito, S., Di Marzio, L., and Carafa, M. (2013). Niosomes encapsulating ibuprofen-cyclodextrin complexes : Preparation and characterization. *Current Drug Targets*, *14*(9), 1070-1078.

Martínez, R. F., Avalos, M., Babiano, R., Cintas, P., Jimenez, J. L., Light, M. E., and Palacios, J. C. (2011). Schiff bases from TRIS and ortho-hydroxyarenecarbaldehydes : Structures and tautomeric equilibria in the solid state and in solution. *European Journal of Organic Chemistry*, 3137-3145.

Mehta, S. K., and Jindal, N. (2013). Formulation of tyloxapol niosomes for encapsulation, stabilization and dissolution of anti-tubercular drugs. *Colloids and Surfaces B: Biointerfaces*, *101*, 434-441.

University of Malaya

Miao, J. Y. (2012). Synthesis, characterization, and crystal structures of two oxidomolybdenum(VI) complexes with hydrazones derived from 3-hydroxy-2-naphthoic hydrazide. *Synthesis and Reactivity in Inorganic, Metal-Organic, and Nano-Metal Chemistry*, *42*(10), 1463-1466.

Mögele, F., Fantauzzi, D., Wiedwald, U., Ziemann, P., and Riege, B. (2009). Two-dimensional assembly of magnetic binuclear complexes: a scanning tunneling microscopy study. *Langmuir*, *25*(23), 13606-13613.

Mohamed, G. G., Omar, M. M., and Hindy, A. M. (2006). Metal complexes of Schiff bases: Preparation, characterization, and biological activity. *Turkish Journal of Chemistry*, *30*(3), 361-382.

Mohamed, G. G., Omar, M. M., and Ibrahim, A. A. (2009). Biological activity studies on metal complexes of novel tridentate Schiff base ligand. Spectroscopic and thermal characterization. *European Journal of Medicinal Chemistry*, *44*(12), 4801-4812.

Mokhtar, M., Sammour, O. A., Hammad, M. A., and Megrab, N. A. (2008). Effect of some formulation parameters on flurbiprofen encapsulation and release rates of niosomes prepared from proniosomes. *International Journal of Pharmaceutics*, *361*(1), 104-111.

Morsy, S. M. I. (2014). Role of surfactants in nanotechnology and their applications. *International Journal of Current Microbiol and Applied Science*, *3*(5), 237-260.

Mosmann, T. (1983). Rapid colorimetric assay for cellular growth and survival: Application to proliferation and cytotoxicity assays. *Journal of Immunological Methods*, *65*(1-2), 55-63.

Muhammad, N., and Guo, Z. (2014). Metal-based anticancer chemotherapeutic agents. *Current Opinion in Chemical Biology*, *19*, 144-153.

Nagaj, J., Stokowa-Soltys, K., Kurowska, E., Fraczyk, T., Jezowska-Bojczuk, M., and Bal, W. (2013). Revised coordination model and stability constants of Cu(II) complexes of *tris* buffer. *Inorganic Chemistry*, *52*(24), 13927-13933.

Nair, P., Kaur, S., and Sharma, Y. P. (2008). Effect of time taken in injecting subcutaneous heparin injection with reference to site pain and bruising among patients receiving heparin therapy. *Nursing and Midwifery Research Journal*, *4*(1), 7-15.

University of Malaya

Nath, M., Saini, P. K. and Kumar, A. (2010). New di- and triorganotin(IV) complexes of tripodal Schiff base ligand containing three imidazole arms: Synthesis, structural characterization, anti-inflammatory activity and thermal studies. *Journal of Organometallic Chemistry*, *695*(9), 1353-1362.

Ndagi, U., Mhlongo, N., and Soliman, M. E. (2017). Metal complexes in cancer therapy–an update from drug design perspective. *Drug Design, Development and Therapy*, *11*, 599-616.

Ng, S. W. (2008). Low-temperature redetermination of 4-chloro-2-[*tris*(hydroxymethyl)methyliminomethyl]phenol as zwitterionic 4-chloro-2-[*tris*(hydroxymethyl)methyliminiomethyl]phenolate. *Acta Crystallographica Section E Structure Reports Online*, 639-642.

Nii, T., and Ishii, F. (2005). Encapsulation efficiency of water-soluble and insoluble drugs in liposomes prepared by the microencapsulation vesicle method. *International Journal of Pharmaceutics*, *298*(1), 198-205.

Nii, T and Ishii, F. (2007). The novel liposome preparation methods based on in-water drying and phase separation : Microencapsulation vesicle method and coacervation method. *Advances in Planar Lipid Bilayers and Liposomes*, *5*, 41-61.

Nikolova-Mladenova, B., Momekov, G., Gerassimova, T., and Topashka-Ancheva, M. (2009). Comparative evaluation of *in silico* and *in vitro* pharmacological activity of some 5-nitrosalicylaldehyde-derived hydrazones. *International Scientific Journal Medical and Biological Sciences*, *1*, 44-48.

Niu, L., Li, Y., and Li, Q. (2014). Medicinal properties of organotin compounds and their limitations caused by toxicity. *Inorganica Chimica Acta*, *423*, 2-13.

Odabaşoğlu, M., Albayrak, Ç., Özkanca, R., Aykan, F. Z., and Lonecke, P. (2007). Some polyhydroxy azo–azomethine derivatives of salicylaldehyde: Synthesis, characterization, spectroscopic, molecular structure and antimicrobial activity studies. *Journal of Molecular Structure*, *840*(1), 71-89.

Ohshima, H., and Makino, K. (Eds). (2014). *Colloid and interface science in pharmaceutical research and development*. Amsterdam: Elsevier.

Onnis, V., Cocco, M. T., Fadda, R., and Congiu, C. (2009). Synthesis and evaluation of anticancer activity of 2-arylamino-6-trifluoromethyl-3-(hydrazonocarbonyl) pyridines. *Bioorganic and Medicinal Chemistry*, *17*(17), 6158-6165.

University of Malaya

Osowole, A. A., Wakil, S. M., and Okediran, E. Q. (2016). Synthesis, characterization and antimicrobial activities of some metal(II) complexes of mixed ligands-dimethyl dithiocarbamic and para aminobenzoic acids. *Applied Chemistry*, *79*, 30375-30378.

Pandit, K. S., Chavan, P. V., Desai, U. V., Kulkarni, M. A., and Wadgaonkar, P. P. (2015). *Tris*-hydroxymethylaminomethane (THAM): A novel organocatalyst for a environmentally benign synthesis of medicinally important tetrahydrobenzo [b] pyrans and pyran-annulated heterocycles. *New Journal of Chemistry*, *39*(6), 4452-4463.

Pavia, D. L., Lampman, G. M., Kriz, G. S., and Vyvyan, J. A. (2014). *Introduction to Spectroscopy* (5th ed.). Bellingham, Washington: Cengage Learning.

Pawanoji, A. A. and Mehta, B. H. (2009). Synthesis, characterization and x-ray diffraction studies of Co(II), Ni(II) and Pd(II) complexes of Schiff base derived from 3-hydroxy benzaldehyde and 3-hydroxy-2-naphthoic hydrazide. *Asian Journal of Chemistry*, *21*(9), 6869-6876.

Pei, X. H., Zhan, X. H., Wang, S. M., Lin, Y. S., and Zhou, L. X. (2010). Effects of a biosurfactant and a synthetic surfactant on phenanthrene degradation by a Sphingomonas strain. *Pedosphere*, *20*(6), 771-779.

Pereyre, M., Quintard, J. P., and Rahm, A. (2013). *Tin in organic synthesis*. United Kingdom: Butterworth-Heinemann.

Piver, W. T. (1973). Organotin compounds: Industrial applications and biological investigation. *Environmental Health Perspectives, 4,* 61-79.

Pourayoubi, M., Saneei, A., Dušek, M., Rostami, S. A., Crochet, A., and Kučeraková, M. (2015). Two new organotin(IV)-phosphoryl complexes: Crystal structure and Hirshfeld surface analysis. *Journal of the Iranian Chemical Society*, *12*(12), 2093-2103.

Prasad, K. S., Kumar, L. S., Prasad, M., and Revanasiddappa, H. D. (2010). Novel organotin(IV)-Schiff base complexes: Synthesis, characterization, antimicrobial activity, and DNA interaction studies. *Bioinorganic Chemistry and Applications*, *2010*, 1-9.

Prasad, K. S., Kumar, L. S., Revanasiddappa, H. D., Vijay, B., and Jayalakshmi, B. (2011). Synthesis, characterization and antimicrobial activity of Cu(II), Co(II), Ni(II), Pd(II) and Ru(III) complexes with clomiphene citrate. *Chemical Sciences Journal, 7,* 28-39.

University of Malaya

Puri, A., Loomis, K., Smith, B., Lee, J. H., Yavlovich, A., Heldman, E., and Blumenthal, R. (2010). Lipid-based nanoparticles as pharmaceutical drug carriers: From concepts to clinic. *Critical Reviews in Therapeutic Drug Carrier Systems*, *26*(6), 1-46.

Qin, W., Long, S., Panunzio, M., and Biondi, S. (2013). Schiff bases: A short survey on an evergreen chemistry tool. *Molecules*, *18*(10), 12264-12289.

Qurban, S. W. (2011). Synthesis and characterization of some transition metal complexes of Schiff bases derived from isonicotinic hydrazide and o-vanillin. *Diyala Journal for Pure Sciences*, *7*(2), 94-104.

Raddatz, S., Mueller-Ibeler, J., Kluge, J., WaB, L., Burdinski, G., Havens, J. R., Onofrey, T., J., Wang, D., and Schweitzer, M. (2002). Hydrazide oligonucleotides: New chemical modification for chip array attachment and conjugation. *Nucleic Acids Research*, *30*(21), 4793-4802.

Revathi, S. and Dhanaraju, M. D. (2014). Hexosomes as a novel drug delivery system: A review. *International Journal of Pharmacy and Pharmaceutical Science*, *6*, 58-63.

Rigaku Oxford Diffraction. (2015). *Crsyalis Pro*. Agilent Technologies Inc. Santa Clara, CA, USA.

Rosen, M. J., and Kunjappu, J. T. (2012). *Surfactants and interfacial phenomena* (4th ed.). New Jersey: John Wiley & Sons Inc.

Saadeh, S. M. (2013). Synthesis, characterization and biological properties of Co (II), Ni (II), Cu (II) and Zn (II) complexes with an SNO functionalized ligand. *Arabian Journal of Chemistry*, *6*(2), 191-196.

Sadler, P. (2009). Dalton transactions themed issue on metal anticancer compounds. *Dalton Transactions, 8*, 10647.

Sahebalzamani, H., Ghammamy, S., Mehrani, K., and Salimi, F. (2010). Synthesis, characterization and thermal analysis of Hg(II) complexes with hydrazide ligands. *Der Chemica Sinica*, *1*(1), 67-72.

Saif, M., El-shafiy, H. F., Mashaly, M. M., Eid, M. F., Nabeel, A. I., and Fouad, R. (2016). Synthesis, characterization, and antioxidant/cytotoxic activity of new chromone Schiff base nano-complexes of Zn(II), Cu(II), Ni(II) and Co(II). *Journal of Molecular Structure*, *1118*, 75-82.

University of Malaya

Sain, N., Krishnan, B., Ormerod, M. G., De Rienzo, A., Liu, W. M., Kaye, S. B., Workman, P., and Jackman, A. L. (2006). Potentiation of paclitaxel activity by the HSP90 inhibitor 17-allylamino-17-demethoxygeldanamycin in human ovarian carcinoma cell lines with high levels of activated AKT. *Molecular Cancer Therapeutics*, *5*(5), 1197-1208.

Sainorudin, M. H., Sidek, N. M., Ismail, N., Rozaini, M. Z. H., Harun, N. A., Anuar, T. N. S. T., and Yusoff, F. (2015). Synthesis, characterization and biological activity of organotin(IV) complexes featuring di-2-ethylhexyldithiocarbamate and *N*-methylbutyldithiocarbamate as ligands. *GSTF Journal of Chemical Sciences*, 1(2), 1-9.

Salager, J. L. (2002). Surfactants types and uses. *FRIP booklet-E300-A teaching aid in surfactant science & engineering*. *2*(3). Merida, Venezuela

Samanta, B., Chakraborty, J., Dey, D. K., Gramlich, V., D., and Mitra, S. (2007). Synthesis, characterisation and structural aspects of a new diorganotin(IV) complex with *N*-(5-bromo-2-hydroxybenzylidene)benzoylhydrazone ligand. *Structural Chemistry*, *18*(3), 287-293.

Sato, H., Wang, Y. M., Adachi, I. and Horikoshi, I. (1996). Pharmacokinetic study of taxol-loaded poly(lactic-co-glycolic acid) microspheres containing isopropyl myristate after targeted delivery to the lung in mice. *Biological and Pharmaceutical Bulletin*, *19*(12), 1596-601.

Saville, M. W., Lietzau, J., Pluda, J. M., Feuerstein, I., Odom, J., Wilson, W. H., Humphrey, R. W., Feigel, E., Steinberg, S. M., Broder, S. and Yarchoan, R. (1995). Treatment of HIV-associated Kaposi's sarcoma with paclitaxel. *The Lancet*, *346*(8966), 26-28.

Sedaghat, T., Yousefi, M., Bruno, G., Rudbari, H. A., Motamedi, H., and Nobakht, V. (2014). Synthesis, spectral characterization, crystal structure and antibacterial studies of diorganotin(IV) complexes with isonicotinoyl hydrazone derivatives. *Polyhedron*, 79, 88-96.

Shaabani, B., Khandar, A. A., Mobaiyen, H., Ramazani, N., Balula, S. S., and Cunha-Silva, L. (2014). Novel pseudohalide-bridged Cu(II) complexes with a hydrazone ligand: Evaluation of antimicrobial activity. *Polyhedron*, *80*, 166-172.

Sharma, S., and Saltz, L. B. (2000). Oral chemotherapeutic agents for colorectal cancer. *The Oncologist*, *5*(2), 99-107.

University of Malaya

Sheldrick, G. M. (2008). A short history of SHELX. *Acta Crystallographica Section A: Foundations of Crystallography*, *64*(1), 112-122.

Sheldrick, G. M. (2015). Crystal structure refinement with SHELXL. *Acta Crystallographica Section C: Structural Chemistry*, *71*(1), 3-8.

Shelke, V. A., Jadhav, S. M., Shankarwar, S. G., Munde, A. S., and Chondhekar, T. K. (2011). Synthesis, characterization, antibacterial and antifungal studies of some transition and rare earth metal complexes of *N*-benzylidene-2-hydroxybenzohydrazide. *Bulletin of the Chemical Society of Ethiopia*, *25*(3), 381-391.

Shinde, N. G., Aloorkar, N. H., and Kulkarni, A. S. (2012). Recent advances in transdermal drug delivery system. *Research Journal of Pharmaceutical Dosage Forms and Technology*, *6*(2), 110-120.

Shujah, S., Shah, A., Muhammad, N., Ali, S., Qureshi, R., Khalid, N., and Meetsma, A. (2010). Diorganotin(IV) derivatives of ONO tridentate Schiff base : Synthesis, crystal structure, *in vitro* antimicrobial, anti-leishmanial and DNA binding studies. *European Journal of Medicinal Chemistry*, *45*(7), 2902-2911.

Shujah, S., Rehman, Z., Muhammad, N., Ali, S., Khalid, N., and Tahir, M. N. (2011). New dimeric and supramolecular organotin(IV) complexes with a tridentate Schiff base as potential biocidal agents. *Journal of Organometallic Chemistry, 696*(15), 2772-2781.

Singh, H. L., and Singh, J. (2014). Synthesis, spectroscopic, molecular structure, and antibacterial studies of dibutyltin (IV) Schiff base complexes derived from phenylalanine, isoleucine, and glycine. *Bioinorganic Chemistry and Applications*, *2014*.

Sinha, R., Kim, G. J., Nie, S., and Shin, D. M. (2006). Nanotechnology in cancer therapeutics: Bioconjugated nanoparticles for drug delivery. *Molecular Cancer Therapeutics*, *5*(8), 1909-17.

Song, J., Shi, F., Zhang, Z., Zhu, F., Xue, J., Tan, X., Zhang, L., and Jia, X. (2011). Formulation and evaluation of celastrol-loaded liposomes. *Molecules*, *16*(9), 7880-7892.

Sreelola, V., and Krishna Sailaja, A. (2014). Preparation and characterisation of ibuprofen loaded polymeric nanoparticles by solvent evaporation technique. *International Journal of Pharmacy and Pharmaceutical Sciences*, *6*(8), 416-421.

University of Malaya

Stan, C. D., Tataringa, G., Gafitanu, C., Dragan, M., Braha, S., Popescu, M. C., Lisa, G., and Stefanache, A. (2013). Preparation and characterization of niosomes containing metronidazole. *Farmacia*, *61*(6), 1178-1185.

Sui, Y., Zeng, X., Fang, X., and Fu, X. (2007). Syntheses, structure, redox and catalytic epoxidation properties of dioxomolybdenum(VI) complexes with Schiff base ligands derived from *tris*(hydroxymethyl)amino methane. *Journal of Molecular Catalysis. A: chemical*, *270*, 61-67.

Sun, R. W. Y., Ma, D. L., Wong, E. L. M., and Che, C. M. (2007). Some uses of transition metal complexes as anti-cancer and anti-HIV agents. *Dalton Transactions*, (43), 4884-4892.

Sundaramurthy, D., Rodriguez, M., Nemr, S., and Braden, G. (2016). Successful treatment of tumor induced lactic acidosis with *tris*(hydroxymethyl)aminomethane (THAM). *American Journal of Kidney Disease*, *67*(5), A1-A118.

Sunitha, M., Jogi, P., Ushaiah, B., and Kumari, C. G. (2012). Synthesis, characterization and antimicrobial activity of transition metal complexes of Schiff base ligand derived from 3-ethoxysalicylaldehyde and 2-(2-aminophenyl)-1-H-benzimidazole. *Journal of Chemistry*, *9*(4), 2516-2523.

Tabassum, S., Yadav, S., and Arjmand, F. (2014). Exploration of glycosylated-organotin(IV) complexes as anticancer drug candidates. *Inorganica Chimica Acta*, *423*, 38-45.

Thadanki, M., Kumari, P. S., and Prabha, K. S. (2011). Overview of cubosomes: A nano particle. *International Journal of Research in Pharmacy and Chemistry*, *1*(3), 535-541.

Thilagavathi, N., Manimaran, A., Padma Priya, N., Sathya, N., and Jayabalakrishnan, C. (2010). Synthesis, characterization, electrochemical, catalytic and antimicrobial activity studies of hydrazone Schiff base ruthenium(II) complexes. *Applied Organometallic Chemistry*, *24*(4), 301-307.

Torchilin, V. (2006). *Nanoparticulates as drug carriers*. London: Imperial College Press.

Tweedy, B. G. (1964). Plant extracts with metal ions as potential antimicrobial agents. *Phytopathology*, *55*, 910-914.

University of Malaya

Vaage, J., Donovan, D., Uster, P., and Working, P. (1997). Tumor uptake of doxorubicin in polyethylene glycol-coated liposomes and therapeutic effect against a xenografted human pancreatic carcinoma. *British Journal of Cancer*, *75*(4), 482-486.

Vasconcelos, T., Sarmento, B., and Costa, P. (2007). Solid dispersions as strategy to improve oral bioavailability of poor water soluble drugs. *Drug Discovery Today*, *12*(23), 1068-1075.

Verma, S., Singh, S. K., Syan, N., Mathur, P., and Valecha, V. (2010). Nanoparticle vesicular systems: A versatile tool for drug delivery. *Journal of Chemical and Pharmaceutical Research*, *2*(2), 496-509.

Waddad, A. Y., Abbad, S., Yu, F., Munyendo, W. L. L., Wang, J., Lv, H., and Zhou, J. (2013). Formulation, characterization and pharmacokinetics of Morin hydrate niosomes prepared from various non-ionic surfactants. *International Journal of Pharmaceutics*, *456*(2), 446-458.

Wan, Y., Shi, Y., and Zhao, D. (2007). Designed synthesis of mesoporous solids *via* nonionic-surfactant-templating approach. *Chemical Communications*, (9), 897-926.

Wang, D. (2002). *Vanadium complexes and clusters for (potential) industrial and medicinal application* (Ph.D. thesis). University Hamburg, Germany.

Wang, F., Yin, H., Cui, J., Zhang, Y., Geng, H., and Hong, M. (2014). Synthesis, structural characterization, *in vitro* cytotoxicities, DNA-binding and BSA interaction of diorganotin(IV) complexes derived from hydrazone Schiff base. *Journal of Organometallic Chemistry*, *759*, 83-91.

Wang, H., Zhao, P., Liang, X., Gong, X., Song, T., Niu, R., and Chang, J. (2010). Folate-PEG coated cationic modified chitosan–cholesterol liposomes for tumor-targeted drug delivery. *Biomaterials*, *31*(14), 4129-4138.

Wang Z. H., Guo Y. Z., Zhang, J., Ma, L., Song, H. B., and Fan, Z. J. (2009). Synthesis and biological activity of organotin. *Journal of Agricultural and Food Chemistry*, *58*(5), 2715-2719.

Westrip, S. P. (2010). publCIF: software for editing, validating and formatting crystallographic information files. *Journal of Applied Crystallography*, *43*(4), 920-925.

University of Malaya

Wu, Y. J. J., Neuwelt, A. J., Muldoon, L. L., and Neuwelt, E. A. (2013). Acetaminophen enhances cisplatin-and paclitaxel-mediated cytotoxicity to SKOV3 human ovarian carcinoma. *Anticancer Research*, *33*(6), 2391-2400.

Xia, Y., Fan, C. D., Zhao, B.-X., Zhao, J., Shin D. S., and Miao, J. Y. (2008). Synthesis and structure-activity relationships of novel 1-arylmethyl-3-aryl-1H-pyrazole-5-carbohydrazide hydrazone derivatives as potential agents against A549 lung cancer cells. *European Journal of Medicinal Chemistry*, *43*(11), 2347-2353.

Yang, Y., Hong, M., Xu, L., Cui, J., Chang, G., Li, D., and Li, C. (2016). Organotin (IV) complexes derived from Schiff base *N*'-[(1E)-(2-hydroxy-3-methoxyphenyl)methylidene]pyridine-3-carbohydrazone: Synthesis, *in vitro* cytotoxicities and DNA/BSA interaction. *Journal of Organometallic Chemistry*, *804*, 48-58.

Yassin, A. E., Anwer, M. K., Mowafy, H. A., El-Bagory, I. M., Bayomi, M. A., and Alsarra, I. A. (2010). Optimization of 5-fluorouracil solid-lipid nanoparticles: A preliminary study to treat colon cancer. *International Journal of Medical Sciences*, *7*(6), 398-408.

Yew, H. C., and Misran, M. (2015). Nonionic mixed surfactant stabilized water-in-oil microemulsions for active ingredient *in vitro* sustained release. *Journal of Surfactants and Detergents*, *19*(1), 49-56.

Zafarian, H., Sedaghat, T., Motamedi, H., Trzybiński, D., and Woźniak, K. (2017). *Bis*-diorganotin(IV) complexes with binucleating hydrazones derived from a methylene-*bis*-aromatic aldehyde as linker: Synthesis, spectral and structural characterization, antibacterial activity and DNA cleavage studies. *Journal of Organometallic Chemistry*, *853*, 184-192.

Zhang, L., Gu, F. X., Chan, J. M., Wang, A. Z., Langer, R. S., and Farokhzad, O. C. (2008). Nanoparticles in medicine: Therapeutic applications and developments. *Clinical Pharmacology and Therapeutics*, *83*(5), 761-769.

Zhang, J., Wu, L. P., Zhuang, L. H., and Wang, G. W. (2009). 3-methoxybenzaldehyde thiosemicarbazone. *Acta Crystallographica Section E: Structure Reports Online*, *65*(4), o884-o884.

Zhang, S. and Morris, M. E. (2005). *Efflux transporters in drug excretion in drug delivery: principles and applications*. In Wang, B., Siahaan, T. and Soltero, R. (Eds.). New Jersey, USA: John Wiley & Sons Inc.

University of Malaya

Zheng, L. W., Wu, L. L., Zhao, B. X., Dong, W. L., and Miao, J. Y. (2009). Synthesis of novel substituted pyrazole-5-carbohydrazide hydrazone derivatives and discovery of a potent apoptosis inducer in A549 lung cancer cells. *Bioorganic and Medicinal Chemistry, 17(*5), 1957-1962.

University of Malaya

LIST OF PUBLICATIONS AND PAPER PRESENTED

PUBLICATION

1. Siti Nadiah Mohd Rosely, Rusnah Syahila Duali Hussen, See Mun Lee, Nathan R. Halcovitch, Mukesh M. Jotani and Edward R. T. Tiekink. (2017). (*N*'-(4-Decyloxy-2-oxidobenzylidene)-3-hydroxy-2-naphthohydrazidato-κ^3*N,O,O'*)dimethyltin(IV): Crystal structure and Hirshfeld surface analysis. *Acta Crystallograhica E. Crystallographic Communications*, *73*(3), 390-396. *(Accepted)*

POSTER PRESENTATIONS

1. Siti Nadiah Binti Mohd Rosely, Rusnah Syahila Duali Hussen, Lee See Mun, Diorganotin compounds for cancer therapy, UM111-Chemistry Symposium, 3rd March 2016, Chemistry Department, University of Malaya, Kuala Lumpur.

2. Siti Nadiah Mohd Rosely, Rusnah Syahila Duali Hussen, Lee See Mun, Synthesis, characterization and formulation of anticancer drugs, 29th Malaysian Analytical Chemistry Symposium (SKAM29), 15-17th August 2016, Bayview Beach Resort, Penang.

University of Malaya